SPECTRAL AND KINETIC STUDIES

OF IRON-SULFUR PROTEINS

Thesis by
Jill Rawlings

In Partial Fulfillment of the Requirements
for the Degree of
Doctor of Philosophy

California Institute of Technology
Pasadena, California
1975

(Submitted October 14, 1974)

ACKNOWLEDGMENT

I would like to thank H. B. Gray for his advice and encouragement.

ABSTRACT

Spectral studies of spinach ferredoxin and Chromatium HiPIP in the near infrared region give indications of inequivalence of the iron. The low energy spectrum of ferredoxin is interpreted in terms of one $[Fe(III)S_4]$ site, which is the reducible site, and one site, which is not tetrahedral and is nonreducible. A band at 720 nm in the oxidized protein is attributed to the first spin forbidden d-d band of a tetrahedral site, while bands at 820 and 920 nm are assigned to the distorted, nonreducible site. A band at 652 nm in the reduced protein is interpreted as an intervalence transition or a spin forbidden band of the iron(II) site.

The near infrared spectrum of reduced HiPIP has a broad band at 1040 nm. This band is absent in the model compound, $(Et_4N)_2[Fe_4S_4(SCH_2Ph)_4]$ and may be indicative of a slight site inequivalence. However, magnetic studies show an antiferromagnetic coupling very similar to the model, with μ_e per iron for protein and model agreeing closely.

A number of redox reactions of these iron-sulfur proteins with inorganic reagents were studied. The second order rate constant for the reaction of spinach ferredoxin with $FeEDTA^-$ is 3.4×10^5 M^{-1} sec^{-1}, while the rate constants for the HiPIP reactions are slower by a factor of 100. The rate constant is 1.7×10^3 M^{-1} sec^{-1}

for the reaction of HiPIP and $FeEDTA^{2-}$ and $2.4 \times 10^{3}\ M^{-1} sec^{-1}$ for the HiPIP-$Fe(CN)_6^{3-}$ reaction. These reactions typically have very small activation enthalpies and very negative activation entropies. Electron tunneling is suggested as a possible mechanism for these reactions.

TABLE OF CONTENTS

CHAPTER I

SPECTRAL STUDIES OF FERREDOXIN

INTRODUCTION

The iron-sulfur proteins have presented interesting structural problems and so have consequently been studied by a great variety of physical techniques.[1,2] Our understanding of structure in this class of metalloproteins is perhaps most extensive for rubredoxin, a one iron protein from C. pasteurianum It is known from X-ray structural studies that rubredoxin has a distorted tetrahedral [FeS_4] coordination, with the sulfur atoms donated by the cysteine residues of the protein.[3] Magnetic susceptibility studies have established high-spin Fe^{2+} and Fe^{3+} for the reduced and oxidized protein, respectively.[4]

Spectral measurements of the reduced protein show charge transfer bands at 310 and 330 nm with no other bands in the visible region.[5] Eaton and co-workers measured the near-infrared spectrum of Fe^{2+}-rubredoxin and located absorption bands at 4 and 6 k cm^{-1} attributed to the components of the ligand field transition $^5E \rightarrow {}^5T_2$ of

a distorted tetrahedral [$Fe(II)S_4$] core structure.[6, 7] This low energy transition is characteristic of Fe(II) in tetrahedral coordination. Other model systems, $Fe[S_2(PPh_3)_2N]_2$[8] and Fe(II) in ZnS,[9] show a bands at 3700-2800 and 330 cm^{-1}, respectively.

The spectrum of oxidized rubredoxin exhibits intense charge-transfer bands throughout the visible region, and a less intense band (ϵ = 360) at 750 nm.[7]

Extension of the electronic spectroscopic work to the two-iron, two-labile-sulfur ferredoxins has shown that one of the sites in the reduced spinach protein (Fd_{red}) is probably very similar to the distorted tetrahedral [$Fe(II)S_4$] site found in reduced rubudoxin;[7] the $^5E \rightarrow {}^5T_2$ transition is found at 1,600 nm . No conclusion was reached concerning the assignment of electronic spectrum of the oxidized ferredoxin (Fd_{ox}), however. Several magnetic susceptibility studies have been reported for oxidized and reduced two-iron ferredoxins. The most recent work, which covered the range 77-300°K, established antiferromagnetic coupling between two $^6A_1$ Fe^{3+} centers in Fd_{ox}.[10] The interpretation of the magnetic data for Fd_{red} was not as definitive, but the evidence favored an antiferromagnetically coupled $Fe^{2+}(^5E)$-$Fe^{3+}(^6A_1)$ model.[10] Mössbauer experiments are also consistent with

a spin-coupled $Fe^{2+}(^5E)$-$Fe^{3+}(^6A_1)$ site in Fd_{red}.[11,12] The spectrum of Fd_{red} consists of two quadrupole split doublets, one centered at the position found in the spectrum of Fd_{ox} and the other at a position typical of Fe^{2+}. Esr studies on ^{33}S analogs indicate that the labile sulfur is also involved at the iron site.[13] The core structure is thus generally represented as two $(cys\text{-}S)_2Fe$ units connected by two sulfide bridges.[1]

Several important features concerning the coordination structure of Fd_{ox} and Fd_{red} remain to be elucidated. The Mössbauer spectrum of Fd_{ox} exhibits a single quadrupole doublet, but the possibility of nonequivalent Fe^{3+} sites has not been eliminated.[11,12] Indeed, the relatively broad Mössbauer line widths observed have been interpreted in terms of a slight nonequivalence,[12] although other factors could be responsible.[11] In addition, the proton contact shifts observed by nmr indicate that protons other than those of cysteine residues are present;[14] the signals, however, have not been identified. Also, Kimura[15] has reported anomalous fluorescence behavior in adrenodoxin. Only one aromatic amino acid, tyrosine 82, is present in the protein, but its fluorescence maximum occurs at 30 nm longer wavelength than for free tyrosine. Normal tyrosine fluorescence is observed in the apoprotein, suggesting that the tyrosine may interact with the metal center.[15] Thus, additional experimental information relating to the structures of the Fe^{3+} sites in both Fd_{ox} and Fd_{red} is needed.

We have found previously that the spin-forbidden sextet-quartet d-d bands of spin-coupled $^6A_1$ Fe^{3+} binuclear complexes are often much more intense than in monomeric reference systems.[16] Intensity enhancements as great as 10^3 would not be unreasonable for the sextet → quartet (Fe^{3+}) and quintet → triplet (Fe^{2+}) bands associated with the strongly spin-coupled binuclear sites of the proteins. Identification of the lowest bands could add significantly to the site characterization, as the d-d transition positions are often diagnostic of geometrical structure. For this reason, we have carefully examined the electronic absorption spectra of Fd_{ox} and Fd_{red} at low temperature in the 1200-600 nm region. Our analysis of the results is presented.

EXPERIMENTAL

The protein was prepared by variations on published procedures.[17,18]

Approximately 20 kg of fresh spinach leaves with 10 ml of 1 M Tris base and 500 "ml" of ice were ground for 5 min in a Waring blender. All subsequent operations were carried out at 4°C. The extract was squeezed through cheesecloth. The ionic strength of the solution was raised to .15 with NaCl. Approximately 500 ml of DEAE-cellulose, Type 52 from Whatman, was then added to the 15 ℓ of filtrate; this was stirred for 2 hr, and then the filtrate was allowed to stand for 1 1/2 hr. Most of the filtrate was siphoned off. The DEAE cellulose was then collected by filtration. This was washed with 2 ℓ of .15 M NaCl, .01 Tris pH 7.5, and finally, the DEAE cellulose was eluted with .15 M Tris, pH 7.5, .8 M NaCl. Ammonium sulfate was then added to 90% saturation; the solution was centrifuged to remove a greenish precipitate. The solution was then dialyzed for 12 hr against 10 ℓ of 0.1 Tris pH 7.5. This was then diluted twofold and absorbed onto a small (2 × 10 cm) column of DEAE, which was eluted with .15 M NaCl, .15 M Tris 7.5. The eluant was diluted threefold, absorbed onto a DEAE column (1 × 2) and again eluted with

.15 M Tris, .8 M NaCl. The concentrated solution was then applied to a Bio Gel P 60 column, equilibrated with .15 M Tris, pH 7.5. The column was washed with .15 M Tris 7.5, and 5 ml fractions were collected. The fractions were analyzed on a Cary 14 spectrophotometer. The ratio of the absorbance at 422 nm to 275 nm was used as the criterion of purity. Fractions with a ratio higher than 0.47 were used.

Samples of ferredoxin were lyophilized and then dissolved in D_2O. An equal volume of ethylene glycol was then added. Addition of ethylene glycol did not affect significantly either the band position or molar extinction coefficients in the visible spectrum of the protein. Spectral measurements were then made on a Cary 14RI spectrophotometer using a liquid nitrogen dewar.

The sample of the reduced protein was obtained by gently bubbling nitrogen through the solution, and then adding a tenfold molar excess of $Na_2S_2O_4$ by syringe.

Thin films of the oxidized protein were obtained by slow evaporation of a concentrated protein solution onto quartz plates.

Adrenodoxin was the gift of T. Kimura and was used without further purification.

The compounds $KFeS_2$ [19] and $KFeSe_2$ [20] were synthesized by literature procedures. Tris(tetraphenylthioxoimidodiphosphinato)-iron(III) was prepared by mixing $Na(OPPh_2NPPh_2S)$ [21] and $FeCl_3$ in a 3:1 molar ratio in water. The dark red precipitate was filtered, dried under vacuum, and recrystallized from acetone-petroleum ether solutions. Anal. Calcd. for $C_{72}H_{60}N_3O_3FeP_6S_3$: C, 63.91; H, 4.47; N, 3.11; O, 3.55; Fe, 4.13; P, 13.73; S, 7.11. Found: C, 6421; H, 4.59; N, 3.19; O, 3.29; Fe, 4.09; P, 13.74; S, 7.42.

RESULTS AND DISCUSSION

The absorption spectra of Fd_{ox} and Fd_{red} in 1:1 ethylene glycol/D_2O are shown in Figures 1 and 2. Lowering the temperature to 77°K results in some sharpening of bands in the visible region, with some weakly resolved bands becoming more apparent at 345 nm and 520 nm. Also, lowering the temperature greatly aids in resolving the region from 600 to 1200 nm. Relatively weak bands are then resolved for Fd_{ox} at 720, 820, and 920 nm. These three features have been observed previously in spectra of Fd_{ox} taken in sucrose solution at -196°C.[22] In addition, band positions in the thin-film spectrum of Fd_{ox} are in close agreement with those obtained in the low temperature glass. The intensities of these bands are somewhat temperature dependent, with the intensity decreasing as the temperature is lowered. Band positions, molar extinction coefficients, and assignments are set out in Table I.

The only major change in the 1200 - 600 nm region which occurs upon reduction of the protein is the disappearance of the 720 nm band and the development of a new band at 652 nm (See Figure 2). Interestingly, the very weak

Figure 1. Electronic absorption spectra of oxidized (a) and reduced (b) spinach ferredoxins in 1:1 D_2O/ethylene glycol at 77 °K. Protein concentration is 1. mg/ml (1 cm pathlength).

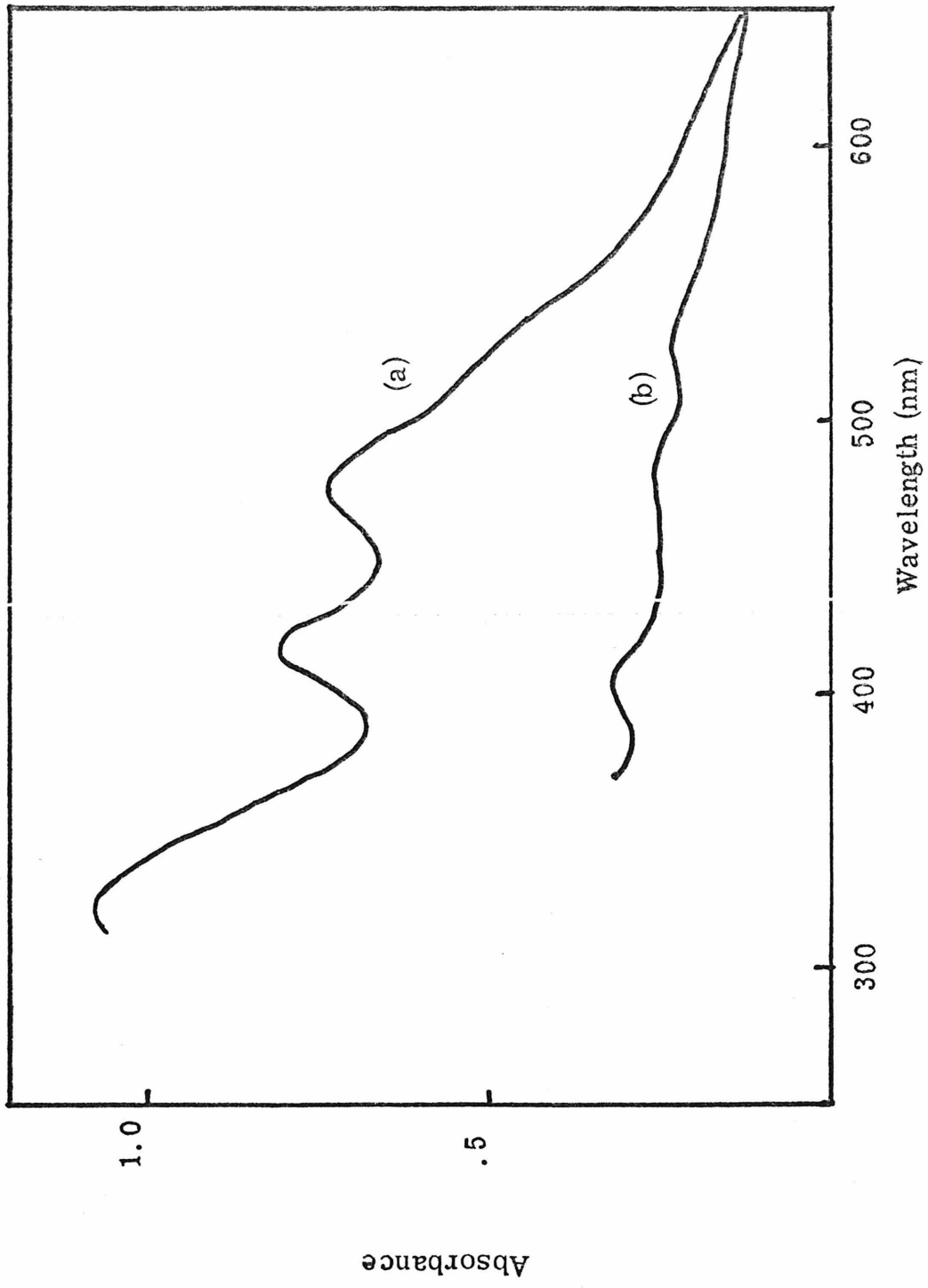

Figure 2. Electronic absorption spectra of oxidized (a) and reduced (b) spinach ferredoxin in 1:1 D_2O/ethylene glycol at 77 °K. Protein concentration is 10 mg/ml (1 cm pathlength).

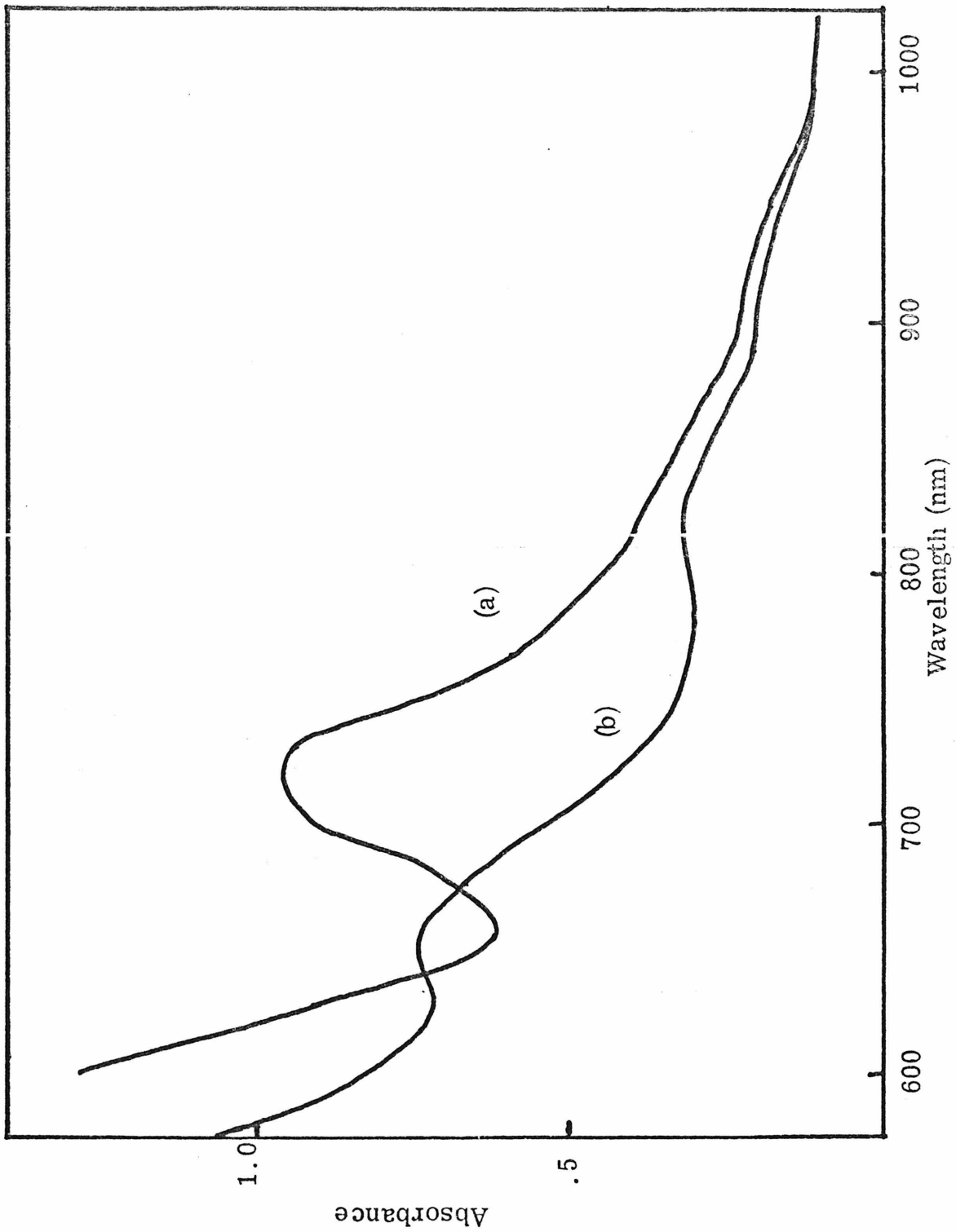

Table I. Electronic Absorption Spectra (1200-600 nm) of Oxidized and Reduced Spinach Ferredoxins in 1:1 D_2O/ethylene glycol at 77°K

	λ_{max}, nm	$\bar{\nu}$, kcm^{-1}	ϵ, ℓ mol Fe^{-1} cm^{-1}	Assignment
Fd_{ox}	920	10.9	80	Nonreducible Fe(III)
	820	12.2	260	Nonreducible Fe(III)
	720	14.1	800	$Fe(III)S_4$ $^6A_1 \rightarrow {}^4T_1$
Fd_{red}	920	11.0	65	Nonreducible Fe(III)
	820	12.2	200	Nonreducible Fe(III)
	652	15.5	600	$Fe(II)S_4$ $^5E \rightarrow {}^3T_1$ or Fe(II) → Fe(III)

features at 820 and 920 nm are still present in Fd_{red}, clearly indicating that the responsible chromophore has not been chemically altered in the electron-transfer process.

The spectral properties outlined above establish that non-equivalent Fe(III) sites are present in Fd_{ox}. The data are nicely accommodated if the site undergoing reduction is formulated as having a tetrahedral $Fe(III)S_4$ core structure, as proposed by Eaton et al.[7] The 13.9 kcm^{-1} peak in Fd_{ox}, which disappears upon reduction, strongly suggests tetrahedral $Fe(III)S_4$, as oxidized clostridial rubredoxin exhibits a similar band at 13.4 kcm^{-1} (ϵ 360).[7] The assignment of the 13.9 kcm^{-1} band to a tetrahedral $Fe(III)S_4$ center is supported by spectral results obtained for $KFeS_2$. The latter compound, which features S^{2-}-bridged $Fe(III)S_4$ tetrahedra,[23] displays a broad absorption system in the 13-16 kcm^{-1} region in a TlCl disk at 77°K (Fig. 3), with no absorption attributable to electronic transitions at lower energies. Thus a band at about 14 kcm^{-1} appears to be characteristic of Fe^{3+} coordinated tetrahedrally by S^{2-} (or $-CH_2S^-$) donor atoms.

Energetic considerations favor assignment of the 14 kcm^{-1} band in tetrahedral $Fe(III)S_4$ to the spin-forbidden $^6A_1 \rightarrow {}^4T_1$ d-d transition. Reasonable values for $Fe(III)S_4$ ligand field parameters (-10 Dq = 6-8, B = 0.6 kcm^{-1}, C/B = 4.5), for example, place the $^6A_1 \rightarrow {}^4T_1$ transition in the 13.5-15 kcm^{-1} range. Additional support

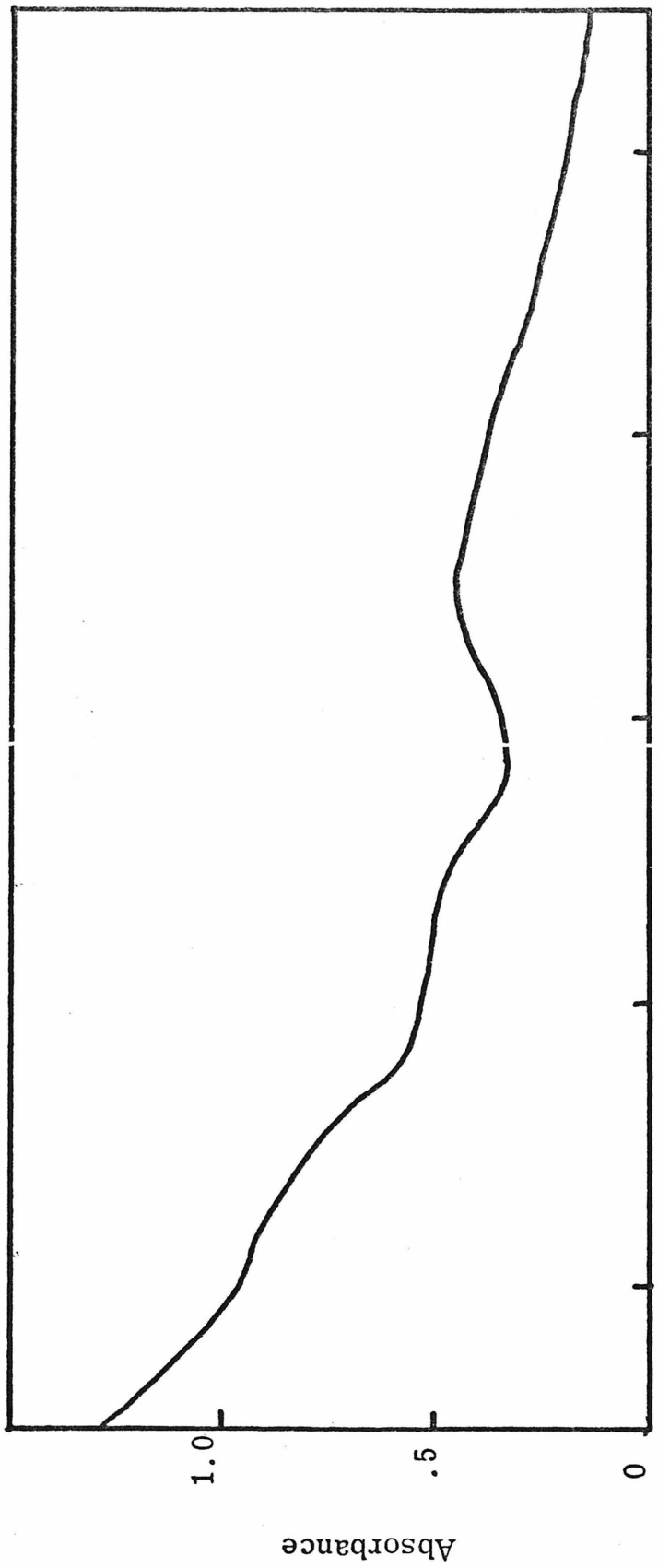

Figure 3. Electronic absorption spectrum of a TlCl pellet of $KFeS_2$ at 77°K.

for a d-d transition is provided by a spectral comparison of $KFeS_2$ and $KFeSe_2$. The lowest absorption system of $KFeSe_2$ is observed in the 11-13 kcm^{-1} region (Fig. 4), which represents a smaller red shift from $KFeS_2$ than would be expected for a transition of the S(Se) → Fe(III) charge transfer type. The moderate red shift, however, is consistent with an excitation of substantial d-d character.

It is interesting that ϵ/Fe value for the 13.4 kcm^{-1} bands in clostridial rubredoxin is not very much smaller than that for Fd_{ox}. This observation makes it clear that there is very little intensity enhancement of the $^6A_1 \rightarrow {}^4T_1$ transition attributable to spin-spin coupling in the binuclear unit of Fd_{ox}. It is probable, therefore, that relaxation of the $^6A_1 \rightarrow {}^4T_1$ spin-forbiddenness results primarily from mixing of the excited $^4T_1$ state with nearby $^6T_2$ transfer states through spin-orbit coupling.

A band at 652 nm (15.3 kcm^{-1}) in Fd_{red} is entirely consistent with the presence of a tetrahedral $Fe(II)S_4$ center. In addition to a spin-allowed $^5E \rightarrow {}^5T_2$ system, tetrahedral $Fe(II)S_4$ should exhibit a large number of quintet → triplet transitions. Taking a reasonable B range of 0.7-0.9 kcm^{-1} (C/B = 4.6), the lowest spin-forbidden transition, $^5E \rightarrow {}^3T_1$, is calculated to fall between 13 and 18 kcm^{-1} in Fd_{red}, due to an intensity-enhanced $^5E \rightarrow {}^3T_1$ transition of the $Fe(II)S_4$ unit of the binuclear site. The proposed assignment derives some

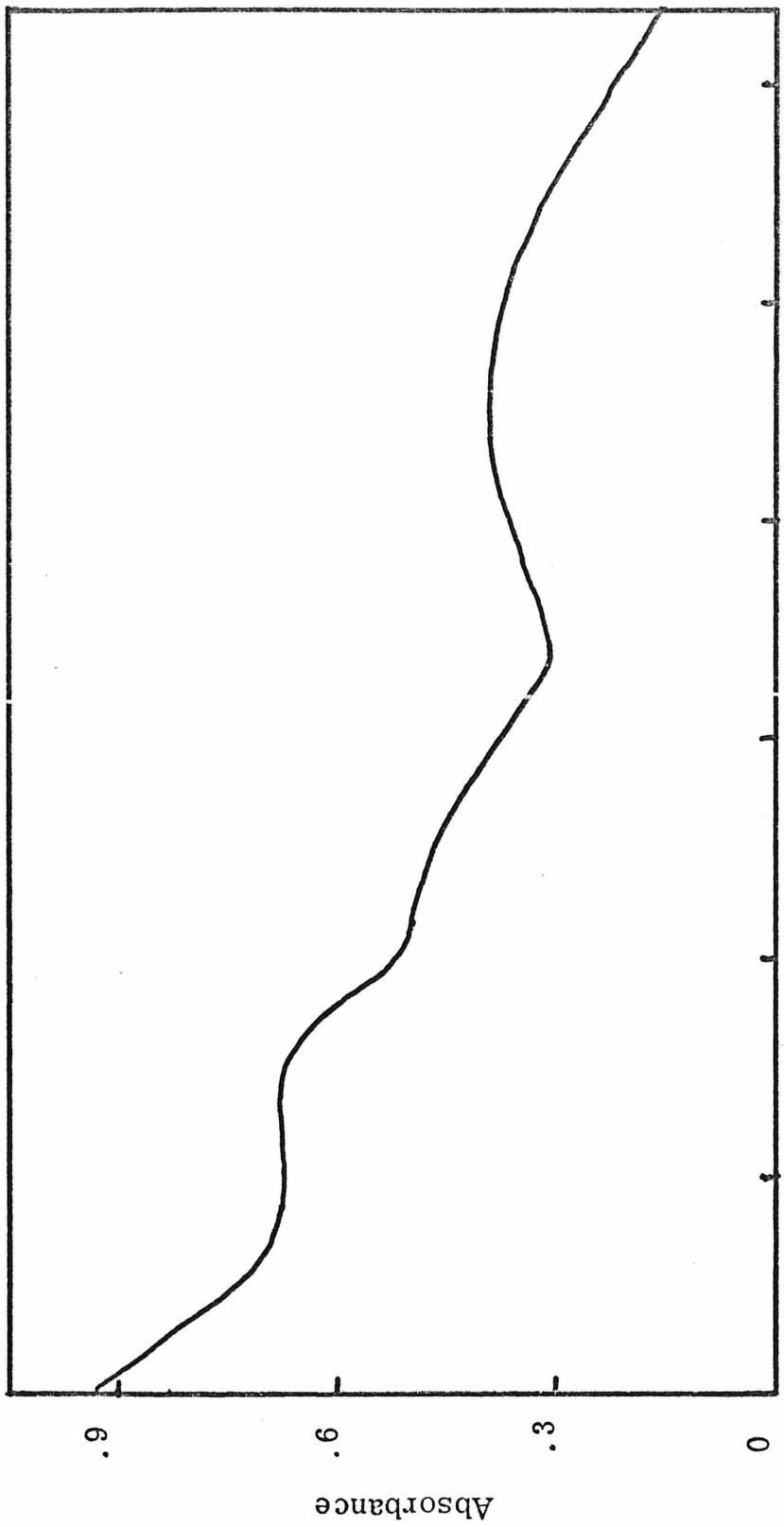

Figure 4. Electronic absorption spectrum of a TlCl pellet of $KFeSe_2$ at 77 °K.

support from spectral measurements on a tetrahedral $Fe(II)S_4$ model compound.[8] The $^5E \rightarrow {}^3T_1$ band has been located at 15.4 kcm^{-1} (ϵ 10) in the absorption spectrum of a single crystal of $Fe[S_2(PPh_2)_2N]_2$.[24] Another very reasonable candidate assignment for the 15.2 kcm^{-1} band in Fd_{red} is an Fe(II) → Fe(III) intervalence transition. It is not possible from the limited information available to make a definite choice between the two proposals.

The absorption peaks at 10.9 and 12.2 nm attributable to the nonreducible Fe(III) site in the protein fall between the $^6A_1 \rightarrow {}^4T_1$ position (about 7 kcm^{-1}) observed for $^6A_1$ $Fe(III)S_6$ complexes[25] and the 13.5-15 kcm^{-1} range predicted for tetrahedral $Fe(III)S_4$. The relatively large band splitting indicates that the structure is significantly distorted from cubic symmetry. Distorted octahedral coordination of the type $Fe(III)S_4X_2$ (X = O or N) appears to be ruled out from the band positions. Even with three sulfur-donor atoms, as in the high-spin (μ_{eff} 5.91, 300°K) $Fe(III)S_3O_3$ complex $Fe(OPPh_2NPPh_2S)_3$, the $^6A_1 \rightarrow {}^4T_1$ band peaks at 8.9 kcm^{-1} (77°K, TlCl disk). Considering the evidence available, then, the most reasonable possibility for the Fe(III) site in Fd_{red} is either a highly distorted (squashed toward D_2d) tetrahedral structure or perhaps an $Fe(III)S_4$ unit involved in additional weak coordination to an available nitrogen or oxygen donor atom.

The spectrum of oxidized adrenodoxin is very similar to the spinach ferredoxin spectrum. Thus, the bands found in spinach ferredoxin at 720, 820, and 920 nm have their counterparts in the adrenodoxin spectrum at 692, 820, and 915 nm. The 692 nm band in adrenodoxin has an extinction coefficient of about 600. It is clear, therefore, that adrenodoxin possesses the same core structure as Fd_{ox}.

References

1. J. C. M. Tsibris and R. W. Woody, Coord. Chem. Res., 5, 417 (1970).

2. W. R. Dunham, G. Palmer, R. H. Sands, and A. J. Bearden, Biochim. Biophys. Acta, 253, 373 (1971).

3. J. R. Heriot, L. C. Sieker, L. H. Jensen, and W. Lovenberg, J. Mol. Biol., 50, 391 (1970).

4. W. D. Phillips, M. Poe, J. F. Wieher, C. C. McDonald, and W. Lovenberg, Nature, 227, 574 (1970).

5. W. Lovenberg and W. M. Williams, Biochemistry, 8, 141 (1969).

6. W. A. Eaton and W. Lovenberg, J. Amer. Chem. Soc., 92, 7195 (1970).

7. W. A. Eaton, G. Palmer, J. A. Fee, T. Kimura, and W. Lovenberg, Proc. Nat. Acad. Sci. U.S., 68, 3015 (1971).

8. A. Davison and E. S. Switkes, Inorg. Chem., 10, 837 (1971).

9. W. Low and M. Weger, Phys. Rev., 118, 1130 (1960).

10. G. Palmer, W. R. Dunham, J. A. Fee, R. H. Sands, T. Iizuka, and T. Yonetani, Biochim. Biophys. Acta, 245, 201 (1971).

11. W. R. Dunham, A. J. Bearden, I. T. Salmeen, G. Palmer, R. H. Sands, W. H. Orme-Johnson, and H. Beinert, Biochim. Biophys. Acta, 253, 134 (1971).

12. K. K. Rao, R. Cammack, D. O. Hall, and C. E. Johnson, Biochem. J., 122, 257 (1971).

13. J. A. Fee and G. Palmer, Biochim. Biophys. Acta, 245, 175 (1971).

14. M. Poe, W. D. Phillips, J. D. Glickson, C. C. McDonald, A. San Pietro, Proc. Nat. Acad. Sci. U.S., 68, 68 (1971).

15. T. Kimura, J. T. Ting, and J. J. Huang, J. Biol. Chem., 247, 4476 (1972).

16. H. J. Schugar, G. R. Rossman, C. G. Barraclough, and H. B. Gray, J. Amer. Chem. Soc., 94, 2683 (1972).

17. D. H. Petering and G. Palmer, Arch. Biochem. Biophys., 141, 456 (1970).

18. S. Keresztes-Nagy and E. Margoliash, J. Biol. Chem., 241, 5955 (1966).

19. J. L. Deutsch and H. B. Jonassen, Inorg. Syn., 6, 179 (1960).

20. W. Bronger, Naturwissenschaften, 53, 525 (1966).

21. A. Schmidpetis and H. Groegen, Chem. Ber., 100, 3052 (1967).

22. D. F. Wilson, Arch. Biochem. Biophys., 122, 254 (1967).

23. J. W. Boon and C. H. MacGillary, Rec. Trav. Chem., 61, 910 (1942).

24. O. S. Siiman and H. B. Gray, in preparation.

25. A. H. Ewald, R. L. Martin, E. Sinn, and A. H. White, Inorg. Chem., 8, 1837 (1969).

CHAPTER II

MAGNETIC AND SPECTRAL STUDIES OF HIPIP

INTRODUCTION

Recent work by Holm and coworkers has provided[1-4] excellent synthetic analogs of the $[Fe_4S_4(S\text{-}Cys)_4]$ cluster found in the iron-sulfur proteins "high potential iron protein" (HiPIP)[5] and bacterial ferredoxins.[6] Holm's model iron cluster, $(Et_4N)_2[Fe_4S_4(SCH_2Ph)_4]$ forms a roughly cubic arrangement of alternating iron and sulfur.[2] The coordination about each iron is roughly tetrahedral, the ligands being three acid-labile sulfur (S*) atoms and one cysteine-like sulfur. Fe-S* distances average 2.286 Å, very similar to other iron-sulfur clusters. The Fe-Fe distances are fairly short, averaging 2.746 Å, thus indicating that some metal-metal interactions may occur. The four iron atoms are structurally indistinguishable.[2]

The model compound has an absorption band at 417 nm (ϵ = 19,400) and magnetic behavior suggesting a singlet ground state.[1] The magnetic moment increases with temperature (μ = 0.3 at 100 °K and μ = 1.04 at 296 °K), suggesting extensive antiferromagnetic coupling.

By considering the bridging sulfur as S^{2-}, one would expect 2 Fe(II) and 2 Fe(III) in the cluster. However, the structure indicates that all the iron atoms are equivalent. Mössbauer spectroscopy[1] is also not consistent with isolated ferric and ferrous ions. Only one quadrupole split doublet is observed,

suggesting extensive delocalization of electrons. Other measurements, such as low temperature optical spectroscopy, also indicate a delocalized electronic structure.[7]

The X-ray studies of the four-iron protein HiPIP reveal a Fe_4S_4 core closely resembling that in Holm's model compound.[5] Two interlocking tetrahedra of iron and sulfur form a roughly cubic array, with each iron also coordinated to a cysteine of the protein (See Figure 1). The iron-iron distances are 2.72 Å for oxidized HiPIP and 2.81 Å for reduced HiPIP; the oxidized cluster is thus slightly smaller than the reduced cluster. All of the iron atoms appear to be equivalent.[5]

Structural work on the eight-iron ferredoxin from Micrococcus aerogenes reveals two four-iron clusters, 12 Å apart.[6] Each of these clusters has a geometry very similar to that described for Holm's model or HiPIP.

Reduced HiPIP shows no esr, and reported magnetic moments are low, indicating a spin = 0 ground state.[8] The oxidized protein has an esr ($g_{\perp} = 2.04$, $g_{||} = 2.12$)[9] and a reported moment consistent with a spin 1/2 state.[8] The visible spectra are relatively featureless; the reduced protein has one intense band ($\epsilon = 16,100$) at 388 nm, while the oxidized protein exhibits a three poorly defined maxima at 450, 375, and 325 nm.[9]

Figure 1. Structure of the Iron Cluster of Chromatium HiPIP

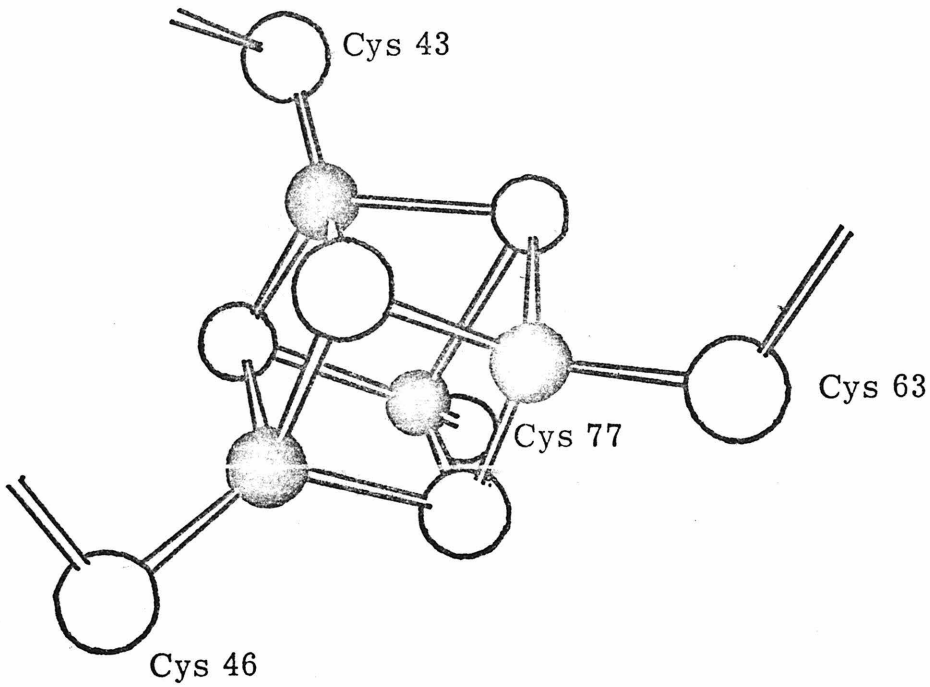

The oxidation-reduction behavior of HiPIP is characterized by a high potential; E^0 = +.35 v for the reduction.[10] However, by adding 80% DMSO, it is possible to further reduce the protein;[11] the typical reduced ferredoxin-type esr signal appears, with g = 2.04, 1.93. The potential of this "super-reduction" is estimated as less than -.4 v. Thus, the protein has been observed in three oxidation states. The middle state is considered to be isoelectronic with Holm's cluster compound and the oxidized state of the eight-iron bacterial ferredoxin (Bac Fd_{ox}), according to the following scheme:

Odd electron state		Even electron state		Odd electron state
	⟶	$[Fe_4S_4(SCH_2Ph)_4]^{2-}$ "2 Fe(II), 2 Fe(III)"	⟶	
$HiPIP_{ox}$	+.35 v ⟶	$HiPIP_{red}$	-.5 v, DMSO ⟶	Super reduced HiPIP
Unknown	? ⟶	Bac Fd_{ox}	-.42 v ⟶	Bac Fd_{red}

Thus, these Fe_4S_4-cluster proteins can be found in several oxidation states. The states found in the biological system differ for HiPIP and Fd_{bac}. Starting in both cases from even electron states, the redox behavior observed for HiPIP involves removing an electron, whereas that for bacterial ferredoxin corresponds to the addition of an electron.

Several questions about the electronic structures of these Fe_4S_4-cluster proteins remain unanswered. For example, is Holm's model compound really isoelectronic with the even electron state found for the proteins? Further, are all iron atoms in the protein equivalent, as is the case for Holm's model compound? If the iron atoms are not equivalent, as some nmr evidence on HiPIP suggests,[12] then what is the nature of this inequivalence? Concerning the latter question, there is also some indication of inequivalence in the Mössbauer spectrum of HiPIP, as the lines are unusually broad.[13] It is possible that incorporating the cluster into the protein perturbs the structure, thereby introducing some inequivalence in the Fe_4 substructure. To help shed light on the above issues, the magnetic susceptibility of reduced HiPIP was measured over a wide temperature range. The electronic absorption spectra of both oxidation states of HiPIP were also recorded at a low temperature.

EXPERIMENTAL

HiPIP was extracted from cells of Chromatium. Stock cultures of Chromatium, strain D, were obtained from the American Type Cell Collection, no. 17899. These cells were then grown as described by Bose.[14] Cells were harvested by continuous centrifugation after four days of growth.

The protein was extracted by variations on published methods.[15,16] The cells were disrupted by freeze-thaw lysing, with 1% Triton-X added. This material was then centrifuged for 1 hr at 10000 rpm. The cells fragments and mitochondrial particles, which were at the top, were removed. To the resulting yellowish solution, ammonium sulfate was added to 90% of saturation. This precipitates most of the material. The precipitate is dissolved in .02 Tris, pH 8 at 4°C, and dialyzed extensively against the same buffer. This was then absorbed onto a column (2 × 10) of DEAE cellulose, type 52, from Whatman. This column was washed with .02 Tris, pH 8 and 40 mM NaCl; a greenish band was collected, with most of the colored material remaining on the column. The greenish fraction was diluted fourfold, and absorbed onto a column of DEAE Sephadex, A-25 equilibrated with .02 M Tris buffer, pH 8. The column was eluted with .02 M Tris buffer, pH 8, plus .05 M NaCl, and fractions were collected. Fractions with the absorbance ratio of 272 nm to 388 nm of 2.52 were collected for this work.

The HiPIP was prepared for spectral work by first obtaining a powder by precipitation with ammonium sulfate. This powder was dissolved in a small amount of D_2O and then dialyzed against D_2O to remove excess salt. Spectra were then taken of this solution. Low temperature solution work was performed by adding an equal volume of ethylene glycol. Thin films were also prepared by evaporation. Spectra were taken on a Cary 17.

The oxidized protein was obtained in two ways. In one, the protein was passed through a small column of Dowex-1X Cl^- charged with $Fe(CN)_6^{3-}$. In the other, a twofold excess of $Fe(CN)_6^{3-}$ was added to the solution, followed by dialysis. Ethylene glycol was added, and then spectra were taken. Thin films were also examined. Both methods gave similar results.

The HiPIP used for the magnetic work was first reduced with mercaptoethanol, followed by dialysis. The concentrated solution was filtered through a millipore filter. The protein was then precipitated with ammonium sulfate. Care was taken to keep the sample out of the air and away from any metallic objects. The magnetism was then measured with a superconducting magnetometer; a description of this instrument has been presented elsewhere.[17] The relative change of susceptibility was measured on a sample of 70 mg of protein in a magnetic field of 150 G from 3 to 150 °K.

RESULTS AND DISCUSSION

The magnetic studies indicate a coupling that closely resembles the four-iron model.[1] A plot of the measured temperature dependent susceptibility against inverse temperature is presented in Figure 2. A paramagnetic component dominates the magnetism at low temperatures; this component is attributed to high spin impurities [1.4% Fe^{3+}(S=5/2) accounts for the observed component]. This paramagnetic component shows a Curie Law behavior ($\chi = 4.1 \times 10^{-6}$ emu/g/T), so it was possible to correct for this component and obtain the temperature dependence of the magnetic moment per iron atom; this is shown in Figure 3. Antiferromagnetic behavior is apparent above 100°K.

Our magnetic susceptibility data on $HiPIP_{red}$ are in good agreement with the results reported for $(Et_2N)_2[Fe_4S_4(SCH_2Ph)_4]$.[1] Perhaps most impressive is the fact that the temperature dependences of μ_e in the tetramer and the protein are within experimental error in the range 100-150°K. It appears, therefore, that the gross electronic structural features of the $[Fe_4S_4(S\text{-}Cys)_4]$ cluster in $HiPIP_{red}$, including the extent of spin-spin coupling, are reproduced very closely by the dianionic tetramer.

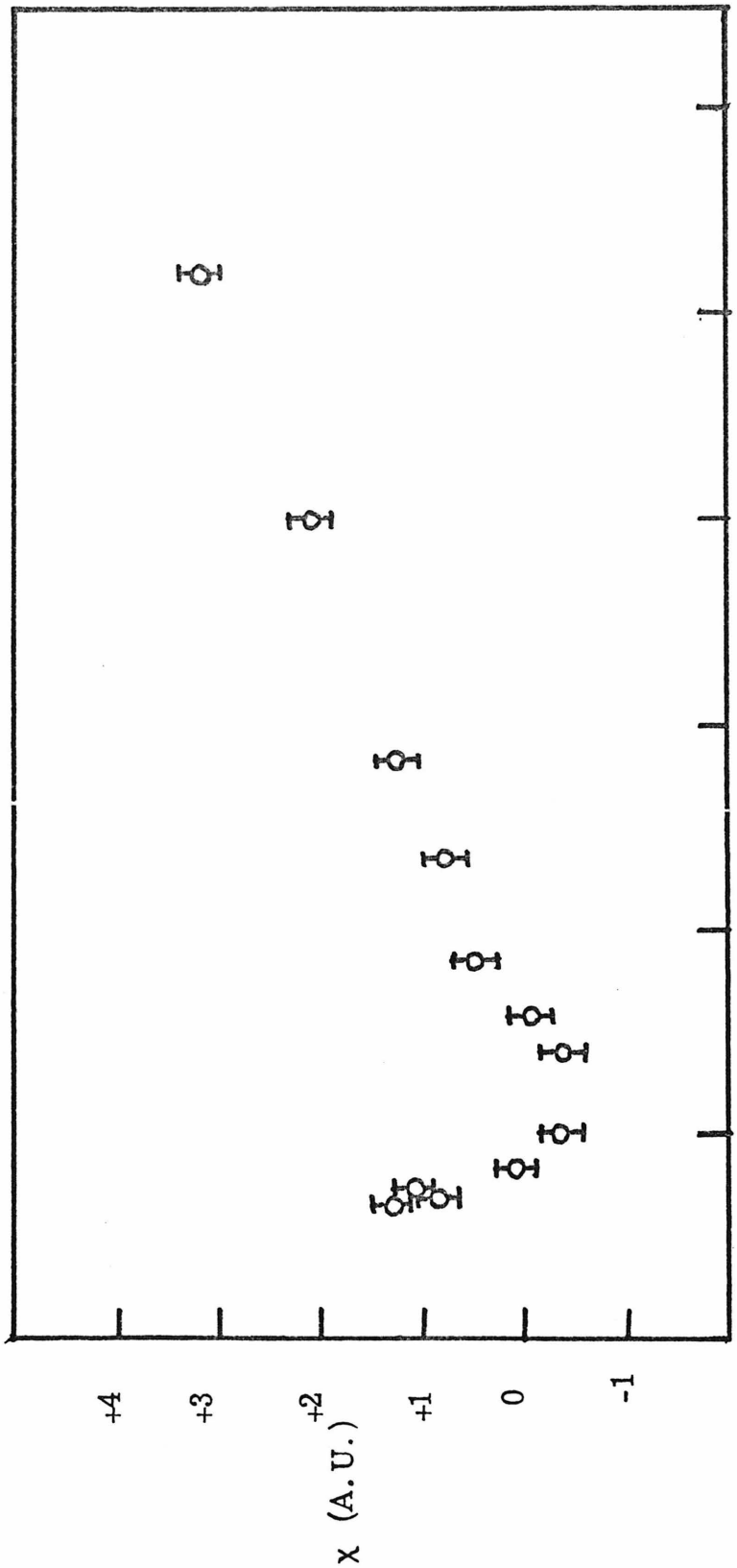

Figure 2. Magnetic susceptibility vs. reciprocal temperature for $HiPIP_{red}$ between 20 and 150 °K.

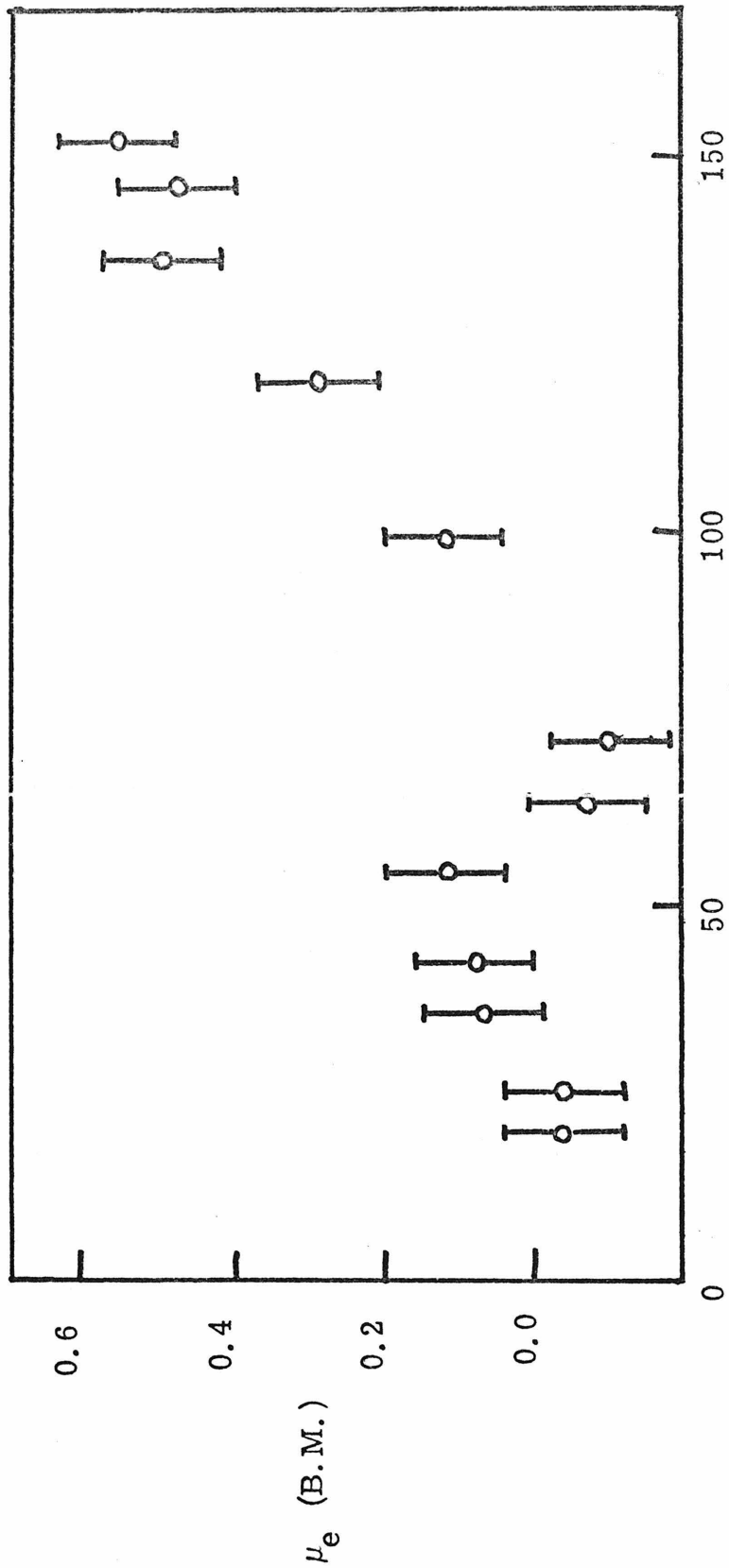

Figure 3. Corrected magnetic moment per iron (μ_e) vs. T for $HiPIP_{red}$ in the region 20 - 150 °K.

The absorption spectra of $HiPIP_{ox}$ and $HiPIP_{red}$ are shown in Figures 4 and 5, and, for comparison, the spectrum of $(Et_4N)_2[FeS_4(SCH_2Ph)_4]$ [7] is shown in Figure 6. Band positions and molar extinction coefficients are listed in Table I.

The near infrared spectrum of Holm's compound is relatively featureless.[7] In particular, no evidence is found for the low energy $^5E \rightarrow {}^5T_2$ transition typical of Fe(II) in a tetrahedral coordination. This spectrum confirms the Mössbauer evidence that all iron atoms are equivalent;[1] the molecule is best thought of in terms of a delocalized ground state, with the electrons equally shared by all four irons. In addition to the intense band at 417 nm, two weaker bands are found at 600 and 780 nm.

Thin film, D_2O, and (two temperature) D_2)/ethylene glycol spectra of reduced HiPIP yield essentially the same results. One prominent band is found at 388 nm, with small variations in band position as the solvent is changed. Three less intense bands are found at 590, 700, and 1040 nm. Attempts to locate a band attributable to tetrahedral $Fe(II)S_4$ yielded inconclusive results, as the spectrum of $HiPIP_{red}$ in the 1500-2500 nm region is dominated by vibrational overtones. A difference spectrum ($HiPIP_{red}$ - $HiPIP_{ox}$) in this region failed to reveal any absorptions with $\epsilon > 200$, but a d-d band of

Figure 4. Electronic absorption spectrum of a thin film of $HiPIP_{red}$ at 77°K.

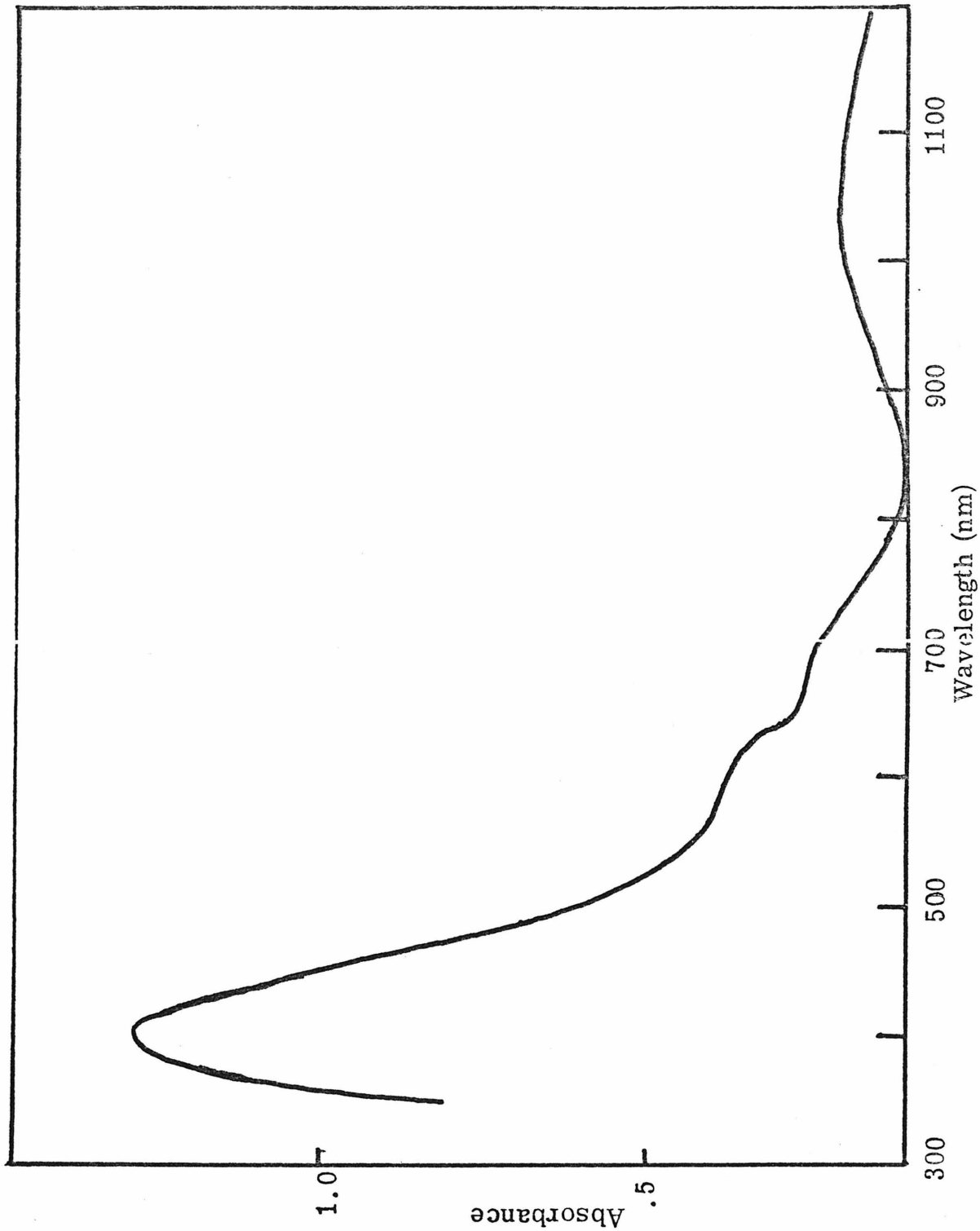
Absorbance
1.0
.5
300
500
700
900
1100
Wavelength (nm)

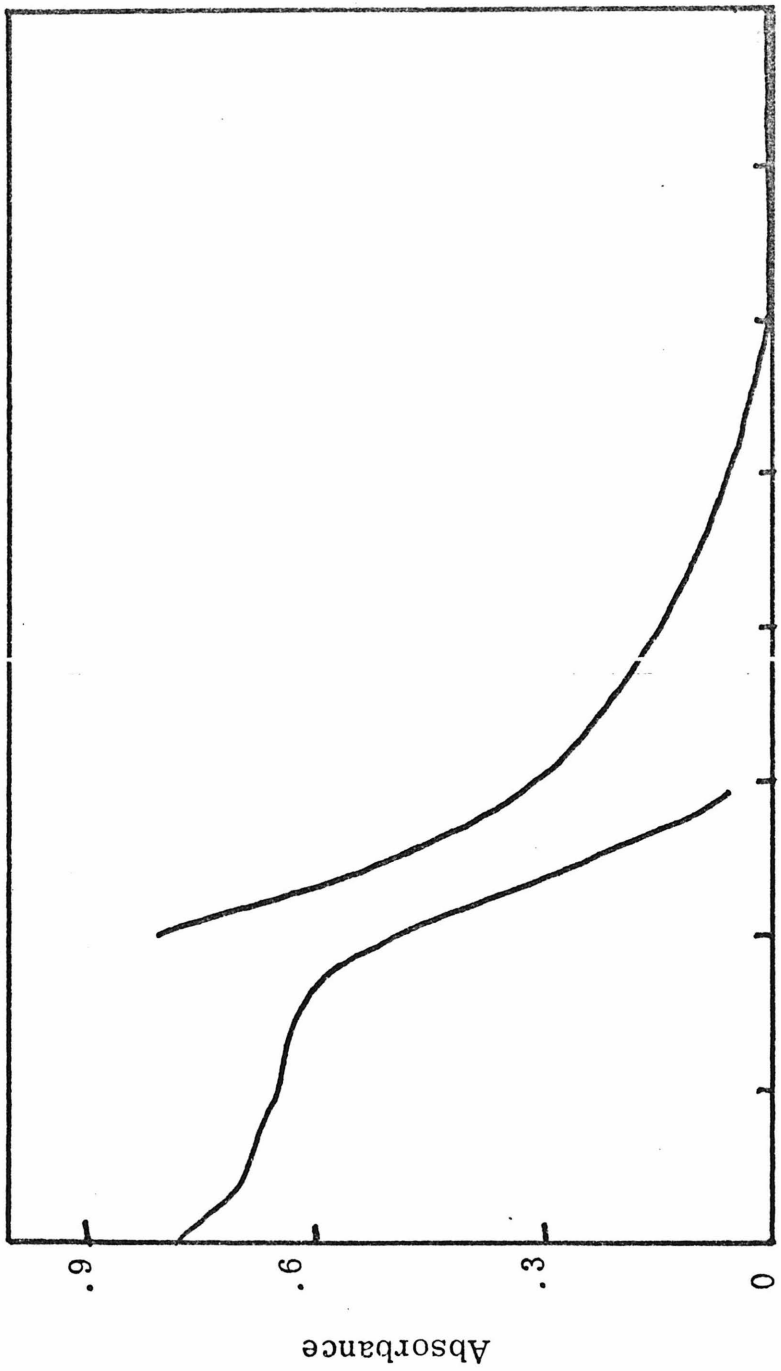

Figure 5. Electronic absorption spectrum of $HiPIP_{ox}$ in a 1:1 ethylene glycol / D_2O glass at 77°K.

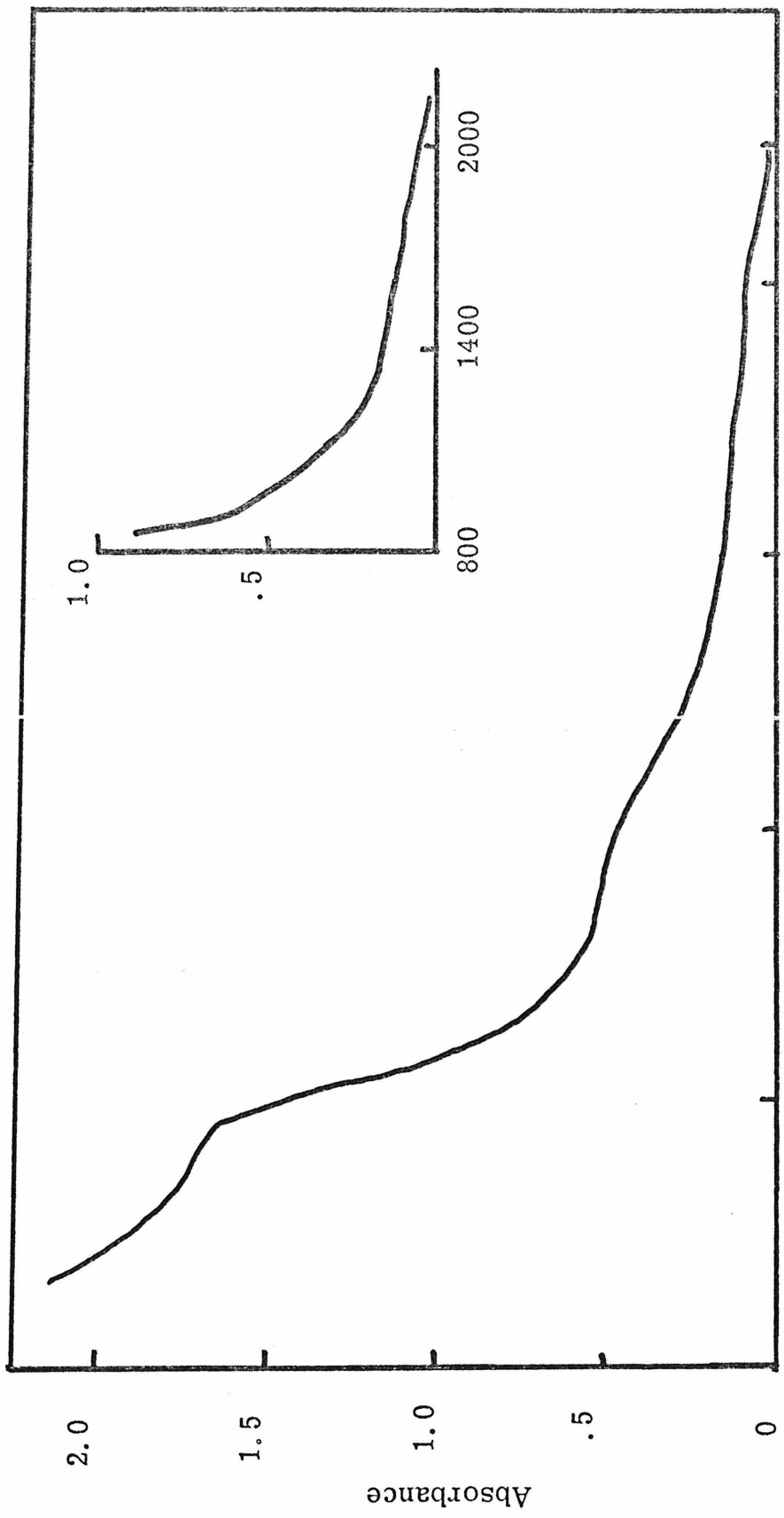

Figure 6. Electronic absorption spectrum of a thin film of $[nPr_4N]_2[Fe_4S_4(SEt)_4]$ at 77°K.

Table I

Spectral Data for Clusters

	λ_{max} (nm)	$\bar{\nu}_{max}$ (cm^{-1})
$HiPIP_{red}$	400	25,000
	590	17,000
	700	14,300
	1040	9,600
$HiPIP_{ox}$	325	30,800
	375	26,700
	450	22,200
$[Fe_4S_4(SCH_2Ph)_4]^{2-}$	429	23,400
	488	20,500
	600	16,700
	780	12,800

moderate intensity could have been masked.

A qualitative comparison between the model and the protein indicates that there must be some differences in the details of the electronic structure of the Fe_4S_4 core in the protein environment. The relatively weak band at 700 nm in $HiPIP_{red}$ is slightly blue-shifted from a similar feature at 780 nm in $(Et_4N)_2[Fe_4S_4(SCH_2Ph)_4]$.[12] More importantly, the broad, low-energy band at 1040 nm appears to have no counterpart in the tetramer. One possibility is that binding the cluster to the protein removes the equivalence of the Fe sites in $[Fe_4S_4(S\text{-}Cys_4)]$. The 1040 nm band could then represent either an intracluster transition between inequivalent Fe sites or possibly one or more d-d excitations at a severely distorted metal center. There is no evidence for a band with $\lambda_{max} > 800$ nm in the thin-film spectrum of $HiPIP_{ox}$ at 77°K. It is possible that on oxidation, with a change of some bond lengths, the core structure is no longer perturbed.

Thus, the magnetic and spectroscopic results confirm a close structural and electronic relationship between $Fe_4S_4(SR)_4^{2-}$ complexes and the $[Fe_4S_4(S\text{-}Cys)_4]$ unit in $HiPIP_{red}$. We conclude that the model and reduced Hi PIP are isoelectronic. However, there is evidence that incorporating the cluster into the protein introduces some inequivalence in the iron atoms. X-ray photoelectron

spectroscopy could provide additional information about the structure of the iron center in the protein environment. Circular dichroism experiments could also provide information about the cluster by identifying low-energy iron (II) d - d bands, if indeed such are present. Experiments along these lines will be required before any more detailed formulations of the electronic structures of the Fe_4S_4 clusters in proteins can be presented.

References

1. T. Herskovitz, B. A. Averill, R. H. Holm, J. A. Ibers, W. D. Phillips, and J. F. Weiher, Proc. Nat. Acad. Sci. U. S., 69, 2437 (1972).

2. B. A. Averill, T. Herskovitz, R. H. Holm, and J. A. Ibers, J. Amer. Chem. Soc., 95, 3523 (1973).

3. R. H. Holm, W. D. Phillips, B. A. Averill, J. J. Mayerle, and T. Herskovits, J. Amer. Chem. Soc., 96, 2109 (1974).

4. B.V. DePamphilis, B. A. Averill, T. Herskovitz, L. Que, Jr., and R. H. Holm, J. Amer. Chem. Soc., 96, 4159 (1974).

5. C. W. Carter, Jr., J. Kraut, S. T. Freer, R. A. Alden, L. C. Seeker, E. Adman, and L. H. Jensen, Proc. Nat. Acad. Sci. US., 69, 3526 (1972).

6. E. T. Adman, L. C. Sieker, and L. H. Jensen, J. Biol. Chem., 248, 3987 (1973).

7. R. H.Holm, B. A. Averill, T. Herskovitz, R. B. Frankel, H. B. Gray, O. Siiman, and F. J. Grunthaner, J. Amer. Chem. Soc., 96, 2644 (1974).

8. T. H. Moss, D. Petering, and G. Palmer, J. Biol. Chem., 244, 2275 (1969).

9. G. Palmer, H. Brintzinger, R. W. Estabrook, and R. H. Sands, in Magnetic Resonance in Biological Systems, A. Ehrenberg, B. G. Malmstrom, and T. Vanngard, eds., Pergamon Press, Oxford, New York, 1967, p. 159.

10. K. Dus, H. DeKlerk, K. Sletten, and R. G. Bartsch, Biochim. Biophys. Acta., 140, 291 (1967).

11. R. Cammack, Biochem. Biophys. Res. Commun., 54, 548 (1973).

12. W. D.Phillips, M. Poe, C. C. McDonald, and R. G. Bartsch, Proc. Nat. Acad. Sci. U. S., 67 682 (1970).

13. M. C. Evans, D. O. Hall, and C. E. Johnson, Biochem. J., 119, 289 (1970).

14. S. K. Bose, in Bacterial Photosynthesis, H. Gest, A. San Pietro, and L. P. Vernon, eds., Antioch Press, Yellow Springs, Ohio, 1963, p. 501.

15. R. G. Bartsch, in Bacterial Photosynthesis, H. Gest, A. San Pietro, and L. P. Vernon, eds., Antioch Press, Yellow Springs, Ohio, 1963, p. 315.

16. R. G. Bartsch, in Methods in Enzymology, A. San Pietro, ed., Vol. 23, Part A, Academic Press, New York, 1971, p. 644.

17. H. E. Hoenig, R. H. Wang, G. R. Rossman, and J. E. Mercereau, Proc. Applied Superconductivity Conf. (Annapolis, Md., May 1-3, 1972), p. 570.

CHAPTER III

KINETIC STUDIES OF HIPIP AND FERREDOXIN WITH INORGANIC REAGENTS

INTRODUCTION

Iron sulfur proteins are involved in a wide variety of electron-transfer reactions.[1,2] The soluble spinach ferredoxin functions in photosystem I to reduce $NADP^+$, using a flavoprotein as a catalyst. The ferredoxin from C. pasteurianum reduces nitrogenase, which itself contains iron-sulfur components. The function of the Chromatium protein (HiPIP) is not known. However, it does undergo photooxidation when the bacterium is exposed to light, thus suggesting that it participates in the photosynthetic electron-transfer chain of the Chromatium organism.[3] Many other proteins involved in redox processes also contain non-heme iron.[2] An iron-sulfur protein is part of the coenzyme Q-cytochrome c reductase complex of the electron-transfer chain of mitochondria. Xanthine oxidase, catalyzing the conversion of xanthine to uric acid, contains molybdenum and flavin adenine dinucleotide (FAD) as well as iron and sulfur. Thus, these proteins are very important in biological electron-transfer reactions.

However, very little information is available concerning the mechanisms of these reactions. Redox reactions between many pairs of metal complexes have been classified as either of the inner or the

outer sphere type,[4, 5] but it remains to be seen whether electron transfer between two metalloproteins can be so simply described. At the very least, though, we can expect to recognize many of the elementary steps of ordinary inner and outer sphere processes. For this reason, it is appropriate to review briefly the principal features of such processes.

Inner Sphere Reactions

Inner sphere reactions require substitution into the coordination sphere of one of the reactants. Thus, one of the reactants must be relatively substitution labile, or at least capable of expanding the coordination sphere to accommodate a bridging ligand. Formation of the precursor complex is followed by an activation process, in which the inner coordination sphere as well as the solvent reorganizes.[6] Electron transfer can then occur, presumably involving the bridging ligand. Breakdown of this bridged successor complex must then occur. Thus, the rate of the reaction can be governed by the rate of substitution or the rate of breakdown as well as the rate of the intramolecular electron transfer.

Some characteristics of inner sphere reaction mechanisms have been worked out for many inorganic reactants.[7, 8] An inner sphere mechanism has often been established by the identification of

products. For example, in the reaction of chloropentaammine-cobalt(III) with aquo chromium(II), the product is chlorochromium(III), thus indicating a precursor complex with a chloride bridge. Another indication of inner sphere pathways with aquo complexes can be a sharp increase in rate on raising the pH, since a hydroxide ligand is a much more effective bridging ligand than is water. The relative effect of azide vs. thiocyanate on the reaction rate can also indicate inner sphere mechanisms, since the transfer of the unsymmetrical SCN^- group in an inner sphere reaction may yield a product in which the "wrong end" of the bridging ligand is attached to the metal center. Thus, the N_3 reaction would be faster.

Another indication of an inner sphere reaction mechanism may exist if the rate of the redox reaction is similar to the rate of the substitution reaction on one metal center. This indicates that the formation of the precursor complex is rate limiting. This situation often occurs with V^{2+} reactions.

It is possible that an inner sphere reaction mechanism exists for the iron-sulfur proteins, with a sulfur of the protein metal center acting as a bridging ligand. It has been demonstrated that sulfur ligands can function as bridging ligands, often much more effectively than the oxygen analog.[9] In such cases, the sulfur compound's reactivity is attributed to the ease with which the metal-ligand bond

could be stretched and to the greater covalency of the bond. Thus, relatively rapid inner sphere reactions of iron-sulfur proteins could occur with reactants that are substitution labile.

Some inorganic complexes are not very labile and cannot increase their coordination number. An inner sphere pathway would then depend on the protein's ability to provide a site for the bridging ligand from the other metal. In cases when the protein metal center cannot coordinate another ligand, an outer sphere mechanism is required. It is also always possible that an outer sphere reaction mechanism would be a lower energy path than the corresponding inner sphere path.

Outer Sphere Reactions

Outer sphere reactions do not involve bond breakage or formation. However, an outer sphere reaction follows a sequence very similar to that of an inner sphere reaction.[6] The two components form a precursor complex which is then activated. Electron transfer occurs which is followed by deactivation and separation of the product species. Several factors are important in determining the rates of exchange reactions. These include the interaction energy, the precursor complex stability, the inner shell reorganization energy, and the solvent reorganization energy.[10]

The probability of electron transfer in the transition state increases with the interaction energy and the interaction energy is increased as the amount of overlap between the redox orbitals is increased. Thus, a closer approach of reactants having orbitals of similar symmetry with no change in spin multiplicity favors reaction.[10] The formation of the precursor complex depends on electrostatic forces and thus should be dependent on the charge type of the reactants. Complex formation is reflected by the ionic strength dependence. The inner sphere reorganization energy depends on the bond distances and force constants of the reactants. Thus, a large change in bond distance will mean a large reorganization energy.[10]

For a cross reaction, or a reaction with a net chemical change, the free energy change of the reaction also influences the rate. Marcus has developed a number of relationships relating the free energies of activation and rate constants of the exchange reactions with similar quantities for the cross reaction.[11,12] The basic relation is: $\Delta G^*_{12} = \left(\frac{\Delta G_1^* + \Delta G_2^*}{2}\right) + \frac{\Delta G^0_r}{2} + \frac{(\Delta G^0_r)}{8(\Delta G_1^* + \Delta G_2^*)}$, with ΔG^0_r the free energy change for the cross reaction when the reactants are a distance r apart. If the precursor and successor complexes have similar stabilities, one can derive the relation that $k_{12} = (k_1 k_2 K_{12} f)^{1/2}$, with $\log f = (\log K_{12})^2 / [4 \log(K_1 K_2 / Z^2)]$ and K_{12} the equilibrium constant for the reaction.[10,13]

Thus, the rate of electron transfer in a cross reaction is governed by an intrinsic factor and a thermodynamic factor. The intrinsic factor depends on the properties of each reactant and is related to the self-exchange rates.

A linear relation for a series of related reactions is often observed between the free energies of activation and the standard free energy change for the electron-transfer step, as predicted by the theory.[13] However, some complexes do not follow the expression for the rate constant. Some of these discrepancies may result from the differing stabilities of the precursor complexes. The formation of an unusually stable precursor complex may be reflected by the enthalpy of activation, since the enthalpy of formation of the precursor complex contributes to the observed enthalpy of activation.[10] Thus, very small or even negative $\Delta H^{\ddagger}$ can be observed if the precursor complex formation has a large negative enthalpy of formation.[14]

Other deviations from Marcus theory can be explained because of spin multiplicity restrictions or other non-adiabatic reaction mechanisms. In a non-adiabatic reaction, the probability that the reactants will be converted to products in the transition state is less than unity.[10] Some of these reactions can be considered to be following an electron tunneling mechanism in which the electron tunnels from one reactant to the other through a large distance.

The sequence of steps for this mechanism are very similar to that of an ordinary outer sphere reaction.[15] The reactants form a complex which is then activated, presumably with the two redox orbitals becoming equal in energy. Electron transfer then occurs, followed by deactivation and separation of the product complex. However, in this case, because of the large separation of the reactants, the interaction between the two redox orbitals is small. Thus, the probability that the electron will transfer in the activated complex is diminished, or the transmission coefficient κ becomes less than unity. Unusual values of $\Delta S^{\ddagger}$ may then be found for electron tunneling reactions because κ is considered to be unity when calculating the activation entropy from the expression $k = \frac{\kappa k_B T}{h} e^{-\Delta H^{\ddagger}/RT} e^{\Delta S^{\ddagger}/R}$.[16] Thus, a very low $\Delta S^{\ddagger}$ may be expected from the conventional calculation if tunneling is occurring.

The problem of electron transfer through large distances in proteins has been treated by Bennett[15] as a one-dimensional tunneling of a particle from the activated reactant complex to the products. The equations that describe this are similar to those of a particle in a finite-walled box. The probability of electron transfer is related to the barrier height, B and width, X; $p = \exp[-\frac{2}{\hbar}(2mB)^{1/2}X]$, where m is the mass of the electron. Barrier widths for proteins would be approximately 3-12 Å, while barrier heights would relate to the ease of

reducing the organic groups of the protein, with values for various groups approximately -3 eV. Rates calculated with these estimations range from 10^3 to 10^{10} sec^{-1} which are in line for expected electron-transfer rates.[15]

Protein Influences

Other questions may arise with metalloprotein reactions that are not important in metal complex reactions. Although the protein may have a small net charge, the protein can provide large local concentrations of charge and a variety of coordinating ligands. Thus, complex formation between the protein and the other reactant may be very favorable, and the reaction may appear to involve two highly charged species. The ionic strength dependence of the rate and the rate law may reflect this charge behavior.

The protein could also impose steric limitations on the path by making it difficult for the reactant to approach the metal center, as noted earlier; reaction may then occur by electron tunneling. Alternately, the protein may show a step in the reaction pathway with the metal center becoming more available to solvent. It has also been suggested that other amino acids could facilitate electron transfer to sterically inaccessible metal centers.[17] A reaction pathway in which the first step is the discrete transfer of an electron to an aromatic residue can

be proposed as a possible mechanism for some of the iron-sulfur proteins. For example, the C-13 nmr of bacterial ferr indicates that some electron density from the iron-sulfur cluster has been transferred to a tyrosine residue.[18] Thus, some overlap of iron-sulfur and aromatic orbitals must occur, perhaps making it possible for the tyrosine to participate in electron transfer.

Other factors which may influence protein reactivity include conformational changes.[2] Possible conformational differences between the oxidized and reduced protein may impose limitations on the reaction. The medium may also have an effect on the reaction, since different protein conformations may exist under different conditions of pH, ionic strength, or buffer composition.

Previous Kinetic Studies

Information on the reaction kinetics of simple iron-sulfur proteins has been limited to one report on rubredoxin.[19] The X-ray structure of this protein indicates that the metal center is exposed to the solvent.[20] The center, a distorted tetrahedron, undergoes very little change in geometry on reduction (bond lengths change by less than .1 Å). The rate constant for reaction with $Ru(NH_3)_6^{2+}$, an outer sphere reductant, is 9.5×10^4 M^{-1} sec^{-1}, indicating a high reactivity for rubredoxin. Reaction with $V(H_2O)_6^{2+}$ ($k = 1.6 \times 10^4$ M^{-1} sec^{-1}) and

$Cr(H_2O)_6^{2+}$ (1.2×10^3 M^{-1} sec^{-1}) also probably proceed by outer sphere mechanisms, even though the possibility exists with Cr^{2+} for an inner sphere mechanism. The activation enthalpies for these reactions are very small (0-1 kcal/mole). This low enthalpy barrier probably reflects the small reorganization of the coordination sphere needed during activation. The reaction is thus controlled by the activation entropy (-30 to -44 eu).

Little information is available to predict the reactivity of more complicated iron-sulfur proteins. The two-iron and four-iron proteins differ greatly in electronic structures and redox potentials[21] and thus might differ considerably in their reactivity patterns. Studies on xanthine oxidase are numerous but have been severely handicapped in the past by impure samples of protein. These studies have primarily been concerned with the sequence of electron flow between the components of the protein. Recent work[2] indicates that the molybdenum transfers the reducing equivalents to the iron-sulfur and flavin components. The iron-sulfur component has a reactivity approximately equal to that of the overall catalytic activity of the protein; the iron-sulfur unit is reduced with a $t_{1/2}$ of 40 msec. It has been suggested that the oxidation of this reduced protein occurs by interaction of oxygen and flavin without directly involving the iron. Thus, although there is some understanding of the electron flow in this enzyme, little information about the inorganic mechanistic details exist.

It is apparent that much more detailed information is needed to elaborate the reaction pathways employed by the iron-sulfur proteins. We have approached this question by studying the reactions of the proteins with some well-understood inorganic reagents. By obtaining kinetic parameters for these reactions, we should be able to decide if the mechanisms are of the inner sphere or outer sphere type. We may also be able to elucidate any special effects attributable to protein structural features.

Experimental Section

Materials and Methods:

Reagent grade chemicals were used without further purification. Distilled deionized water was used in making solutions.

Crystals of $Na(FeEDTA) \cdot 3\,H_2O$[22] and of $Fe(HEDTA) \cdot 1\frac{1}{2}\,H_2O$[23] were prepared as described by Schugar (EDTA = ethylenediaminetetracetate and HEDTA = N-hydroxy ethylethylenediaminetriacetate). Standard solutions for kinetics work were prepared from weighed samples and analyzed by iodometry;[24] less concentrated solutions were prepared by dilutions.

$K_3Fe(CN)_6$ solutions were prepared from weighed samples; concentrations were checked by absorbance measurements at 420 nm (ϵ=1033).[25]

Standard solutions of Fe^{2+} were prepared by dissolving iron wire in a twofold excess of hydrochloric acid. These solutions were analyzed by the ceric method, using ferroin as an indicator.[26] An aliquot of the Fe^{2+} solution was transferred to a solution containing buffer, a 20% excess of Na_2H_2EDTA, and enough base to neutralize the excess acid. Other solutions were obtained by dilution. These solutions contained a 0.05 M potassium phosphate buffer and enough

sodium chloride to keep the ionic strength constant at 0.1. The pH was adjusted when necessary by addition of small amounts of acid or base. The pH was monitored by using a Brinkmann pH 101 meter with a Brinkmann glass combination electrode. All of these operations were carried out under a nitrogen atmosphere; the nitrogen was passed through two chromous towers before being bubbled gently through all buffer solutions. Hamilton air-tight syringes and standard syringe techniques were used.

$[Co(phen)_3]Cl_3 \cdot 7H_2O$ was synthesized by refluxing $[(NH_3)_5CoCl]Cl_2$ obtained from Alfa Inorganics with 1,10-phenanthroline for 5 hours.[27] This solution was then oxidized with chlorine. The isolated crystals were then characterized spectrally in the region 380-220 nm. Concentrations of solution used for kinetics were determined by optical absorbance at 350 nm (ϵ = 3700 M^{-1} cm^{-1}) and 330 nm (ϵ = 4680 M^{-1} cm^{-1}).[28]

The iron-sulfur proteins were prepared as described previously. Protein solutions for the kinetic measurements were made by dialyzing the protein against the desired buffer. The solutions were then diluted to the desired concentration with buffer; concentrations were established by optical measurements (420 nm ϵ = 9400 for ferrodoxin[29] and 388 nm ϵ = 16,100 for HiPIP).[3]

For work at variable temperature using Tris buffers, separate protein solutions were prepared for every temperature. The protein was dialyzed against a Tris buffer chosen so that the pH of this buffer would be 7.8 at the temperature desired.

The ferredoxin solutions were reduced under a nitrogen atmosphere by using 0.1 ml of a standardized $Na_2S_2O_4$ solution. The dithionite solution was standardized by reaction with $K_3Fe(CN)_6$. The amount of $Na_2S_2O_4$ was adjusted so that there was a 20% excess of reducing agent. Typically, however, as judged by the absorbance change, only 80% of the ferredoxin was reduced. Presumably, some of the reduced ferredoxin reacted with trace amounts of oxygen present.

Complete reduction of HiPIP was assured by adding a few drops of mercaptoethanol, followed by dialysis against the desired buffer. Oxidation of HiPIP was accomplished by passing a concentrated, low ionic strength ($\mu = 0.001$) solution of protein through a small Bio-Rad Ag 1X-8 column charged to 50% of capacity with $Fe(CN)_6^{3-}$.[3] Negligible amounts of $Fe(CN)_6^{3-}$ were eluted from the column if low ionic strength solutions were used. Enough NaCl was then added to bring up the ionic strength to 0.1. The protein was then diluted with potassium phosphate buffer of ionic strength 0.1.

Titrations were performed on the Cary 17, using the 0 – .2 OD slide wire.

Nitrogen was carefully bubbled through all solutions for 45 minutes prior to measurement. Traces of glucose oxidase and glucose were added to solutions in certain control experiments to insure completely anaerobic conditions; no significant differences in the kinetic results were found in these cases.

Most solutions were stored in nitrogen-purged, serum-capped bottles. They were then transferred from the serum bottles to the stopped-flow drive syringes by means of stainless steel needles and teflon tubing with Hamilton fittings connected to the inlet port. The work with $Co(phen)_3^{3+}$ was done using an all-glass system. The $Co(phen)_3^{3+}$ solution was stored in serum-capped, round-bottom flask fitted with a nitrogen inlet tube and a glass luer-lock fitting. Solutions were then transferred to the stopped-flow apparatus through teflon tubing connected to the inlet port.

Stopped-Flow Spectrophotometer

Kinetic measurements were made on a Durrum Model D-110 stopped-flow spectrophotometer. The Durrum uses a Kel-F flow system with a 2 cm path length. A tungsten lamp, with a Power/Mate power supply, was the light source. A Kepco Model ABC 1500/M power supply was used for the photomultiplier tubes.. The Durrum has glass drive syringes fitted with O-ring seals to insure a water-tight fit. Temperature was controlled with circulating water from a Forma

Scientific temperature control unit.

Analysis of Data

Absorbance changes as a function of time were displayed on a Tektronix 564 B oscilloscope. The earlier data were recorded by taking pictures of the oscilloscope trace; data points were then obtained by measuring these pictures. Plots of log $(A_t - A_\infty)$ vs t were made to verify first-order dependence; the pseudo first-order rate constant was obtained from the slope of the line determined by a linear least-squares method.

Later data were taken by use of an analog input buffer in conjunction with the PDP-10 computer. These data were recorded, plotted, and computed using the program "IDC".

With several of the fast reactions, when only a small excess of the reagent could be used, the data were also calculated in terms of a second-order reaction. The rate equation in this case is $\frac{1}{B_0 - A_0} \ln \frac{A_0 B}{B_0 A} = kt$, and k is determined from the slope of the line log B/A vs t, where A and B are the reactants. With second-order conditions, a slight distortion is obtained in the absorbance because of the finite flow deadtime of the system.

Alternately, as has been found by Corbett,[30] a reaction with only a twofold excess of one reagent can be treated as a pseudo first-

order reaction, with an error in the calculated k of less than 2% for 60% conversion. For the fastest reactions, this is well in line with experimental error, and thus, most of these data were treated this way.

RESULTS

Ferredoxin

Adding one equivalent of $FeEDTA^-$ to a solution of reduced ferredoxin restores the spectrum of the oxidized ferredoxin solution. This establishes a one-electron process and also indicates that the protein is not denatured by this reagent.

The reaction was found to follow pseudo-first-order kinetics when the oxidizing agent was in excess ($-\frac{d[Fd]}{dt} = k_{obs}[Fd]$). A typical curve of the progress of the reaction is shown (Figure 1), as well as a plot of log $(A_t - A_\infty)$ vs. t (Figure 2). This plot was usually linear for $\geq 90\%$ of the reaction. Duplicate reactions were performed, with good agreement found in k_{obs}. Nearly the same rate was found for the alfalfa protein as for the spinach protein ($k_{obs,\,spinach} = 54\ sec^{-1}$, $k_{obs,\,alfalfa} = 53\ sec^{-1}$). Most work was done at 465 nm. However, the reaction rate was the same at 420 and 540 nm.

A plot of the pseudo-first-order rate constant vs. concentration of oxidizing agent is linear (see Figure 3). This indicates the reaction is first order with respect to oxidizing agent ($\frac{d[Fd]}{dt} = k_1[Fd][FeEDTA^-]$). The reaction was found to be very fast; the second-order rate constant is $3.4 \times 10^5\ M^{-1}\ sec^{-1}$ ($\mu = .1$, pH = 7.8, T = 12.5°). Thus, only a limited concentration range for the oxidizing agent could be studied.

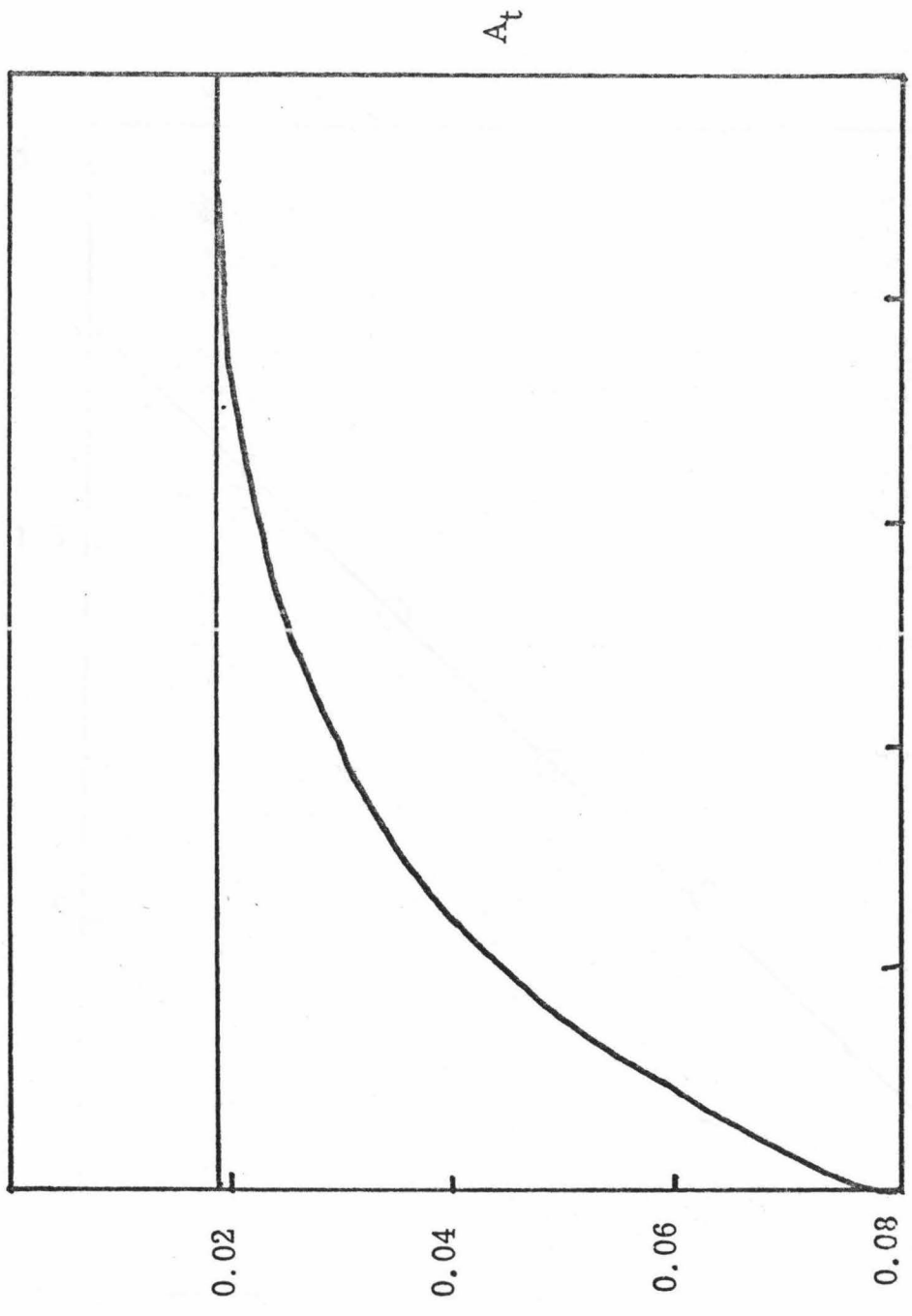

Figure 1. Typical Oscilloscope Trace Showing Absorbance vs. Time for the Reaction of Ferredoxin and $FeEDTA^-$ (25.5 °C, $\mu = 0.1$ Tris-Cl, pH 7.2 $[FeEDTA^-] = 1.9 \times 10^{-4}$ M, $[Fd] = 10^{-5}$ M).

Figure 2. Typical plot of log $(A_t - A_\infty)$ vs. t for the Reaction of Ferredoxin with $FeEDTA^-$ (25.5 °C, $\mu = 0.1$ Tris-NaCl, $[FeEDTA^-] = 1.9 \times 10^{-4}$ M, $[Fd] = 10^{-5}$ M).

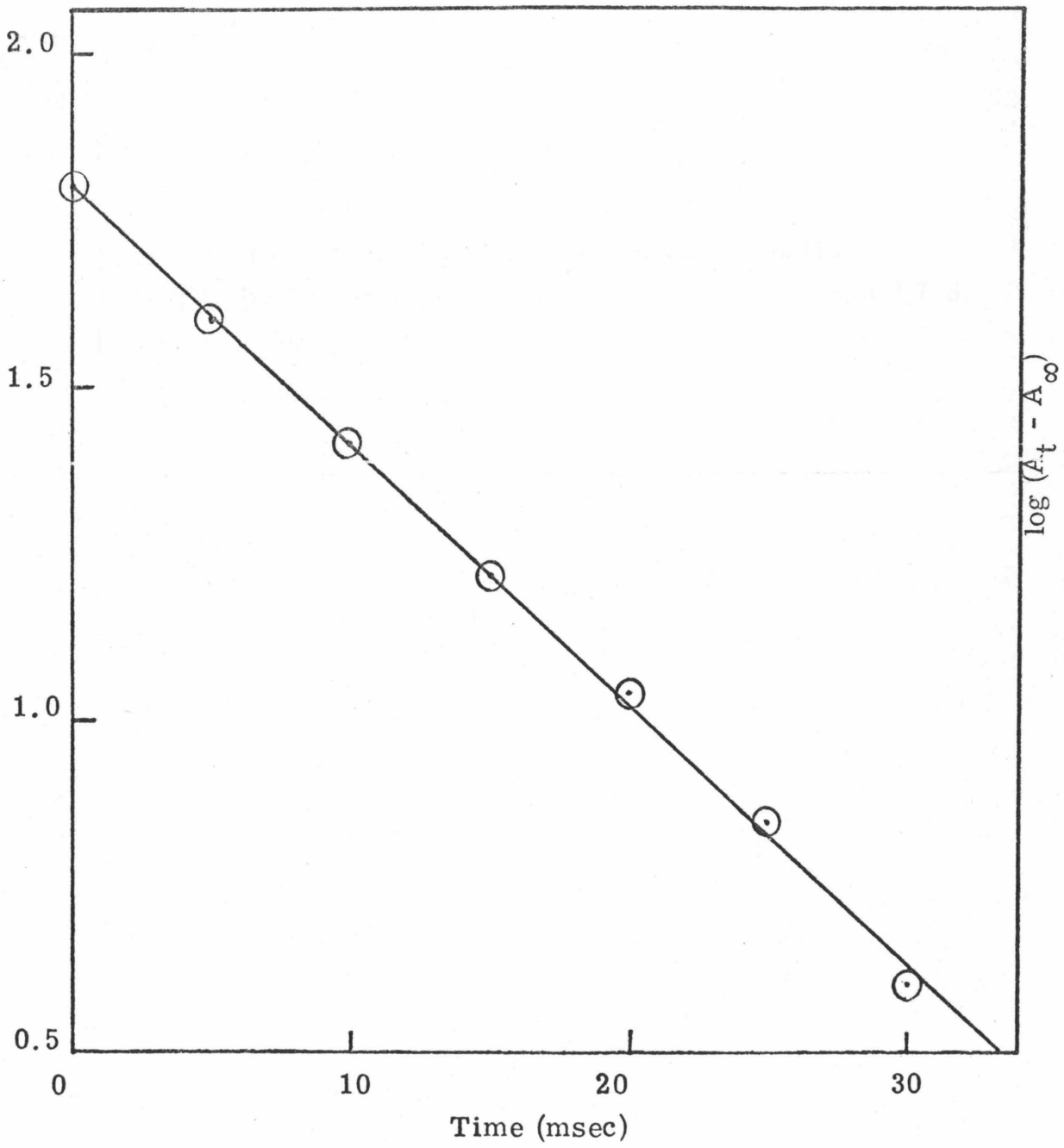

Figure.3. Observed Rate Constants for the Reduction of $FeEDTA^-$ by Ferredoxin (12.5 °C, $\mu = 0.1$ Tris-Cl, pH 7.8, $[Fd] = 10^{-5}$ M).

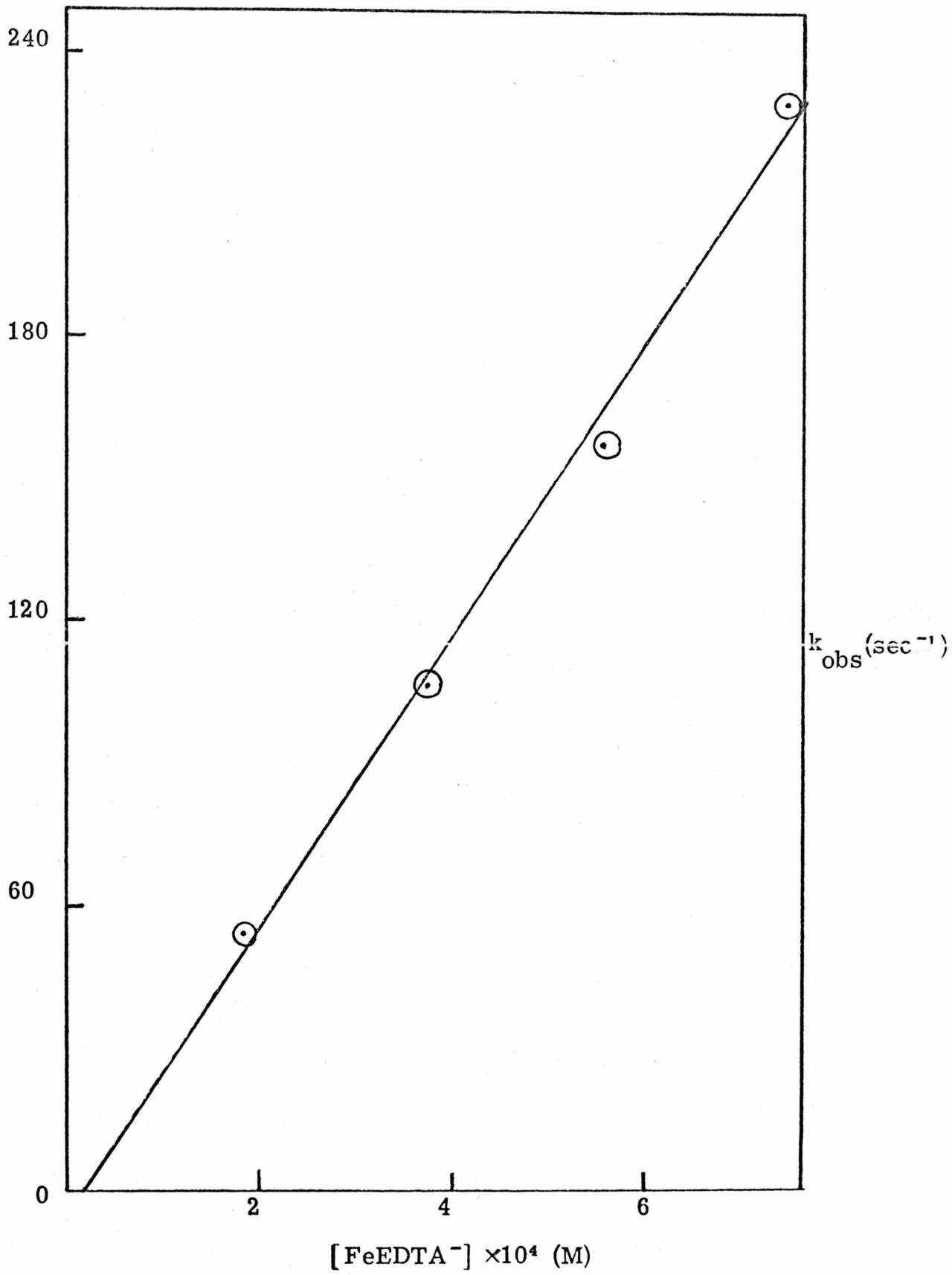
240
180
120
60
0
2
4
6
$k_{obs}(sec^{-1})$
[FeEDTA$^-$] ×10^4 (M)

By changing the ligand to HEDTA, a tenfold drop in the pseudo-first-order rate constant was observed. This slower rate allowed a wider concentration range to be studied ($2 \times 10^{-4} \leq c \leq 2 \times 10^{-3}$ M). No evidence for rate saturation was observed. The second-order rate constant is 2.5×10^{4} M^{-1} sec^{-1} (.1 μ Tris-Cl, pH 7.8, 26°). These data are collected in Appendix I.

The rate of the reaction was found to be nearly independent of temperature for both $FeEDTA^-$ and $FeHEDTA^-$. Standard Eyring plots of log k/T vs. 1/T were found to be linear over the narrow temperature range of protein stability (see Figure 4 and Appendix I). Linear least-squares analysis of the data gives the slope of this line, which is related to the activation enthalpy. The activation parameters for oxidation by $FeEDTA^-$ are $\Delta H^{\ddagger}$ = +.7 kcal mole and $\Delta S^{\ddagger}$ = -31 eu, while parameters for $FeHEDTA^-$ are $\Delta H^{\ddagger}$ = +.3 kcal/mole and $\Delta S^{\ddagger}$ = -37.2 eu.

The reaction of ferredoxin with $FeEDTA^-$ was studied in the pH range 6.7 to 9. A tenfold increase in rate was observed as the pH was lowered. In the pH range 6.7 to 8, a plot of log k_{obs} vs. pH was linear. In the pH range 8 to 9, the rate was further decreased by increased pH. The ionic strength dependence of this reaction was studied over a wide range; rates were found to increase as the ionic strength was raised. These plots are available (Appendix I).

Figure 4. Eyring plot for the reaction of ferredoxin with $FeEDTA^-$ (μ= 0.1 Tris-Cl, pH 7.8, $[FeEDTA^-] = 1.9 \times 10^{-4}$ M, $[Fd] = 10^{-5}$ M).

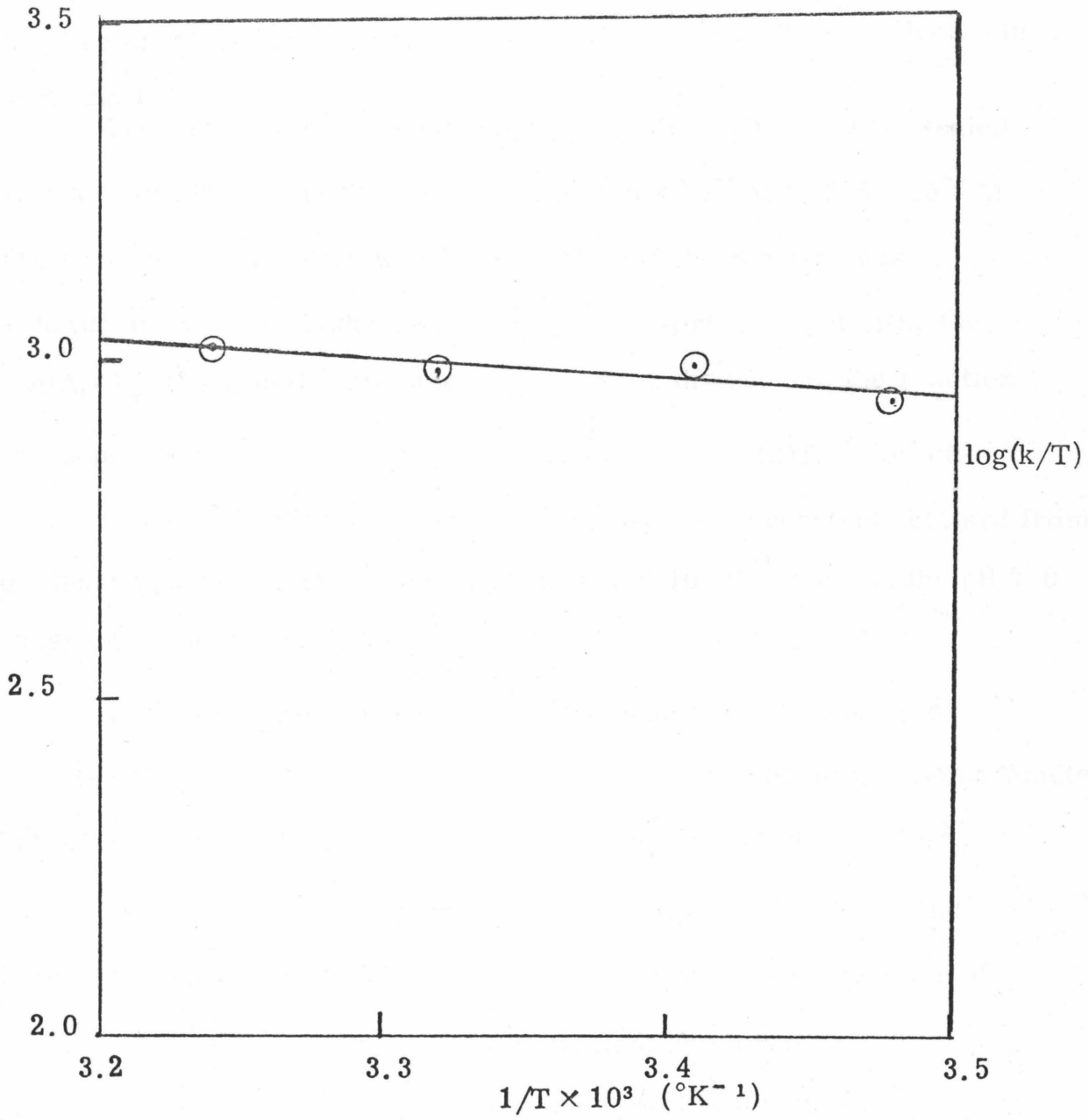

HiPIP

The reactions of high potential iron protein with three inorganic reagents were studied; reagents were chosen so that both the oxidation and reduction of the protein could be followed. Typical examples of the data are presented here, while the remainder of the data is collected in Appendix I.

The reaction of the oxidized protein with $FeEDTA^{=}$ was studied over a $FeEDTA^{=}$ concentration range of 1.5×10^{-4} M to 2.5×10^{-3} M. The protein concentration was 5×10^{-6} M, and the reaction was followed at 480 nm. Under these pseudo-first-order conditions, the $\log(A_t - A_\infty)$ vs. t plots were linear for greater than 90% of the reaction The dependence of the observed rate constants on $FeEDTA^{=}$ concentration is shown in Figure 5. The second-order rate constant obtained from the least-squares slope of these data is 1.7×10^{3} M^{-1} sec^{-1} in the pH 7.0 phosphate-chloride buffer.

The temperature dependence of the reaction was analyzed in terms of a standard Eyring plot (see Figure 6); the activation parameters obtained from the slope are $\Delta H^{\ddagger}$ = +.4 kcal/mole and $\Delta S^{\ddagger}$ = -41 eu.

The oxidation of the protein was studied using $Fe(CN)_6^{3-}$ and $Co(phen)_3^{3+}$. Judging by the observed absorbance change, reaction of HiPIP with $Fe(CN)_6^{3-}$ involved one equivalent and left the protein intact, in contrast to the $Fe(CN)_6^{3-}$ reaction with ferredoxin, which resulted in complete loss of the visible ferredoxin spectrum.It was also observed that after several hours, solutions of

Figure 5. Observed Rate Constants for the Reduction of HiPIP by $FeEDTA^{2-}$ (25 °C, $\mu = 0.1$ phosphate-NaCl, pH 7.0, $[HiPIP] = 8.1 \times 10^{-6}$ M).

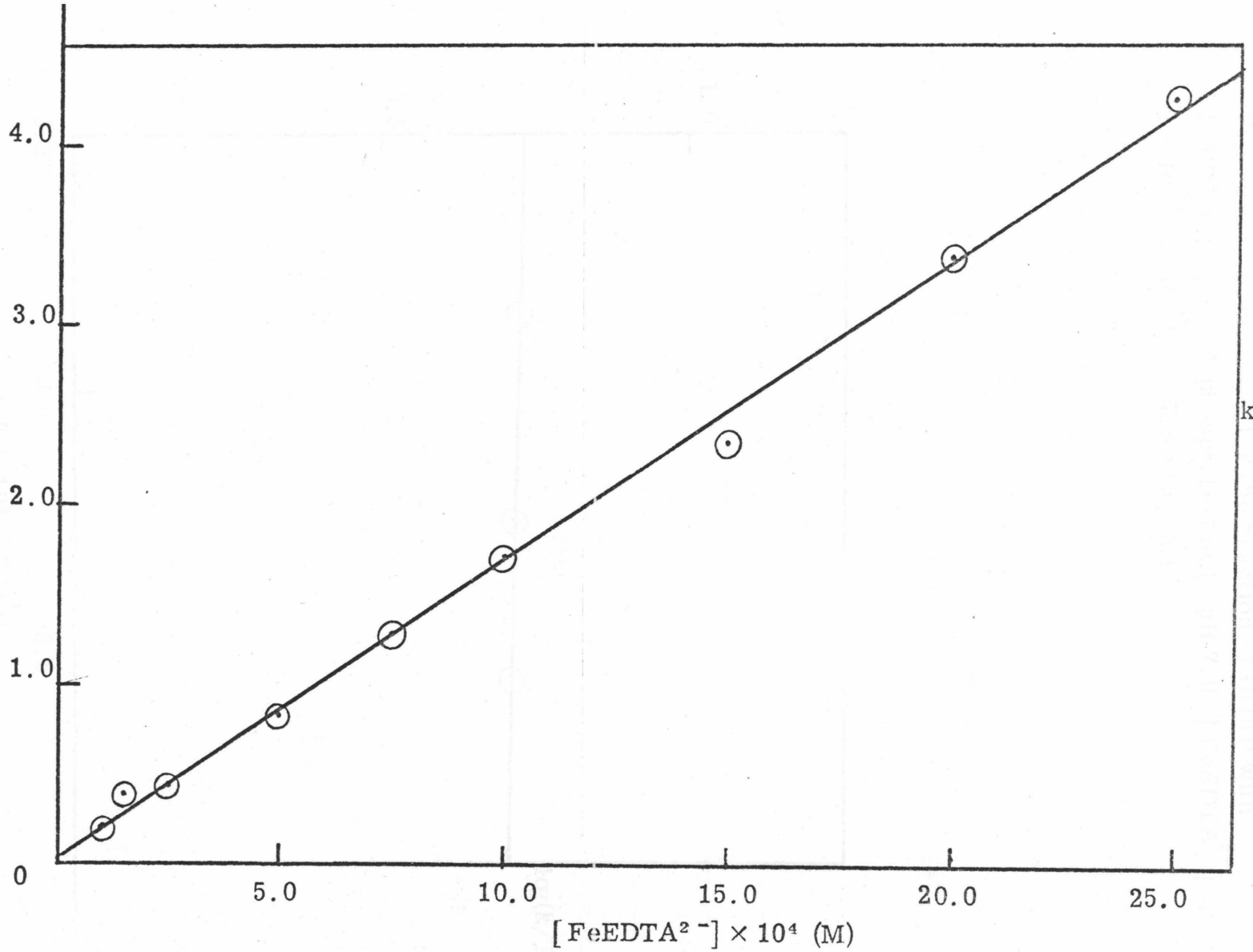
4.0
3.0
2.0
1.0
0
5.0
10.0
15.0
20.0
25.0
$k_{obs}(sec^{-1})$
$[FeEDTA^{2-}] \times 10^4$ (M)

Figure 6. Eyring plot for the reaction of HiPIP with $FeEDTA^{2-}$ ($\mu = 0.1$ phosphate-NaCl, pH 7.0, $[FeEDTA^{2-}] = 5 \times 10^{-4}$ M, $[HiPIP] = 7.5 \times 10^{-6}$ M).

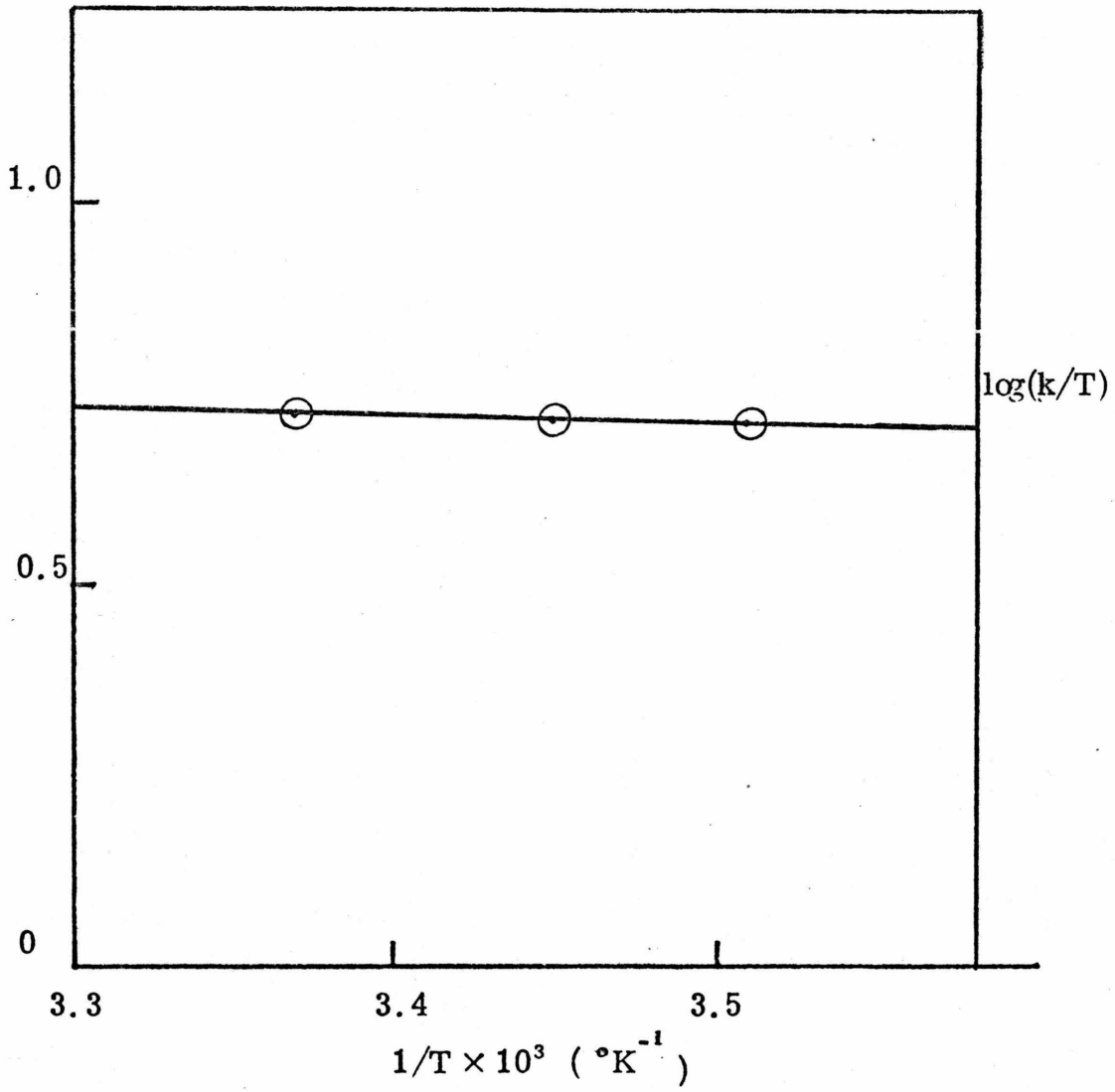

HiPIP mixed with large excesses of $Co(phen)_3^{3+}$ turned pinkish, perhaps indicating that the phenanthroline complex had pulled the iron out of the protein. However, this is not expected to interfere with the observed kinetics, since the denaturation reaction is much slower than the oxidation. The observed absorbance change during the kinetics experiment agreed well with the change expected for protein oxidation, while a different absorbance change would be expected if the protein were denaturing during the redox reaction.

Under pseudo first-order conditions, a plot of the log $(A_t - A_\infty)$-time data for both reactions is linear. Both of these reactions show a first-order dependence of rate constants on the oxidant concentration over a fairly wide range; for $Fe(CN)_6^{3-}$, this range was a 20 to 1000 fold excess. No rate saturation was observed with any of these reagents. All data are given in Appendix I.

Second-order rate constants obtained by least-squares analysis at 25°, pH 7 are 2.4×10^3 M^{-1} sec^{-1} for reaction with $Fe(CN)_6^{3-}$ and 2.8×10^3 M^{-1} sec^{-1} for reaction with $Co(phen)_3^{3+}$. The Eyring plots for these reactions are linear over the narrow temperature range studied. Activation parameters obtained from least-squares analysis of the Eyring plot are $\Delta H^{\ddagger} = -.2$ kcal/mole and $\Delta S^{\ddagger} = .44$ eu for reaction with $Fe(CN)_6^{3-}$. For reaction with $Co(phen)_3^{3+}$, $\Delta H^{\ddagger} =$

14 kcal/mole and $\Delta S^{\ddagger} = +4.2$ eu.

The pH dependence of the reaction with $Co(phen)_3^{3+}$ was studied in the range 5.2 to 8. A small increase in rate was observed as the pH was raised.

The second order rate constants and the activation parameters for all of the reactions studied here are summarized in Table I.

Table I

Comparison of Reactions

Protein	Reactant	k_1 (M^{-1} sec^{-1})	$\Delta H^{\ddagger}$ (kcal/mole)	$\Delta S^{\ddagger}$ (e.u.)
Red Fd	$FeEDTA^-$	3.4×10^5	+ 0.7	-31
Red Fd	FeHEDTA	2.5×10^4	+ 0.3	-37
Ox HiPIP	$FeEDTA^{2-}$	1.7×10^3	+ 0.4	-41
Red HiPIP	$Fe(CN)_6^{3-}$	2.4×10^3	- 0.2	-44
Red HiPIP	$Co(phen)_3^{3+}$	2.8×10^3	+14	+ 4.2

DISCUSSION

The rates of reaction of ferredoxin and HiPIP with the inorganic reagents ($Fe(CN)_6^{3-}$, $FeEDTA^-$, $FeEDTA^{2-}$, and $Co(phen)_3^{3+}$) showed a first-order dependence on the concentration of the inorganic reagent. Over the concentration range studied, plots of k_{obs} vs. oxidant or reductant concentration were linear with a zero intercept. None of these reactions showed any evidence of rate saturation, in which the observed rate constant becomes independent of the inorganic reagent concentration. Thus, over the chosen concentration range, complex formation between protein and redox reagent or a protein rearrangement does not become the rate-limiting step of the overall reaction.[31]

Thus, the rate law is of the form k_1[Protein][Inorganic], with k_1 including any pH dependence. This simple rate is the same as the rate law found for many inorganic electron-transfer reactions. The kinetic parameters obtained for some of these reactions can be compared to those obtained for some simple inorganic systems. For example, the reaction between $FeEDTA^{2-}$ and $Fe(CyDTA)^-$ has a $k(25°) = 3 \times 10^4\ M^{-1}\ sec^{-1}$, $\Delta H^{\ddagger} = 4.0$ kcal/mole and $\Delta S^{\ddagger} = -19$ eu.[32] The protein reaction of $FeEDTA^-$ and ferredoxin has $k(25°) = 3.4 \times 10^5\ M^{-1}\ sec^{-1}$, $\Delta H^{\ddagger} = 1.7$ kcal/mole, and $\Delta S^{\ddagger} = -31$ eu. Thus, the reaction parameters of the iron-sulfur proteins are similar to

those of the inorganic complexes.

The inorganic reagents chosen for study were, for the most part, substitution inert. Thus, $Fe(CN)_6^{3-}$ and $Co(phen)_3^{3+}$ would not be expected to lose a ligand during the course of an electron-transfer reaction; these complexes could not accommodate a protein sulfur ligand to form a bridge for an inner sphere path. Thus, for inner sphere electron transfer, the small molecule must substitute into the protein's coordination sphere.

Structural knowledge about spinach ferredoxin is limited. However, since the pmr indicates that no water exchanges into the first coordination sphere,[33] the metal center is not particularly open and is thus unlikely to be able to accommodate a bridging ligand. A comparison of the rates of reaction of $FeEDTA^-$ and FeHEDTA with ferredoxin also indicates that an inner sphere path is not favored. It would be expected that FeHEDTA could react more rapidly than $FeEDTA^-$ if an inner sphere mechanism were favored. However, the rate of FeHEDTA reaction is ten times slower than the $FeEDTA^-$ rate.

In addition, in the reaction of $FeEDTA^-$ and ferredoxin, the pH behavior indicates that an inner sphere mechanism is not favored. $FeEDTA^-$ is a seven-coordinate species, with one water molecule as the seventh ligand.[34] If this water molecule were acting as a bridging ligand to the ferredoxin, the rate should increase as the pH is

increased, since hydroxide ligands are much better bridges than aquo ligands. However, the pH behavior is opposite this expected behavior; the rate increases as the pH is decreased. This behavior gives some indication that the reaction is proceeding by an outer sphere mechanism. Thus, from our studies, it would appear that the protein-inorganic reactions are of the outer sphere type; no evidence has been found that the reactions proceed by an inner sphere mechanism.

The iron-sulfur proteins as a class would seem to be characterized by very low activation enthalpies. Rubredoxin, the single iron protein, has reported activation enthalpies of 0.1 to 1.1 kcal/mole for reactions with inorganic systems. The activation enthalpies reported here for ferredoxin and HiPIP are in the range -0.5 to +1.1 kcal/mole, with the exception of the reaction of $Co(phen)_3^{3+}$ and HiPIP, with $\Delta H^{\ddagger}$ = +14 kcal/mole. The low $\Delta H^{\ddagger}$ is indicative of a low Franck-Condon barrier, or equivalently, the $\Delta H^{\ddagger}$ for reorganizing the iron coordination sphere during the redox reaction is very small. Thus, these three proteins, although differing greatly in electronic structure and potential, are related by having somewhat similar activation features; on oxidation or reduction, very little rearrangement of the metal center is needed. The X-ray structural data on HiPIP and rubredoxin are consistent with this, since bond lengths change by only 0.1 Å on electron transfer.[35,36] Thus, the protein can accommodate an extra electron without much rearrangement.

The electron involved in the ferredoxin electron transfer is probably in a nonbonding orbital of a tetrahedral FeS_4 center. Thus, minimal rearrangement would be expected on reduction, since the redox orbitals are directed away from ligands. Electron transfer of t_2 electrons would have a greater effect on the ligand bond lengths, since the t_2 orbitals point toward the ligands. Thus, for ferredoxin, low rearrangement barriers are easily rationalized.

The comparison with HiPIP raises an interesting point about the electronic structure of the cluster. It is well-established that localized Fe^{2+} and Fe^{3+} exist in the ferredoxin molecule, thus resulting in transfer of an e electron;[37] rubredoxin also transfers an e electron. The electronic structure of HiPIP is much less certain. However, the similarity of activation enthalpies among the three proteins suggests that orbitals of similar symmetries are involved in each case. Thus, a structural picture of HiPIP in which the extra electron is somewhat localized in an e orbital is consistent with a low Franck-Condon barrier and a low activation enthalpy.

One can consider that the $\Delta H^{\ddagger}$ observed is made of several contributions, or $\Delta H^{\ddagger} \cong \frac{1}{2} (\Delta H_{11}^{\ddagger} + \Delta H_{22}^{\ddagger} + \Delta H^{0})$. Thus, although the activation enthalpy of the protein reactant may be small, the inorganic reactant would be expected to contribute several kilocalories of

enthalpy to the observed $\Delta H^{\ddagger}$, resulting in a $\Delta H^{\ddagger}$ which is greater than zero. The very low $\Delta H^{\ddagger}$ found for these systems must then be rationalized by considering the ΔH^{0} of the reaction, which might be expected to be negative.

An unusually low $\Delta H^{\ddagger}$ can also be explained as a result of a very favorable $\Delta H^{\ddagger}$ for the formation of the precursor complex between protein and reactant.[10] However, for these reactions, precursor complex formation is not very favorable. For the HiPIP reactions, the equilibrium constant for complex formation could be no larger than 10-100 M^{-1}, or deviation from first-order dependence on the redox agent concentration would have been observed. Also, the ionic strength dependence of the ferredoxin-$FeEDTA^{-}$ reaction indicates that the active site contains reactants of the same charge type, since the rate increases as the ionic strength increases. Thus, the low $\Delta H^{\ddagger}$ found for these reactions is attributed to a low Franck-Condon barrier and a negative ΔH^{0} for the reaction and not to favorable complex formation.

The reaction of HiPIP and $Co(phen)_3^{3+}$ is an exception to the generally low activation enthalpies. Reactions of cobalt complexes typically show a moderate $\Delta H^{\ddagger}$; the reaction of $Co(terpy)_2^{2+}$ and $Co(phen)_3^{3+}$ has an activation enthalpy of 6.9 kcal/mole.[38] However, the $Co(phen)_3^{3+}$-HiPIP reaction has a $\Delta H^{\ddagger}$ of 14 kcal/mole. It is thus suggested that the reaction of HiPIP with $Co(phen)_3^{3+}$ may be showing a considerably different mechanism than the other reactions; this mechanism may require a substantial rearrangement of the reactants to allow the phenanthroline rings to overlap the iron-sulfur cluster.

Other protein redox reactions have shown similar patterns. For example, while the cytochrome c-$FeEDTA^{2-}$ reactions shows a low $\Delta H^{\ddagger}$ of 6 kcal/mole and $\Delta S^{\ddagger}$ of -18 eu,[39] the reaction of cytochrome c with $Co(phen)_3^{3+}$ has a high $\Delta H^{\ddagger}$ (11.3 kcal/mole) and a relatively high $\Delta S^{\ddagger}$ (-6.2 eu).[40] Thus, the much higher $\Delta H^{\ddagger}$ for reaction with $Co(phen)_3^{3+}$ may be interpreted in terms of rearrangements of the reactants necessary to insure good overlap of the redox orbitals, which in the ordinary conformation may not be large. Thus, in the reactions of $Co(phen)_3^{3+}$ with both cytochrome c and HiPIP, the reactants may have to rearrange significantly before efficient electron transfer can occur.

Using the activation parameters, it would seem possible to divide protein redox reactions into three loose classifications.

The first group is characterized by a high activation enthalpy, perhaps caused by a requirement for large rearrangements of the reactants. The $Co(phen)_3^{3+}$-cytochrome c and $Co(phen)_3^{3+}$-HiPIP reactions would fall in this category. Many of the reactions of laccase, the four copper oxidase, would also fit this criterion. For example, the laccase-$FeEDTA^{2-}$ reaction has a $\Delta H^{\ddagger}$ = 13 kcal/mole,[41] which is attributed to protein rearrangement.

The second group has activation parameters typical of many other inorganic redox reactions; $\Delta H^{\ddagger}$ has a value of several kilocalories and $\Delta S^{\ddagger}$ is approximately -20 to -30 eu. The cytochrome c-$FeEDTA^{2-}$ reaction would be classed with this group, as would several of the one-copper protein reactions. The plastocyanin-Cr^{2+} reaction, for example, shows a $\Delta H^{\ddagger}$ of 1.5 kcal/mole and $\Delta S^{\ddagger}$ of -34 eu.[42]

The third group is represented by most of the iron-sulfur protein reactions and by another of the copper proteins, azurin. The determining characteristic for this class is a $\Delta H^{\ddagger}$ which is quite small and a $\Delta S^{\ddagger}$ which is very negative. The azurin-$FeEDTA^{2-}$ reaction, for example, is very slow and has activation parameters of approximately 2 kcal/mole for $\Delta H^{\ddagger}$ and -40 eu for $\Delta S^{\ddagger}$.[43] These parameters are very similar to many of the HiPIP, rubredoxin, and ferredoxin reactions which have been studied. Although this classification scheme should not be applied rigidly to protein redox reactions,

some patterns for describing these reactions are beginning to emerge. With reference to Figure 7, most of the iron-sulfur reactions are Type III. In these reactions, little rearrangement of the reactants is needed. However, the reaction is slow, probably because of a large distance separating the reactants. The other type of reaction found for the iron-sulfur proteins is one in which large rearrangement of the reactants are needed, and this is designated as Type I.

Since the Type III iron-sulfur reactions have a very small $\Delta H^{\ddagger}$, the rate of the reaction is controlled by the $\Delta S^{\ddagger}$. The activation entropy for these reactions is large and negative. One would expect a $\Delta S^{\ddagger}$ of -13 eu for the loss of translational and rotational motion on formation of the collision complex.[2] An additional loss of about 15 eu might be expected because of solvent rearrangement. Since no large conformational changes are observed in the X-ray structures of rubredoxin or HiPIP, protein rearrangements can not contribute to the low $\Delta S^{\ddagger}$. Inorganic reactions can have a fairly low $\Delta S^{\ddagger}$; in the reaction of $Co(terpy)_2^{2+}$ and $Co(phen)_3^{3+}$, the $\Delta S^{\ddagger}$ is reported to be -31 eu.[38] However, the $Fe(CN)_6^{3-}$-HiPIP reaction has an even more negative entropy change; $\Delta S^{\ddagger}$ is -44 eu. One possible cause for such a negative entropy is that the reaction mechanism has become nonadiabatic and is proceeding by a tunneling mechanism.[15] In this case, the transmission coefficient has become less than unity, and this is reflected in the observed entropy change. A tunneling mechanism would be forced if there were little overlap of redox orbitals caused by steric restriction and no alternative low-energy pathway available.

It is known from the X-ray structure that the cluster in HiPIP is buried in the hydrophobic interior of the protein.[15] This inaccessi-

Figure 7. Possible Reaction Mechanisms of a Metalloprotein with an Inorganic Reactant M'

Type I: Large protein rearrangement allowing close approach of metal centers

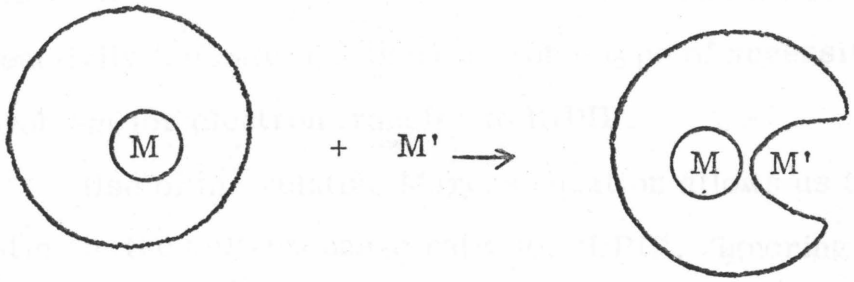

Type II: Ordinary outer sphere reaction with close contact between metal centers; no protein rearrangement necessary

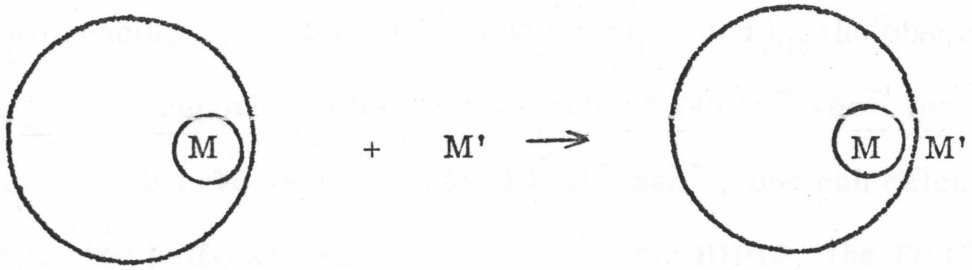

Type III: No protein rearrangement with large distance between metal centers.

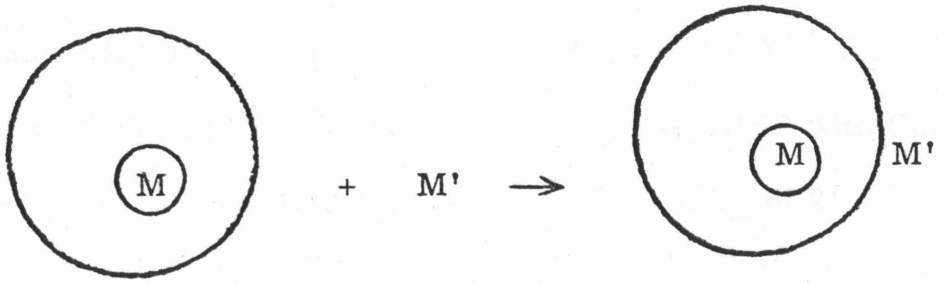

bility leads one to the problem of how this cluster is reduced or oxidized by the relatively bulky $FeEDTA^{2-}$ or $Co(phen)_3^{3+}$. Models of the protein indicate that the nearest approach of a small molecule to the cluster is about 3.5 Å,[15] and the low rates of reactivity indicate that there is some type of accessibility problem for electron transfer to HiPIP.

Use of the relative Marcus equation allows us to estimate the self-exchange rate for HiPIP. Ignoring the correction factor f, the equation can be written $\log k_{12} = \frac{1}{2}(\log k_{11} + \log k_{22} + \Delta E^0/.059)$, with ΔE^0 the difference in standard potential between the two reactants, k_{11} the self-exchange rate, and k_{12} the observed rate. Using the reported self-exchange rate of 740 M^{-1} sec^{-1} for $Fe(CN)_6^{3-}$ [44] and the observed rate of 2.4×10^3 M^{-1} sec^{-1}, one can calculate the expected self-exchange rate of the protein HiPIP; the $Fe(CN)_6^{3-}$ reaction gives a k_{11} of 5×10^3 M^{-1} sec^{-1}. This self-exchange rate is much lower than that found for typical reactions of rubredoxin with its less buried metal center. The self-exchange rate for rubredoxin obtained from the reaction with $Ru(NH_3)_6^{2+}$ is 10^8 M^{-1} sec^{-1}.[5] The self-exchange rate calculated for reaction of HiPIP with $Co(phen)_3^{3+}$ is also much lower than this value. Using a k_{22} of 21 M^{-1} sec^{-1} for

$Co(phen)_3^{3+}$,[45] the k_{11} is 2.7×10^4 M^{-1} sec^{-1}, in rough agreement with that obtained from the $Fe(CN)_6^{3-}$ reaction.

Calculating protein self-exchange rates from the $FeEDTA^{n-}$ reactions proves to be much more ambiguous, since the value of the self-exchange rate for the $FeEDTA^{n-}$ system has not been independently determined. By calculating k_{11} for $FeEDTA^{n-}$ from the cytochrome c-$FeEDTA^{2-}$ reaction, one obtains a value of approximately 10^3 M^{-1} sec^{-1}. Using such a value, we estimate that k_{11} for HiPIP is approximately 1 M^{-1} sec^{-1} and that for ferredoxin is 0.1 M^{-1} sec^{-1}. Although a more accurate determination of the $FeEDTA^{n-}$ self-exchange rate is needed, it is apparent that there is an inconsistency in the calculated k_{11} from data on the oxidation and reduction of HiPIP. It is possible that HiPIP has a reduction pathway that is significantly different from that employed in oxidation.

We suggest that electron tunneling may be a feasible redox mechanism in these proteins. The observed rates can be accounted for by physically reasonable barrier heights and widths. The observed $\Delta S^{\ddagger}$ can also be accounted for by barrier widths of 10-12 Å and a barrier height of approximately 3.5 eV, corresponding to a κ of 10^{-6} to 10^{-8}[15]. Considering the inaccessible nature of the metal cluster in HiPIP, a tunneling mechanism is certainly not unexpected. Similar remarks apply to the redox reactions of ferredoxin.

In terms of the previous classification, a type II reaction would be of the ordinary outer sphere variety. Little rearrangement of the reactants is needed for good overlap of the redox orbitals.

A type I reaction involves a large rearrangement so that the reactants are near each other; an adiabatic reaction can then occur. A type III reaction would involve tunneling; the reactants would not have to rearrange significantly, but the reactant metal centers would never approach each other very closely, and a nonadiabatic reaction would occur. Thus, $\Delta S^{\ddagger}$ would be very negative.

Our studies of the iron-sulfur proteins have established that their redox reactions probably do not follow an inner sphere mechanism. In addition, reaction patterns have emerged; most of the iron-sulfur proteins show reactions characterized by a small $\Delta H^{\ddagger}$ and a large, negative $\Delta S^{\ddagger}$; these reactions show little protein rearrangement. However, one reaction, between $Co(phen)_3^{3+}$ and HiPIP has a large $\Delta H^{\ddagger}$, indicative of a large rearrangement. These types of reactions can be found with other metalloproteins, and thus, a rough classification of protein reactions has emerged. Iron-sulfur proteins follow Type I or Type III behavior. The effect of the protein on the metal center has been demonstrated, as easy accessibility to the metal center is apparently not possible.

References

1. R. Malkin and J. C. Rabinowitz, Ann. Rev. Biochem., 36, 113 (1967).

2. L. E. Bennett, in Current Research Topics in Bioinorganic Chemistry, S. J. Lippard, ed., Wiley, New York, 1973, p. 1.

3. R. G. Bartsch, in Bacterial Photosynthesis, H. Gest, A. San Pietro, and L. P. Vernon, eds., Antioch Press, Yellow Springs, Ohio, 1963, p. 315.

4. F. Basolo and R. G. Pearson, Mechanisms of Inorganic Reactions, Wiley, New York, 1967, p. 454.

5. W. L. Reynolds and R. W. Lumry, Mechanisms of Electron Transfer, The Ronald Press, New York, 1966.

6. N. Sutin, Chem. Brit., 8, 148 (1972).

7. N. Sutin, Acct. Chem. Res., 1, 225 (1968).

8. H. Taube and E. S. Gould, Acct. Chem. Res., 2, 321 (1969).

9. R. H. Lane and L. E. Bennett, J. Amer. Chem. Soc., 92, 1089 (1970).

10. N. Sutin, in Inorganic Biochemistry, G. L. Eichorn, ed., Vol. 2, Elsevier, Amsterdam, 1973, p. 611.

11. R. A. Marcus, A. Rev. Phys. Chem., 15, 155 (1964).

12. R. A. Marcus, J. Phys. Chem., 72, 891 (1968).

13. R. J. Campion, N. Purdie, and N. Sutin, Inorg. Chem., 3, 1091 (1964).

14. H. Taube, Adv. Inorg. Chem. Radiochem., 7, 1 (1959).

15. L. E. Bennett and W. P. Jones, to be published.

16. A. A. Frost and R. G. Pearson, Kinetics and Mechanism, Wiley, New York, 1951, p. 97.

17. T. Takano, O. B. Kallai, R. Swanson, and R. E. Dickerson, J. Biol. Chem., 248, 5234 (1973).

18. E. L. Packer, H. Steinlickt, and J. C. Rabinowitz, Proc. Nat. Acad. Sci. U.S., 69, 3278 (1972).

19. C. A. Jacks, L. E. Bennett, W. N. Raymond, and W. Lovenberg, Proc. Nat. Acad. Sci. U.S., 71, 1118 (1974).

20. J. R. Heriot, L. C. Sieker, L. H. Jensen, and W. Lovenberg, J. Mol. Biol., 50, 391 (1970).

21. J. C. M. Tsibris and R. W. Woody, Coord. Chem. Rev., 5, 417 (1970).

22. H. J. Schugar, A. T. Hubbard, F. C. Anson, and H. B. Gray, J. Amer. Chem. Soc., 91, 71 (1969).

23. H. J. Schugar, G. R. Rossman, C. G. Barraclough, and H. B. Gray, J. Amer. Chem. Soc., 94, 2683 (1972).

24. E. H. Swift, J. Amer. Chem. Soc., 51, 1682 (1929).

25. C. K. Jorgensen, Acta Chem. Scand., 10, 518 (1956).

26. D. A. Skoog and D. M. West, Fundamentals of Analytical Chemistry, Holt, Rinehart and Winston, New York, 1963, p. 346.

27. P. Pfeiffer and B. Werdelman, Zeit. Anorg. Allgemeine Chem., 263, 36 (1950).

28. T. J. Przystas and N. Sutin, J. Amer. Chem. Soc., 95, 5545 (1973).

29. D. H. Petering and G. Palmer, Arch. Biochem. Biophys., 141, 456 (1970).

30. J. F. Corbett, J. Chem. Educ., 49, 663 (1972).

31. J. K. Yandell, D. P. Fay, and N. Sutin, J. Amer. Chem. Soc., 95, 1131 (1973).

32. R. G. Wilkins and R. E. Yelin, Inorg. Chem., 7, 2667 (1968).

33. A. S. Mildvan, R. W. Estabrook, and G. Palmer, in Magnetic Resonance in Biological Systems, A. Erhenberg, B. G. Malmastrom, and T. Vanngard, eds., Pergamon Press, Oxford, New York, 1967, p. 175.

34. M. D. Lind and J. L. Hoard, Inorg. Chem., 3, 34 (1964).

35. K. D. Watenpaugh, L. C. Sieker, J. R. Herriott, and L. H. Jensen, Cold Springs Harbor Symp. Quant. Biol., 36, 359 (1971).

36. C. W. Carter, Jr., J. Kraut, S. T. Freer, R. A. Alden, L. C. Sieker, E. Adman, and L. H. Jensen, Proc. Nat. Acad. Sci. U.S., 69, 3526 (1972).

37. W. R. Dunham, G. Palmer, R. H. Sands, and A. J. Bearden, Biochim. Biophys. Acta, 253, 373 (1971).

38. R. Farina and R. G. Wilkins, Inorg. Chem., 7, 514 (1968).

39. H. L. Hodges, R. A. Holwerda, and H. B. Gray, J. Amer. Chem. Soc., 96, 3132 (1974).

40. J. V. McArdle, H. B. Gray, C. Creutz, and N. Sutin, J. Amer. Chem. Soc., 96, 5737 (1974).

41. R. A. Holwerda, Thesis, California Institute of Technology, 1973.

42. J. W. Dawson, H. B. Gray, R. A. Holwerda, and E. W. Westhead, Proc. Nat. Acad. Sci. U.S., 69, 30 (1972).

43. R. C. Rosenberg, personal communication.

44. R. J. Campion, C. F. Deck, P. King and A. C. Wahl, Inorg. Chem., 6, 672 (1967).

45. B. R. Baker, T. Basolo, and H. M. Neumann, J. Phys. Chem., 63, 371 (1959).

CHAPTER IV

STUDIES OF THE REACTIONS OF FERREDOXIN WITH FAD, FMN, RIBOFLAVIN, AND $NADP^+$-REDUCTASE

INTRODUCTION

Soluble spinach ferredoxin interacts in the cell with an FAD-containing protein of molecular weight 37,000.[1] The flavoprotein exhibits a variety of activities, including a diaphorase activity (NADPH → $Fe(CN)_6^{3-}$), transhydrogenase activity (NADPH → $NADP^+$), and a hemoprotein reductase activity (NADPH → cyt f). However, the main cellular function of the enzyme is the production of reduced pyridine nucleotides using ferredoxin as the reducing agent. The cellular system preferentially produces NADPH instead of NADH.

The redox properties of this enzyme have been studied by others. The enzyme is slowly reduced by $Na_2S_2O_4$ in a two-electron process, with no spectroscopic evidence for the formation of a semiquinone.[1] With excess NADPH, the protein "rapidly" forms a semiquinone. The semiquinone has an esr signal, with g = 2.0024, and it shows an absorption spectrum characteristic of many semiquinones; a low energy wavelength band is centered at 700 nm.[2] The protein then slowly forms the fully reduced flavin. The potentials for these reductions have been reported; E_1 is found to be -.32 v, and E_2 is -.40 v.[3]

Recent work by Forti[2] in chloroplasts indicates that the enzyme is only reduced to the semiquinone level during the photoprocess; Forti indicates that the ferredoxin-flavoprotein reaction does not produce the fully reduced flavin.

It has been found that ferredoxins from different plant sources are less effective than the ferredoxin from spinach in the reaction with the spinach flavoprotein;[4] very specific interactions between the ferredoxin and the reductase are to be found.[5] Recent work indicates that a complex is formed between the two proteins. This complex has been characterized by a difference spectrum and by sedimentation analysis. Apparently, the reductase reacts with ferredoxin in less than 3 msec to form the 1:1 complex.[6] The dissociation constant has been reported as 5×10^{-8} M. The complex dissociates at a high ionic strength, indicating that electrostatic forces are largely responsible for the binding. At low ionic strengths, a tightly bound complex is formed which has low catalytic activity. Maximum activity is found at .1 ionic strength. This ionic strength is close to that observed for maximal activity in the chloroplast, and thus, it has been suggested that the complex is important in the in vivo behavior of the system. The complex dissociates completely at high ionic strength. However, the exact nature of the specificity for one iron-sulfur protein (or the binding mechanism) is unknown. Both the reductase and the ferredoxin are acidic proteins (pI for the reductase is 5.1), and thus, gross electrostatic forces cannot be responsible for the specificity or the

binding. There are indications that sulfhydryl groups are responsible for much of the activity, and they may thus be implicated in the mechanism.

Other work has shown complex interactions between the enzymes. Apparently, a complex is formed with ferredoxin, ferredoxin reductase, and cytochrome c which exhibits a greatly enhanced reactivity toward oxygen.[7] The binding of cytochrome c greatly alters the catalytic activity of the complex. This system has been suggested as a model for other complex reaction systems.[7]

In an attempt to understand the forces that a protein can exert on an active center, kinetic studies of the ferredoxin reduction of FAD were performed. FAD, a low molecular weight compound, should have fewer steric restrictions than the enzyme complex during reactions. The potentials for reduction of FAD are $E_1 = -.13$ v and $E_2 = -.33$ v.[3] Solutions of partially reduced FAD contain FAD, $FADH_2$, FAD; and a complex of FAD and $FADH_2$, all in rapid equilibrium. Equilibrium and rate constants for the FMN system have been determined. The reaction of two semiquinone radical anions to give FMN and $FMNH_2$ has an equilibrium constant of 10^3.[8] Thus, the disproportionation of the radical is greatly favored. The enzyme and the FAD show very little absorbance change in the region of 510 nm as they are successively reduced. Thus, this region was used to follow the reaction.

EXPERIMENTAL SECTION

Flavin adenine dinucleotide (FAD), flavin mononucleotide (FMN), and riboflavin were obtained from Sigma; concentrations of solutions for kinetics work were obtained from optical absorbance at 450 nm (ϵ = 10700).[1] $FADH_2$ was prepared by reducing FAD solutions with $Na_2S_2O_4$ in a nitrogen atmosphere.

Ferredoxin-TPN reductase (FTR) was extracted from spinach leaves by Shin's method.[1] The activity of the enzyme was assayed by its reduction of cytochrome c in the presence of ferredoxin and NADPH. The NADPH was obtained from Sigma. The A_{458}/A_{275} ratio was .125. The concentration of protein solutions was determined by the absorbance at 456 nm (ϵ = 10740).[1]

The preparation of ferredoxin solutions, kinetic procedures, and apparatus were described in previous chapters.

RESULTS

A spectroscopic titration indicates that two moles of reduced ferredoxin are consumed per mole of $FADH_2$ formed.

Kinetic measurements were made on ferredoxin solutions 2×10^{-5} M in protein. Measurements were made at 540 nm, which is a wavelength of very little absorption for the FAD species. The concentration dependence for the oxidation of ferredoxin by FAD is seen in Figure 1. Over a narrow concentration range, the reaction is first order in FAD, with a zero intercept. The observed rate constants are fairly high, with a k_{obs} of 59 sec^{-1} for the lowest concentration studied. The k_{obs} are slightly higher using FMN as the oxidant and are much higher using the less bulky riboflavin. The addition of $FADH_2$ stimulates the reaction; a plot of k_{obs} versus $[FADH_2]^{1/2}$ is linear, with the intercept for this plot having the same value for k_{obs} as the reaction with no added $FADH_2$ (Figure 2).

The reaction of ferredoxin with FAD does not show a strong temperature dependence. An Eyring plot is linear, with the activation parameters of $\Delta H^{\ddagger}$ = 4.4 kcal/mole and $\Delta S^{\ddagger}$ = -16 eu. The k_{obs} values depend to some extent on ionic strength, increasing fivefold as the ionic strength is increased to .8 M. All data are given in Appendix I.

Reactions of ferredoxin with ferredoxin-TPN reductase were studied with ferredoxin in excess. The observed absorbance change

Figure 1. Observed Rate Constants for the Reaction of Ferredoxin and FAD (26 °C, $\mu = 0.1$ Tris-NaCl, pH 7.8, $[Fd] = 1.5 \times 10^{-5}$ M).

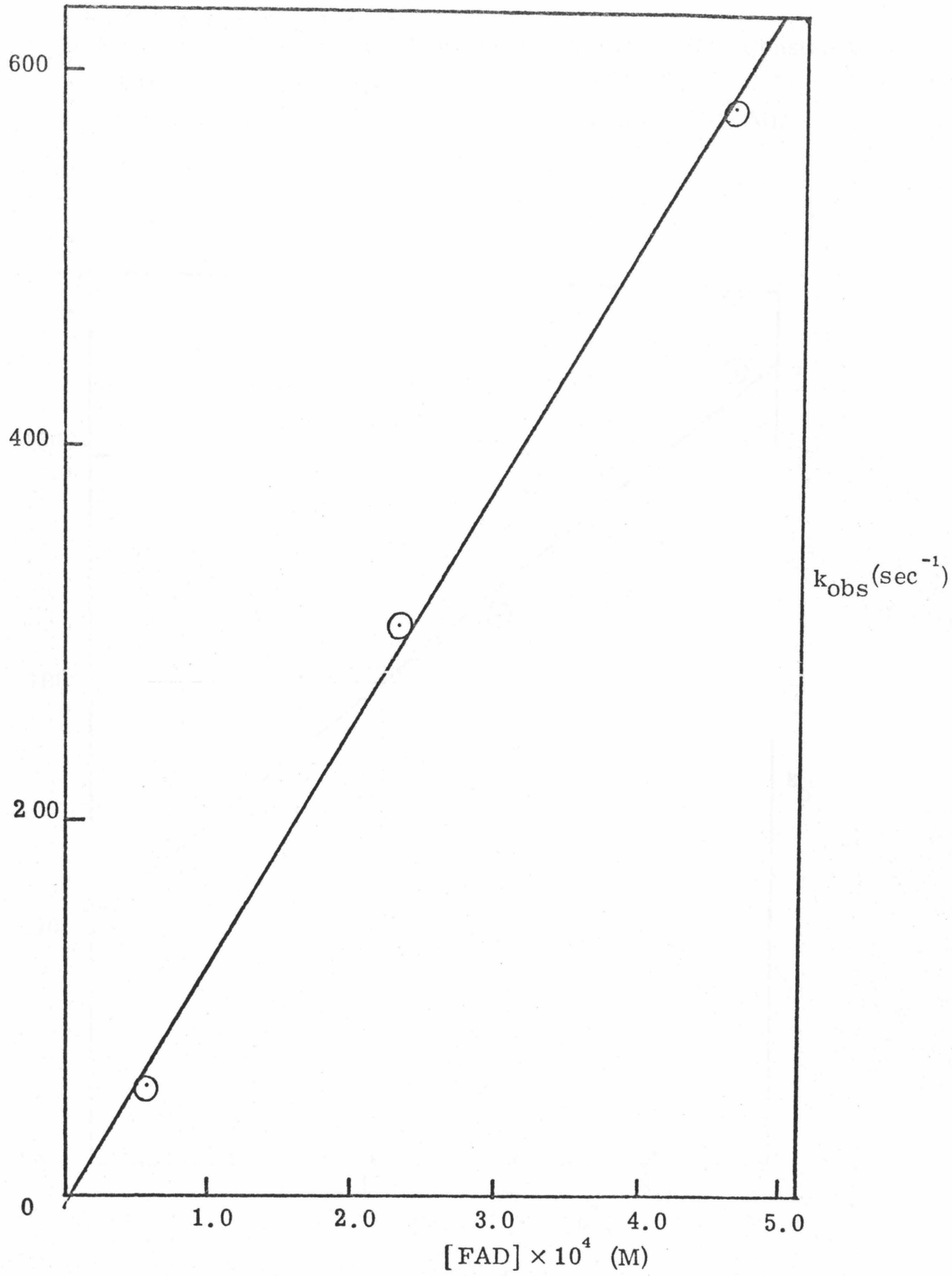
600
400
200
0
1.0
2.0
3.0
4.0
5.0
[FAD] × 10^4 (M)
k_obs (sec^-1)

Figure 2. $FADH_2$ Dependence of the Observed Rate Constants for the Reaction of Ferredoxin and FAD (26 °C, $\mu = 0.1$ Tris-NaCl, $[FAD] = 6.8 \times 10^{-5}$ M, $[Fd] = 1.5 \times 10^{-5}$ M).

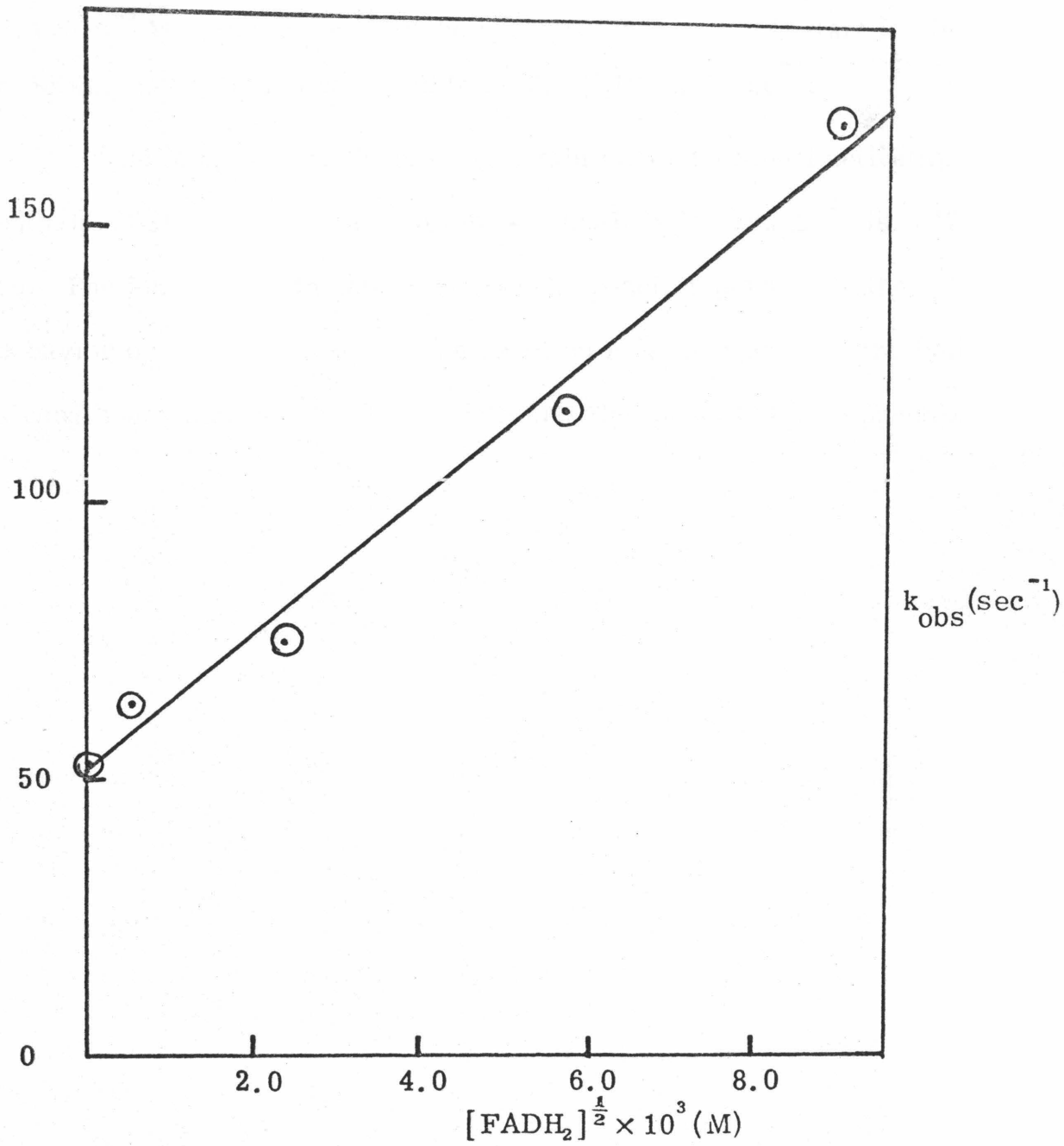

would indicate that only a one-electron reduction of the flavoprotein to the semiquinone level occurred; one mole of ferredoxin was oxidized per mole of flavoprotein. The k_{obs} for a ferredoxin concentration of 5.4×10^{-5} M was 0.5 sec^{-1}. The second-order rate constant for the reaction may then be estimated to be 9.2×10^{3} M^{-1} sec^{-1}.

The temperature dependence again showed a small activation enthalpy; $\Delta H^{\ddagger}$ for the reaction is -.4 kcal/mole, and $\Delta S^{\ddagger}$ is -42 eu. The ionic strength dependence of the reaction paralleled the behavior observed with FAD; the reaction rate increased as the ionic strength was increased. These data are also tabulated in Appendix I.

DISCUSSION

The reaction of reduced ferredoxin with the two-electron acceptor FAD proceeds with a 2:1 stoichiometry. Over a narrow concentration range, the reaction is first order in FAD. The addition of $FADH_2$ stimulates the reaction, indicating that the reaction of ferredoxin with the FAD semiquinone must be rapid.

The observed data can be interpreted in terms of the scheme below (where Fd_{red} is abbreviated Fd_r):

$$1)\quad Fd_r + FAD \xrightarrow{k_1} Fd_{ox} + FAD\cdot$$

$$2)\quad Fd_r + FAD\cdot \xrightarrow{k_2} Fd_{ox} + FADH$$

$$3)\quad 2\,FAD\cdot \underset{k_4}{\overset{k_3}{\rightleftharpoons}} FAD + FADH$$

Reactions 1 and 2 are presumed to go to completion, as is indicated by the E^0 values. All protonations are presumed rapid. The rate equation for this scheme is:

$$-d[Fd_r]/dt = k_1[FAD][Fd_r] + k_2([FAD][FADH_2]K)^{1/2}[Fd_r]$$

with K the equilibrium constant for the disproportionation of the FAD and $FADH_2$. When FAD and $FADH_2$ are in excess compared to ferredoxin, this law simplifies to $\frac{-d[Fd_r]}{dt} = k_{obs}[Fd_r]$

$$k_{obs} = k_1[FAD] + k_2([FAD][FADH_2]K)^{1/2}$$

Thus, the decay in ferredoxin concentration should follow pseudo first-order kinetics. When the $FADH_2$ concentration is low, the reaction should show a first-order dependence on the [FAD]. A plot of k_{obs} vs. $[FADH_2]^{1/2}$ should be linear with the intercept having the same value for k_{obs} as the reaction with no added $FADH_2$. All of these characteristics were observed in the ferredoxin-FAD reaction. Thus, with no added $FADH_2$, the reaction with ferredoxin is essentially a one-electron reduction to the semiquinone of FAD; the semiquinone produced then reacts with other semiquinone present to form one mole of $FADH_2$. The rate of this disproportionation is 10^9 M^{-1} sec^{-1}.[8]

By using an estimated K of 10^{-3} M^{-1},[8] one can obtain values of k_1 and k_2. Thus, k_1, the second-order rate constant for reaction of FAD and reduced ferredoxin is 8.6×10^5 M^{-1} sec^{-1}, and k_2, the reaction rate with semiquinone is 1.3×10^7 M^{-1} sec^{-1}. Thus, even though the potential difference involved in the reaction is small,[3] the rate constants are relatively large.

The temperature dependence of the reaction was not very marked, increasing 50% over 12°C. Since in the absence of added $FADH_2$, the rate observed is essentially the rate of formation of the

semiquinone, this temperature dependence directly reflects the temperature dependence of formation of semiquinone. Thus, activation parameters can be calculated for formation of the semiquinone; $\Delta H^{\ddagger}$ is 4.4 kcal/mole and $\Delta S^{\ddagger}$ = -16 eu.

The reaction of the flavoprotein with ferredoxin was carried out with the ferredoxin in excess. However, from observed optical changes, the reaction had a one to one stoichiometry, indicating that only the semiquinone form of the protein was formed during reaction. This behavior could reflect the specific protein-protein interaction during the reaction,[6] since dissociation of the complex could be slow. The potential for the reduction of the semiquinone is also unfavorable.[3] Thus, it would seem that the in vivo and in vitro reactions of ferredoxin-FTR are one-electron reductions.[2]

Thus, this reaction was treated as a one-electron transfer process. The second-order rate constant for the production of the protein semiquinone is 9.2×10^{3} M^{-1} sec^{-1}. This is a factor of 100 fold less than the similar reaction with FAD. Since the potential for this reaction is less favorable than for reaction with FAD,[3] one would expect a drop in the rate when the flavin grouping is substituted into a protein environment; a drop in potential of 0.2 volt would be expected to give a 100 fold drop in rate constant.

The temperature dependence of the reaction shows a very small activation enthalpy (-.4 kcal/mole) and a very negative activation entropy (-42 eu). These parameters are in the range considered before to indicate that a tunneling mechanism may be operative. The temperature dependence of the reaction with FAD is more normal ($\Delta H^{\ddagger}$ = 4 kcal/mole, $\Delta S^{\ddagger}$ = -16 eu) perhaps indicating that an isolated FAD grouping is more flexible and can react by an ordinary outer sphere mechanism. One notes that FMN and riboflavin, which are smaller than FAD, have larger k_{obs} values.

One other explanation for a small $\Delta H^{\ddagger}$ may be a very favorable enthalpy term for the complex formation between the two proteins;[9] this $\Delta H^{\ddagger}$ would not exist for the FAD. However, the ionic strength dependences of the flavoprotein and the FAD reaction are very similar, increasing by a factor of four as the ionic strength is increased. This may indicate that the complex formation between the proteins is not very important in determining the reaction rates, since the amount of complex formation drops off very sharply as the ionic strength is increased.[6] Thus, the very small $\Delta H^{\ddagger}$ and negative $\Delta S^{\ddagger}$ may again be indicative of steric restrictions for the protein-protein reaction.

References

1. M. Shin, in Methods in Enzymology, Vol. 23, Part A, A. San Pietro, ed., Academic Press, New York, 1971, p. 440.
2. G. Forti, Arch. Biochem. Biophys., 140, 167 (1970).
3. J. J. Kierns and J. H. Wang, J. Biol. Chem., 247, 7374 (1972).
4. C. F. Yocum, J. N. Siedow, and A. San Pietro, in Iron-Sulfur Proteins, W. Lovenberg, ed., Vol. 1, Academic Press, New York, 1973, p. 111.
5. S. Nakamura and T. Kimura, J. Biol. Chem., 246, 6235 (1971).
6. G. P. Forest, S. G. Mayhew, and V. Massey, J. Biol. Chem., 244, 964 (1969).
7. S. Nakamura and T. Kimura, J. Biol. Chem., 247, 6462 (1972).
8. B. G. Barman and G. Tollin, Biochemistry, 11, 4768 (1972).
9. N. Sutin, in Inorganic Biochemistry, G. L. Eichhorn, ed., Vol. 2, Elsevier, Amsterdam, 1973, p. 611.

CHAPTER V

KINETICS OF

FERREDOXIN-HEMOPROTEIN REACTIONS

INTRODUCTION

Iron-sulfur proteins are involved in redox reactions with several heme proteins.[1] Adrenodoxin, for example, reacts with cytochrome P450. Also, iron-sulfur centers are involved in the mitochondrial electron transport chain, possibly functioning between cytochromes b_1 and c_1. Thus, it should be valuable to measure the rates of reactions of hemoproteins and iron-sulfur proteins. By doing so, it should prove possible to learn more about the steric constraints imposed on reactions between large molecules.

The heme proteins studied were the commonly available ones, cytochrome c (cyt c) and metmyoglobin (mMb). Both proteins have their hemes located in somewhat similar environments; one edge of the heme is exposed to solvent, while the rest of the heme is buried in the protein interior.[2,3] However, these proteins have different spin states and ligands. Horse heart metmyoglobin is a high spin ferric heme protein, with imidazole and water as the fifth and sixth iron ligands. The water may be replaced by other anions, such as F^-.[4] Cytochrome c is a low spin heme protein. The fifth and sixth coordination sites of the iron are occupied by histidine and methionine.[2]

The reaction mechanisms of cytochrome c have been studied extensively; several possible reduction paths have been suggested. Work with Cr^{2+} as the reducing agent has indicated that the Cr^{2+} can

enter the interior region of the protein and then reduce the heme iron, perhaps with the assistance of a tyrosine.[5] This mechanism may involve breaking the heme Fe-methionine bond. Other reagents, such as $FeEDTA^{2-}$ [6] or $Co(phen)_3^{3+}$,[7] may react with the protein at the exposed heme edge, transferring the electron through the porphyrin ring to or from the iron. It has also been suggested that electrons may use the nearly parallel aromatic rings found in cytochrome c to reduce the heme iron.[2] Thus, the reaction mechanism of the protein may depend largely on the properties of the other reactant.

By using a large molecule such as ferredoxin as the other reactant, we have placed some limitations on the possible mechanism of reduction of cytochrome c. Unless protein-protein interactions accidentally lead to a direct match of the exposed heme edge and iron-sulfur center, it is likely that either a Type I or a Type III pathway will be required for reaction.

EXPERIMENTAL SECTION

Horse heart cytochrome c (Type III), obtained from Sigma, was used without further purification. Horse heart myoglobin (Type III) was obtained from Nutritional Biochemical Corp. and from Sigma. Solutions of the protein were centrifuged to remove an insoluble material. Solutions were then oxidized with a twofold excess of $K_3Fe(CN)_6$, followed by extensive dialysis. The protein that was used for kinetics had ratios ≥ 5 for the optical absorbances of the Soret band to the protein band. Metmyoglobin fluoride solutions were prepared by dialyzing metmyoglobin against a potassium phosphate buffer solution (μ = 0.05) with .8 M NaF added. The concentrations of the solutions for kinetics work were determined by optical absorbances at 550 nm for cytochrome c (ϵ = 9000),[8] 560 nm for mMb (ϵ = 3700)[9] and at 610 nm (ϵ = 8700) for mMbF.[10]

The ferredoxin solutions were prepared as described in earlier chapters. The apparatus, procedure, and data analysis have also been described.

RESULTS

The reactions of ferredoxin with cytochrome c and metmyoglobin were carried out with the heme proteins in excess. The reaction with cytochrome c was followed at 550 nm which is a wavelength of large absorbance change for this protein. Reduced ferredoxin concentrations were thus quite low; the usual reaction concentration was 2.5×10^{-6} M. The observed absorbance change was consistent with a one-electron change for the ferredoxin. Reactions with metmyoglobin and metmyoglobin- fluoride (mMbF) were followed at 560 and 610 nm, respectively; again, ferredoxin concentrations could be kept low. The data are collected in Appendix I.

With the heme proteins in excess, pseudo first-order kinetics were observed. The concentration dependences for the reactions of ferredoxin with cyt c and mMb indicate a first-order dependence on the heme protein concentration. A typical example is shown in Figure 1. The second-order rate constant for reaction with mMb at 25°, .1 μ is 2.3×10^{6} M^{-1} sec^{-1}, while k_1 for cytochrome c is 8.1×10^{4} M^{-1} sec^{-1}.

The Eyring plots of log k/T versus 1/T were linear for both proteins (see Figure 2 and Appendix I). The activation enthalpy for the mMb reaction is -0.9 kcal/mole, while the $\Delta H^{\ddagger}$ for the cytochrome c reaction is much larger, $\Delta H^{\ddagger}$ = 9.6 kcal/mole. The activation entropies are -32 eu for mMb and -4 eu for cytochrome c.

Figure 1. Observed Rate Constants for the Reduction of Cytochrome c by Ferredoxin (25 °C, $\mu = 0.1$ phosphate, pH 7.0, $[Fd] = 2.5 \times 10^{-6}$ M).

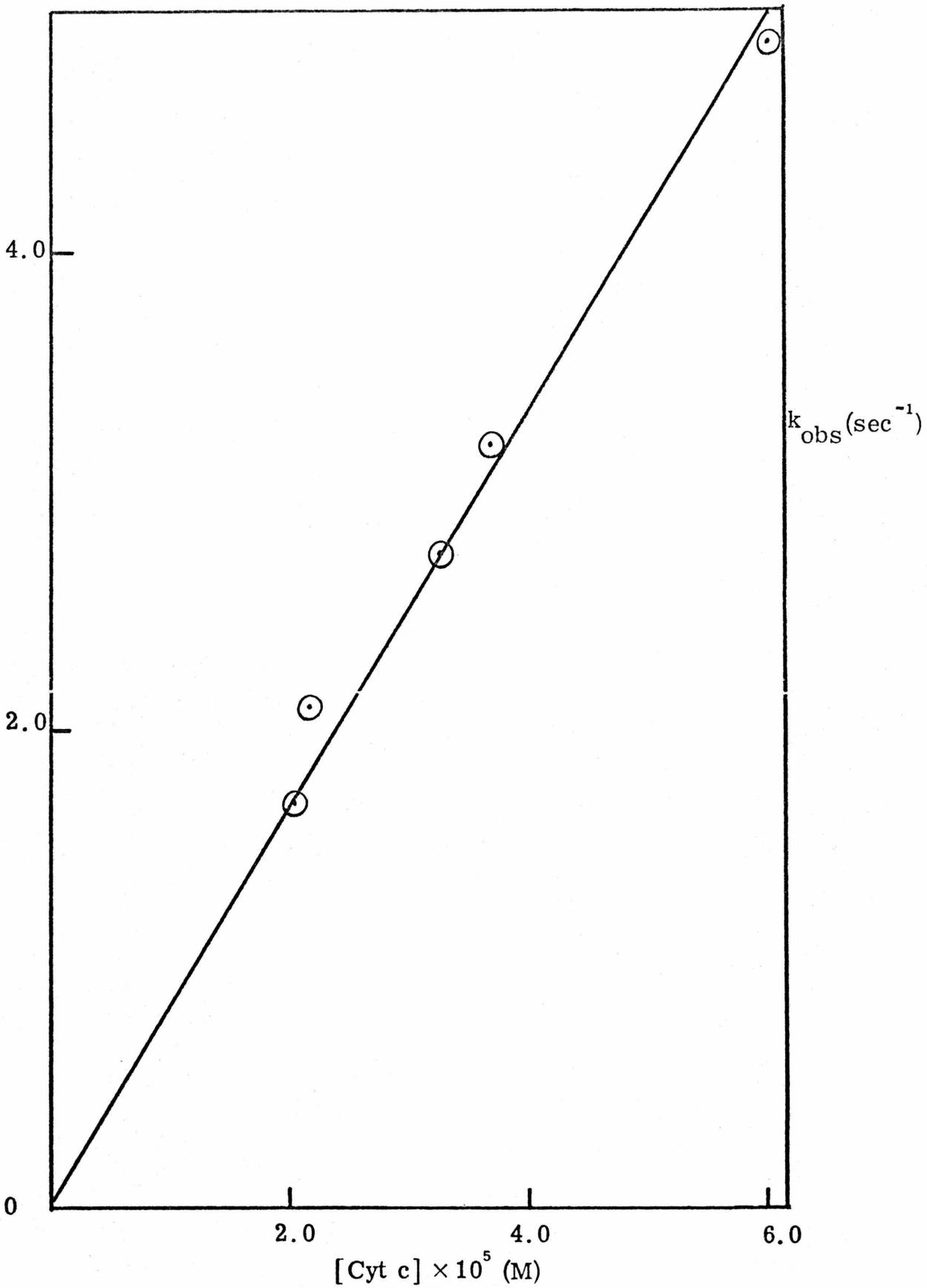
4.0
2.0
0
2.0
4.0
6.0
$k_{obs}(sec^{-1})$
[Cyt c] $\times 10^5$ (M)

Figure 2. Eyring plot for the reaction of Ferredoxin with Cytochrome c (μ =0.1 phosphate, pH 7.0, [Cyt c] = 2.05×10^{-5} M, [Fd] = 2.5×10^{-6} M).

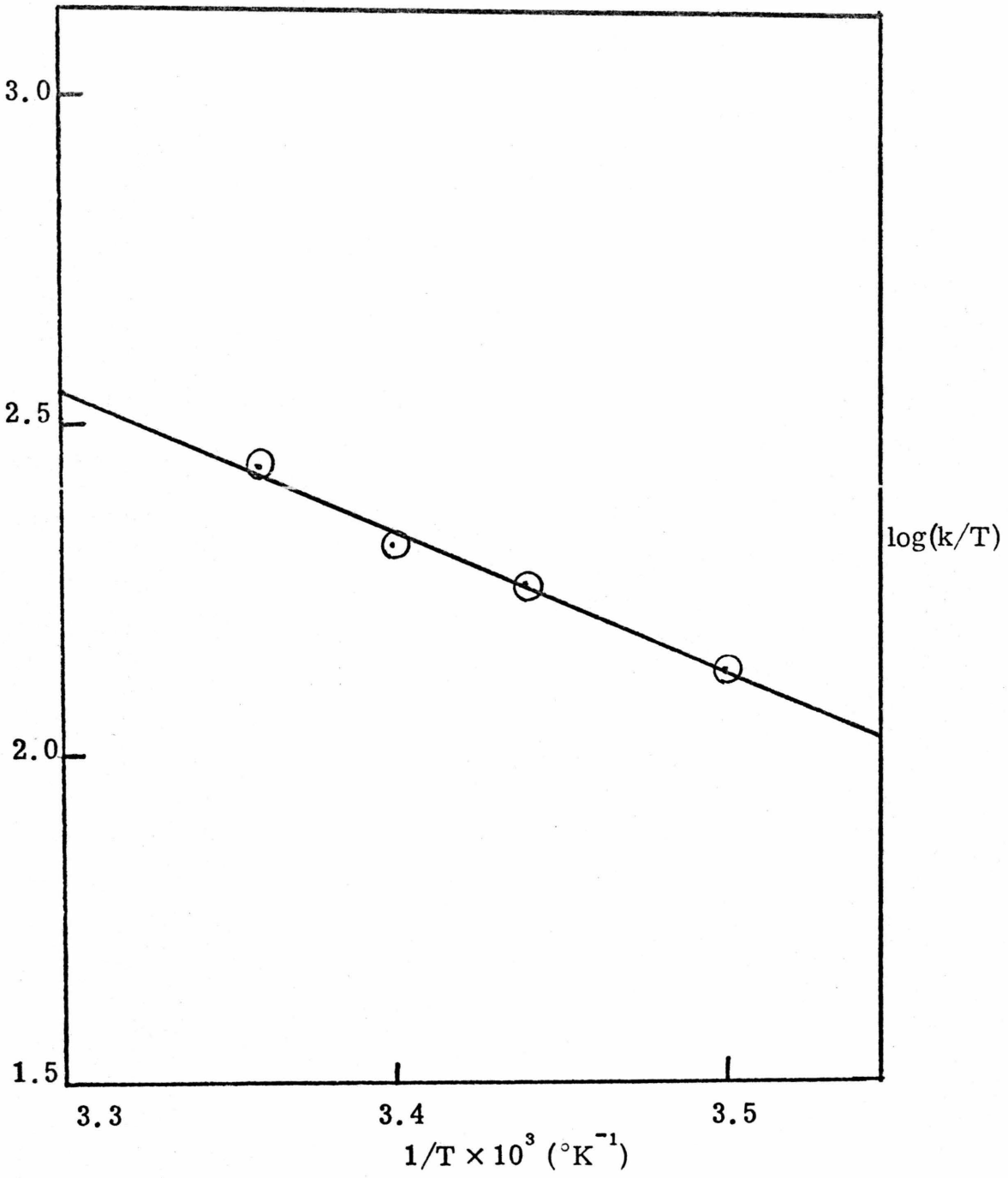

The pH dependence of the mMb reaction was studied over the range 6 to 8. With mMb, this yields a similar pH dependence as for $FeEDTA^-$; log k_1 vs. pH is linear.

By adding a large excess of F^-, the rate of the reaction drops to a much lower value; k_{obs} is 0.4 sec^{-1} (μ = 0.8) compared with a k_{obs} value of 80 sec^{-1} (μ = 0.1) in the absence of F^-. The reaction shows no dependence on the metmyoglobin-fluoride concentration (see Figure 3).

The rate of formation of the mMb-F complex was determined by using the stopped-flow apparatus; one-drive syringe contained metmyoglobin and the other contained a concentrated fluoride solution. The reaction was followed at 610 nm, a wavelength of strong absorption for the fluoride complex. The rate constant obtained for the formation of the fluoride derivative was 4.6 M^{-1} sec^{-1}.

Figure 3. Observed Rate Constants for the Reaction of Ferredoxin with MetMyoglobin-Fluoride (25 °C, $\mu = 0.8$ Tris-NaF, pH 7.7, [Fd] $= 5 \times 10^{-6}$ M).

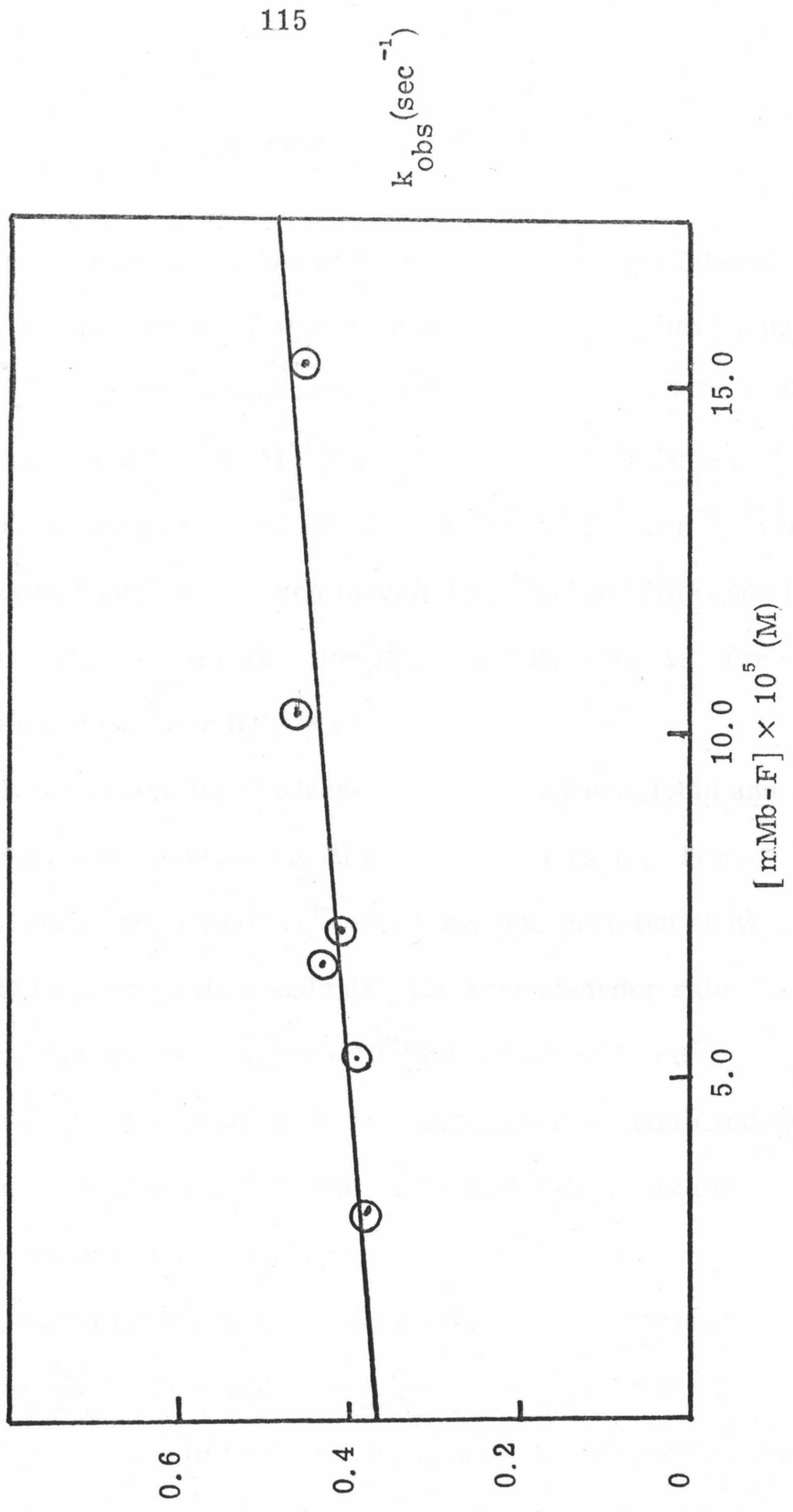
$k_{obs}(sec^{-1})$
0.6
0.4
0.2
0
5.0
10.0
15.0
[mMb-F] × 10^5 (M)

DISCUSSION

The reactions of ferredoxin with the heme proteins follow second-order kinetics over a fairly narrow range of concentrations. A large difference in the second-order rate constant is observed; k_1 for metmyoglobin is 2.3×10^6 M^{-1} sec^{-1} while the cytochrome c reaction is slower by a factor of 30; k_1 is 8.1×10^4 M^{-1} sec^{-1}. This difference in reactivity exists even though the potential difference for the ferredoxin-cytochrome c reaction is greater than the ΔE^0 for reaction with metmyoglobin by 0.2 v.[1]

This large reactivity difference between metmyoglobin and cytochrome c does not exist in small molecule reactions. For example, the reactions of $Fe(CN)_6^{3-}$ with the heme proteins show approximately the same rate constants; the second-order rate constants for mM b and cyt c are 2×10^6 and 8×10^6 M^{-1} sec^{-1}, respectively.[11,12] The small reactivity difference is attributed to differences in the self-exchange rates from such factors as differences in the spin states of the heme groups.

Thus, one would predict that approximately the same rate would be observed for the heme proteins reaction with ferredoxin. However, the large difference in rate constant between the heme proteins suggests that a different mechanism may be operating. A basic difference in the reaction mechanism is shown by the activation parameters. The

reaction with mMb proceeds with an almost negligible $\Delta H^{\ddagger}$ (-.9 kcal/mole) and a fairly large negative $\Delta S^{\ddagger}$ (-32 eu). The ferredoxin-cytochrome c reaction, however, has a sizeable activation enthalpy ($\Delta H^{\ddagger}$ = 9 kcal/mole) and a relatively favorable activation entropy (-4 eu). This value of $\Delta H^{\ddagger}$ for the cytochrome reaction is fairly consistent with other reactions of cytochrome c which show $\Delta H^{\ddagger}$ in the 6-9 kcal/mole range. This suggests that the cytochrome c must undergo some rearrangement before reaction can occur. These activation parameters for the ferredoxin-cytochrome c reaction are fairly similar to the cyt c-$Co(phen)_3^{3+}$ reaction. Instead of Type III behavior, then, it appears that a Type I pathway is preferred.

The Fd-mMb reaction has the activation parameters typical of a Type III process. We propose, therefore, that the structures of these two heme proteins differ significantly enough that a tunneling mechanism is favored in the metmyoglobin reaction while a protein rearrangement with an adiabatic electron transfer is favored for the cytochrome c reaction.

By adding F^- to the medium, a drop in the rate of reduction of myoglobin was observed, and the rate became independent of the mMb-F concentration. This behavior suggests that the dissociation of the fluoride from the heme protein has become the rate-limiting step, followed by rapid electron transfer. The rate of dissociation of F^-

is calculated to be 0.3 sec^{-1}, obtained from $k_d = K_{eq}/k_a$, with $K_{eq} = 15\ M^{-1}$. [4] K_a, the rate constant for the association of mMb and F^-, was measured to be 4.6 $M^{-1}\ sec^{-1}$. This k_d is in close agreement with the observed value of the rate constant for the reduction of metmyoglobin-fluoride.

References

1. L. E. Bennett, in Current Research Topics in Bioinorganic Chemistry, S. J. Lippard, ed., Wiley, New York, 1973, p. 1.
2. T. Takano, O. B. Kallai, R. Swanson, and R. E. Dicherson, J. Biol. Chem., 248, 5234 (1973).
3. C. L. Nobbs, H. C. Watson, and J. C. Kendrew, Nature, 209, 334 (1966).
4. H. Theorell and A. Ehrenberg, Acta Chem. Scand., 5, 823 (1951).
5. E. Fleischer, personal communication.
6. H. L. Hodges, R. A. Holwerda, and H. B. Gray, J. Amer. Chem. Soc., 96, 3132 (1974).
7. J. V. McArdle, H. B. Gray, C. Creutz, and N. Sutin, J. Amer. Chem. Soc., 96, 5737 (1974).
8. E. Margoliash and N. Frohwist, Biochem. J., 71, 570 (1959).
9. P. George, J. Beetlestone, and J. S. Griffith, Rev. Mod. Phys., 36, 441 (1964).
10. H. Theorell and A. Ehrenberg, Acta Chem. Scand., 5, 823 (1951).
11. E. Antonini, M. Brunori, and J. Wyman, Biochemistry, 4, 545 (1965).
12. K. G. Brandt, P. C. Parks, G. Czeslinski, G. B. Hess, J. Biol. Chem., 241, 4180 (1966).

APPENDIX I

SUPPLEMENTAL TABLES AND

FIGURES FOR THE KINETICS

Table 1

Observed Rate Constants for the Oxidation of Ferredoxin by $FeEDTA^-$ and FeHEDTA

$FeEDTA^-$ and Ferredoxin;
12.5°, μ = 0.1 Tris-Cl, pH 7.8, [Fd] = 10^{-5} M, 465 nm

$[FeEDTA^-] \times 10^4$ (M)	k_{obs} (sec^{-1})
1.84	54
	56.1
	53 (Alfalfa protein)
3.76	106
	111
5.6	156
	151
7.5	228
	210

FeHEDTA and Ferredoxin;
26°C, μ = 0.1 Tris-NaCl, pH 7.8, [Fd] = 10^{-5} M, 465 nm

[FeHEDTA] $\times 10^3$ (M)	k_{obs} (sec^{-1})
0.20	5.6
	5.1
0.56	14.0
	13.6
1.06	24.0
	25.7
1.97	50.0
	48.2

Figure 1. Observed Rate Constants for the Reduction of FeHEDTA by Ferredoxin (26 °C, $\mu = 0.1$ Tris-NaCl, pH 7.8, $[Fd] = 10^{-5}$ M).

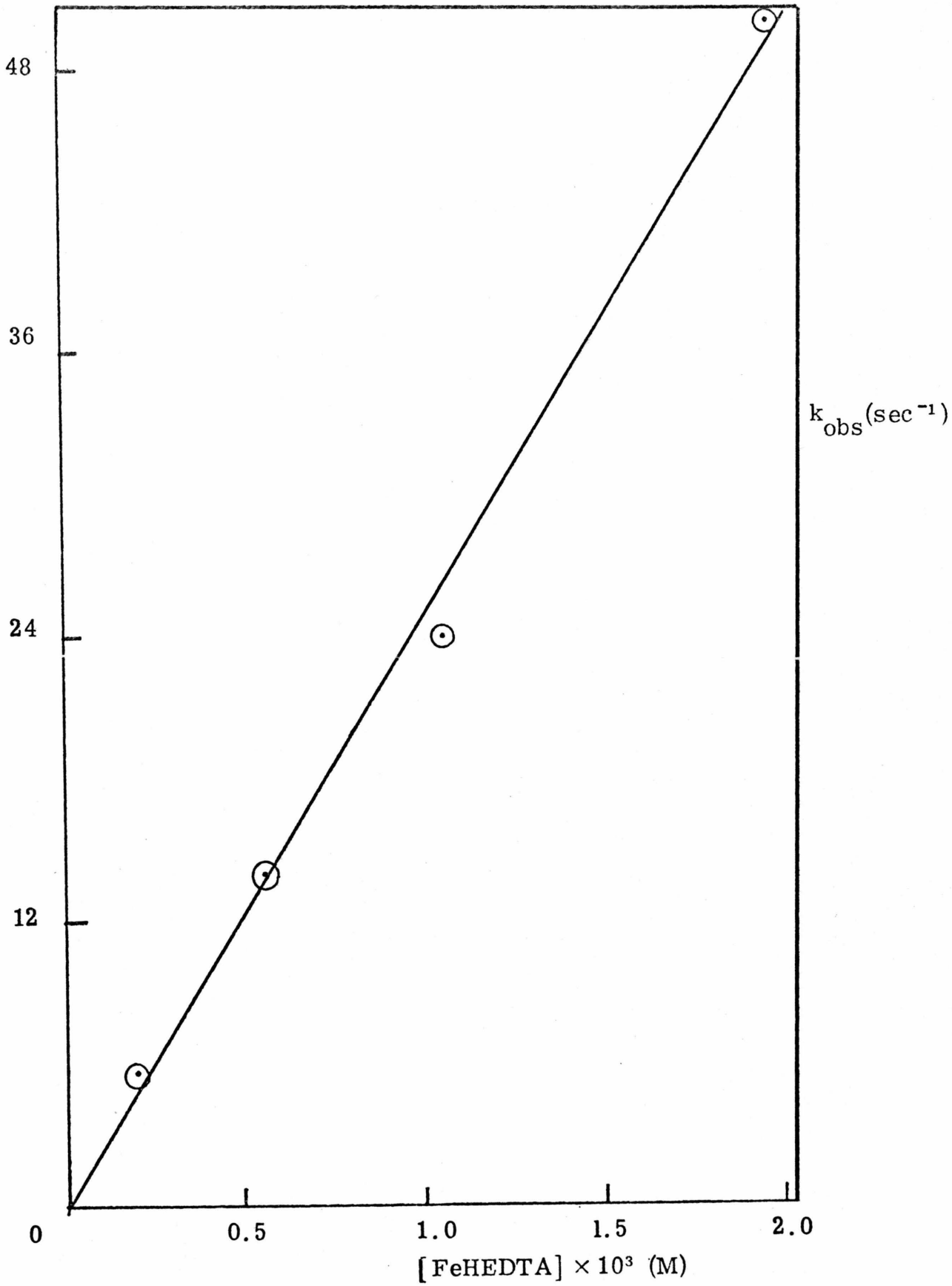
48
36
24
12
0
0.5
1.0
1.5
2.0
$k_{obs}(sec^{-1})$
[FeHEDTA] × 10^3 (M)

Table 2

Temperature Dependence of the Observed Rate Constants for the Reaction of $FeEDTA^-$ and FeHEDTA with Reduced Ferredoxin

$FeEDTA^-$ and Ferredoxin;
$\mu = 0.1$ Tris-Cl, pH 7.8, $[FeEDTA^-] = 1.9 \times 10^{-4}$ M, $[Fd] = 10^{-5}$ M, 465 nm

Temperature (°C)	k_{obs} (sec^{-1})
6.0	46.7
	48.0
12.5	53.8
	53.2
19.0	54.0
	54.5
26.0	60.0
	58.0
32	57.5
	59.2

FeHEDTA and Ferredoxin;
$\mu = 0.1$ Tris-NaCl, pH 7.8, $[FeHEDTA] = 2 \times 10^{-4}$ M, $[Fd] = 10^{-5}$ M, 465 nm

Temperature (°C)	k_{obs} (sec^{-1})
12.0	5.8
	5.5
26.0	5.6
	5.9
32.0	6.7
	6.4

Figure 2. Eyring plot for the reaction of ferredoxin with FeHEDTA ($\mu = 0.1$ Tris-NaCl, pH 7.8, [FeHEDTA] = $.2 \times 10^{-4}$ M, [Fd] = 10^{-5} M).

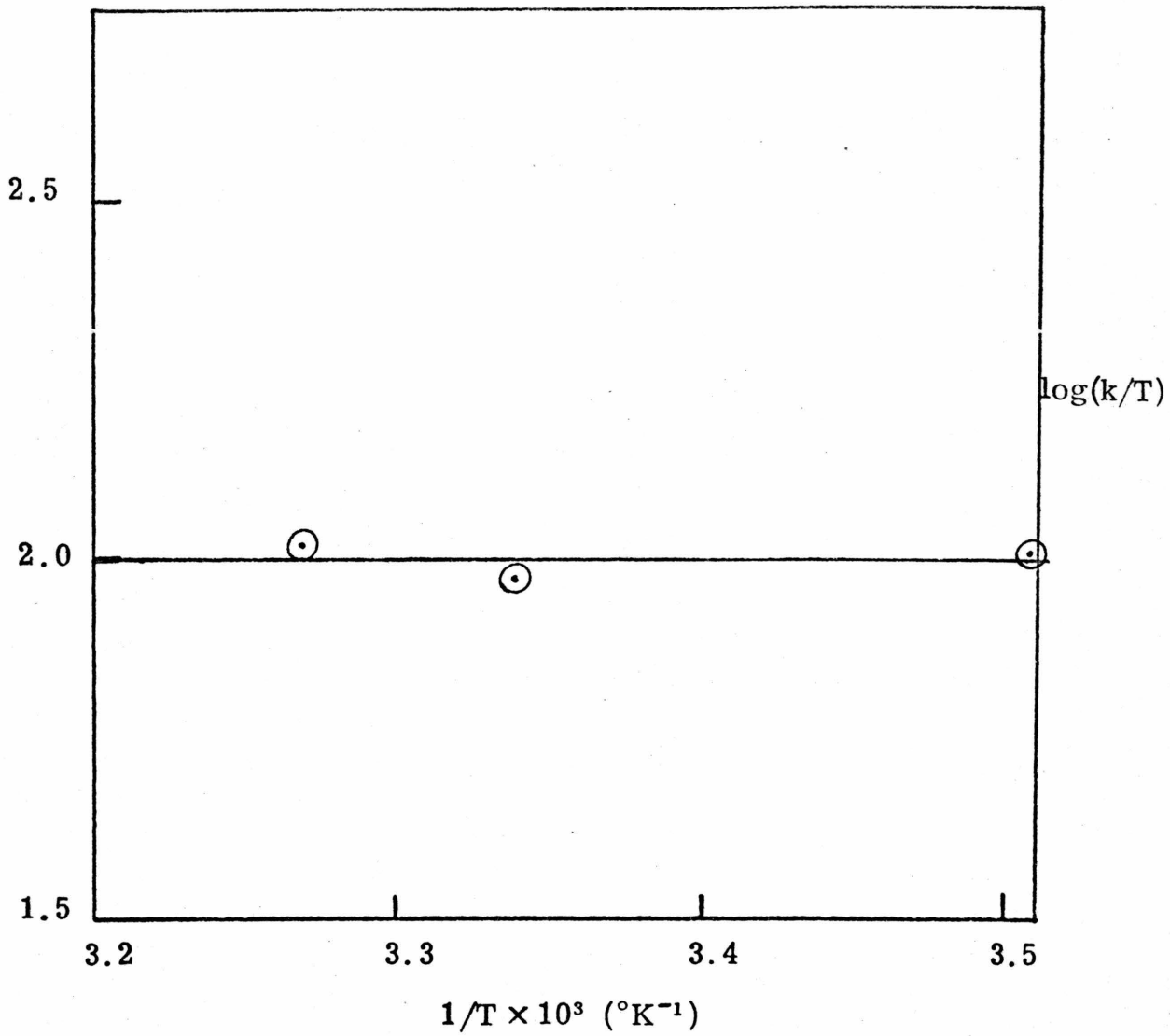

Table 3

pH Dependence of Observed Rate Constants for the Oxidation of Ferredoxin by $FeEDTA^-$; 25.5°C, $\mu = 0.1$ Tris-NaCl, $[FeEDTA^-] = 1.9 \times 10^{-4}$ M, $[Fd] = 10^{-5}$ M, 465 nm

pH	k_{obs} (sec^{-1})
6.7	121.2
	118.4
7.2	74.1
	76.5
7.8	47.8
	49.2
8.1	35.4
	34.8
8.7	19.5
	19.8
9.0	11.5
	11.1

Figure 3. pH Dependence of the Observed Rate Constants for the Oxidation of Ferredoxin by $FeEDTA^-$ (25.5 °C, $\mu = 0.1$ Tris-NaCl, $[FeEDTA^-] = 1.9 \times 10^{-4}$ M, $[Fd] = 10^{-5}$ M).

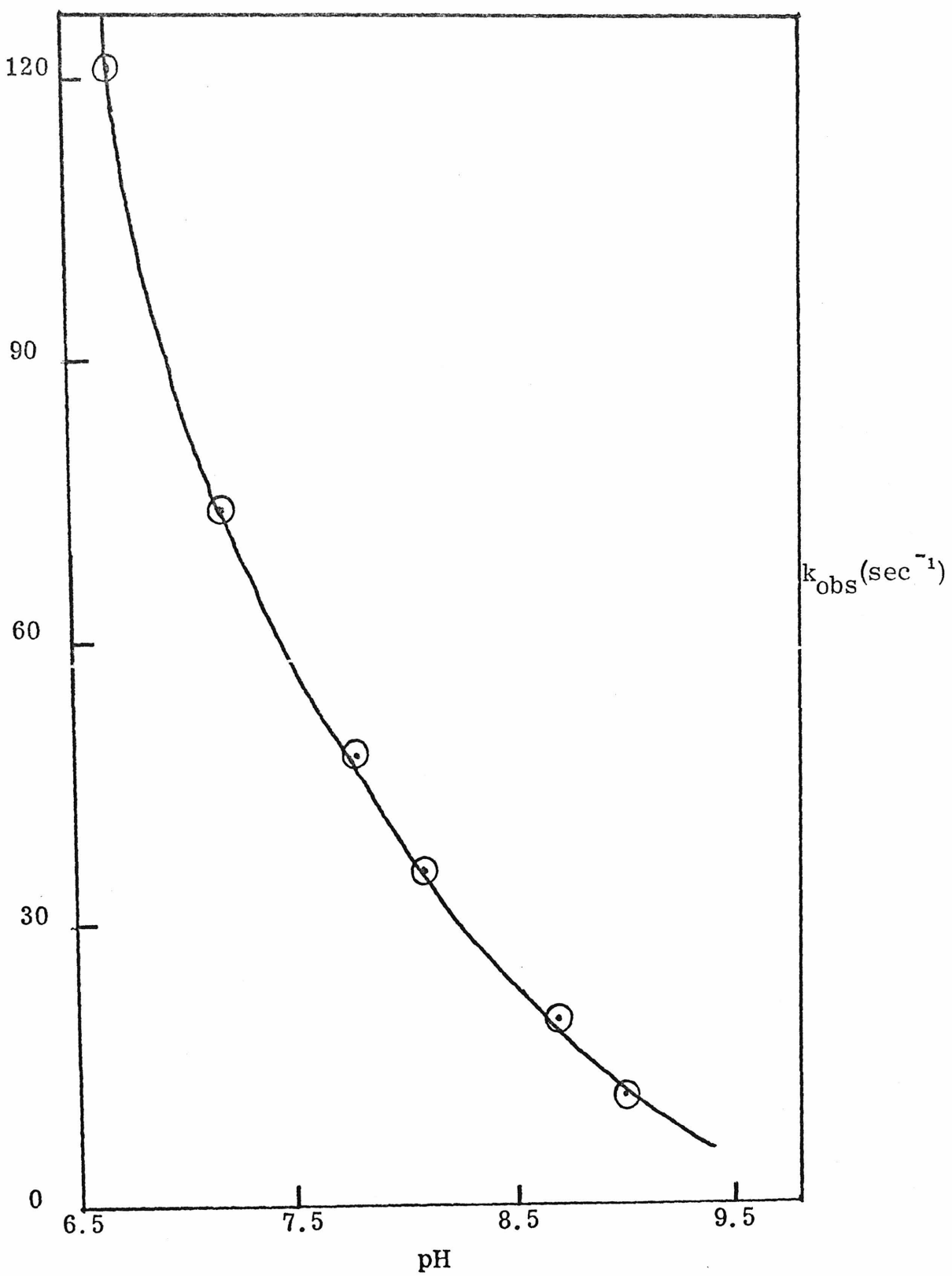
120
90
60
30
0
6.5
7.5
8.5
9.5
pH
$k_{obs}(sec^{-1})$

Table 4

Ionic Strength Dependence of Observed Rate Constants for the Oxidation of Ferredoxin by $FeEDTA^-$; 25.8 °C, pH 7.8, $[FeEDTA^-] = 2 \times 10^{-4}$ M, $[Fd] = 10^{-5}$ M, Tris-NaCl buffer, 465 nm

μ	k_{obs} (sec^{-1})
0.10	58.7
	56.5
0.24	74.5
	77.1
0.38	83.7
	85.2
0.59	93.4
	92.3
0.80	106.8
	103.9

Figure 4. Ionic Strength Dependence of Observed Rate Constants for the Oxidation of Ferredoxin by $FeEDTA^-$ (25.8 °C, Tris-NaCl buffer, pH 7.8, $[FeEDTA^-] = 2 \times 10^{-4}$ M, $[Fd] = 10^{-5}$ M).

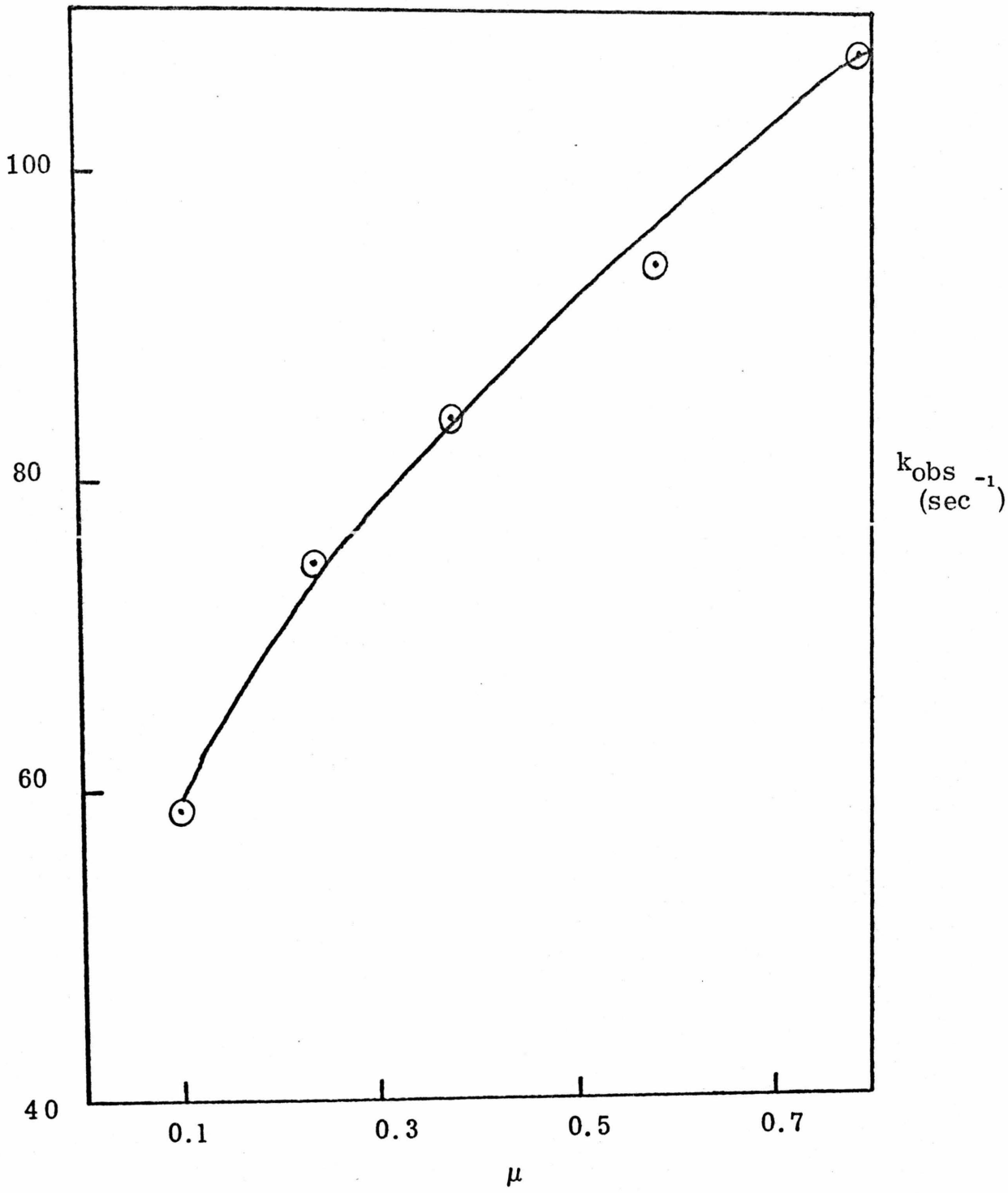

Table 5

Observed Rate Constants for the Reduction of HiPIP by $FeEDTA^{2-}$;
25°C, $\mu = 0.1$ phosphate-NaCl, pH 7.0,
$[HiPIP] = 8.1 \times 10^{-6}$ M, 480 nm

$[FeEDTA^{2-}] \times 10^4$ (M)	k_{obs} (sec^{-1})
1.0	0.20
	0.22
1.5	0.39
	0.36
2.5	0.44
	0.43
5.0	0.83
	0.74
7.5	1.28
	1.21
10.0	1.71
	1.59
15.0	2.1
	2.05
20.0	3.39
	3.30
25.0	4.29
	4.21

Table 6

Temperature Dependence of the Observed Rate Constants for the Reaction of $FeEDTA^{2-}$ with Oxidized HiPIP;
μ = 0.1 phosphate-NaCl, pH 7.0,
$[FeEDTA^{2-}] = 5 \times 10^{-4}$ M, [HiPIP] = 7.5×10^{-6} M, 480 nm

Temperature (°C)	k_{obs} (sec^{-1})
12.0	0.735
	0.70
17.0	0.75
	0.76
24.0	0.79
	0.83

Table 7

Observed Rate Constants for the Oxidation of HiPIP by $Fe(CN)_6^{3-}$;
25 °C, μ = 0.1 phosphate, pH 7.0
[HiPIP] = 8.1×10^{-6} M, 480 nm

$[Fe(CN)_6^{3-}] \times 10^4$ (M)	k_{obs} (sec^{-1})
1.04	0.189
	0.187
2.60	0.50
	0.49
5.20	1.04
	1.00
10.40	2.10
	2.10
26.0	5.70
	5.65
52.0	12.30
	12.25

Figure 5. Observed Rate Constants for the Oxidation of HiPIP by $Fe(CN)_6^{3-}$ (25 °C, $\mu = 0.1$ phosphate, pH 7.0, [HiPIP] $= 8.1 \times 10^{-6}$ M).

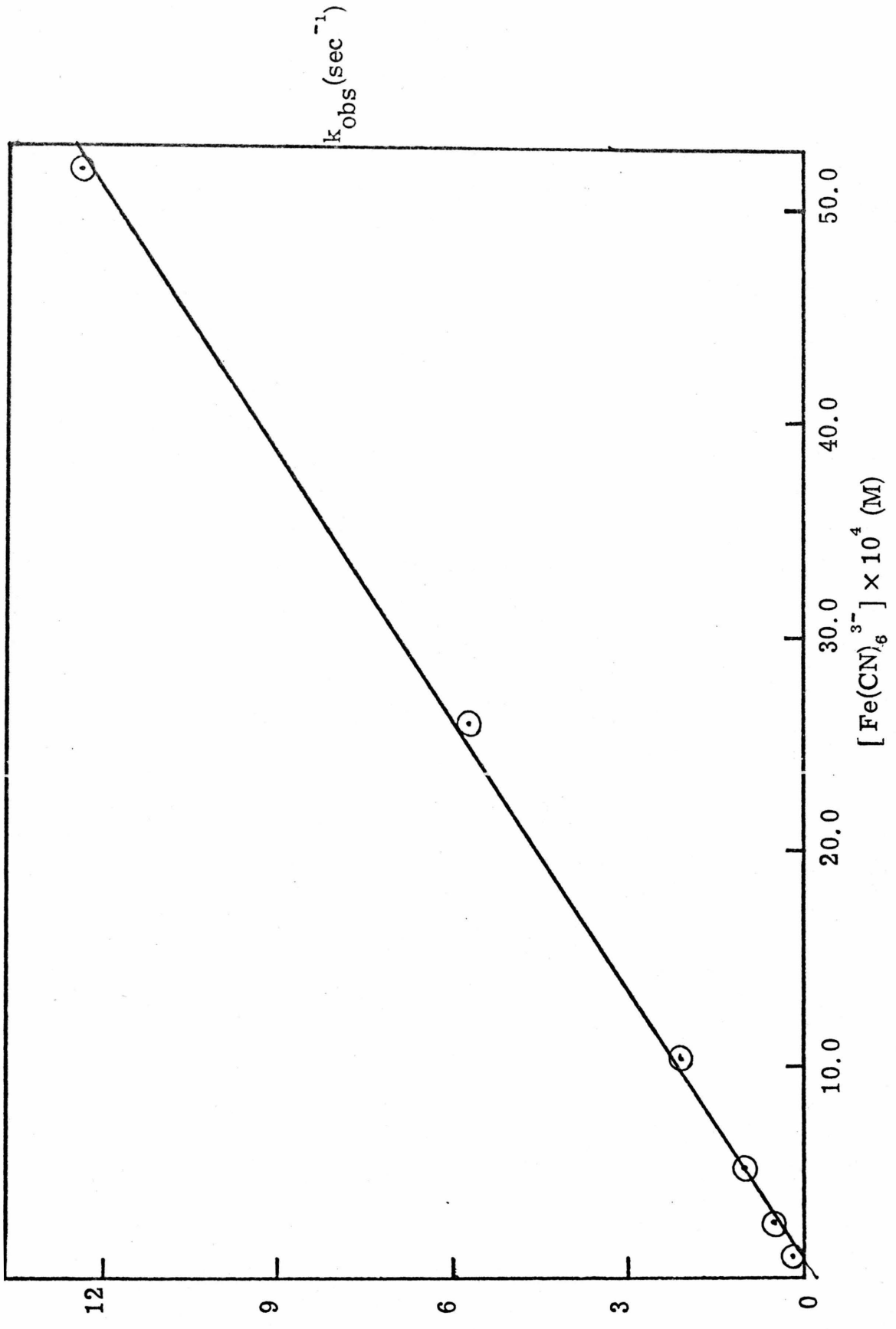
$k_{obs}(sec^{-1})$
12
9
6
3
0
10.0
20.0
30.0
40.0
50.0
$[Fe(CN)_6^{3-}] \times 10^4$ (M)

Table 8

Observed Rate Constants for the Oxidation of HiPIP by $Co(phen)_3^{3+}$; 26°C, $\mu = 0.1$ phosphate, pH 7.0, [HiPIP] = 7.0×10^{-6} M, 480 nm

$[Co(phen)_3^{3+}] \times 10^4$ (M)	k_{obs} (sec^{-1})
0.64	0.20
	0.18
1.27	0.38
	0.39
2.34	0.73
	0.79
5.85	1.66
	1.59
11.70	3.35
	3.28

Figure 6. Observed Rate Constants for the Reduction of $Co(phen)_3^{3+}$ by HiPIP (26 °C, $\mu = 0.1$ phosphate, pH 7.0, [HiPIP] $= 7.0 \times 10^{-6}$ M).

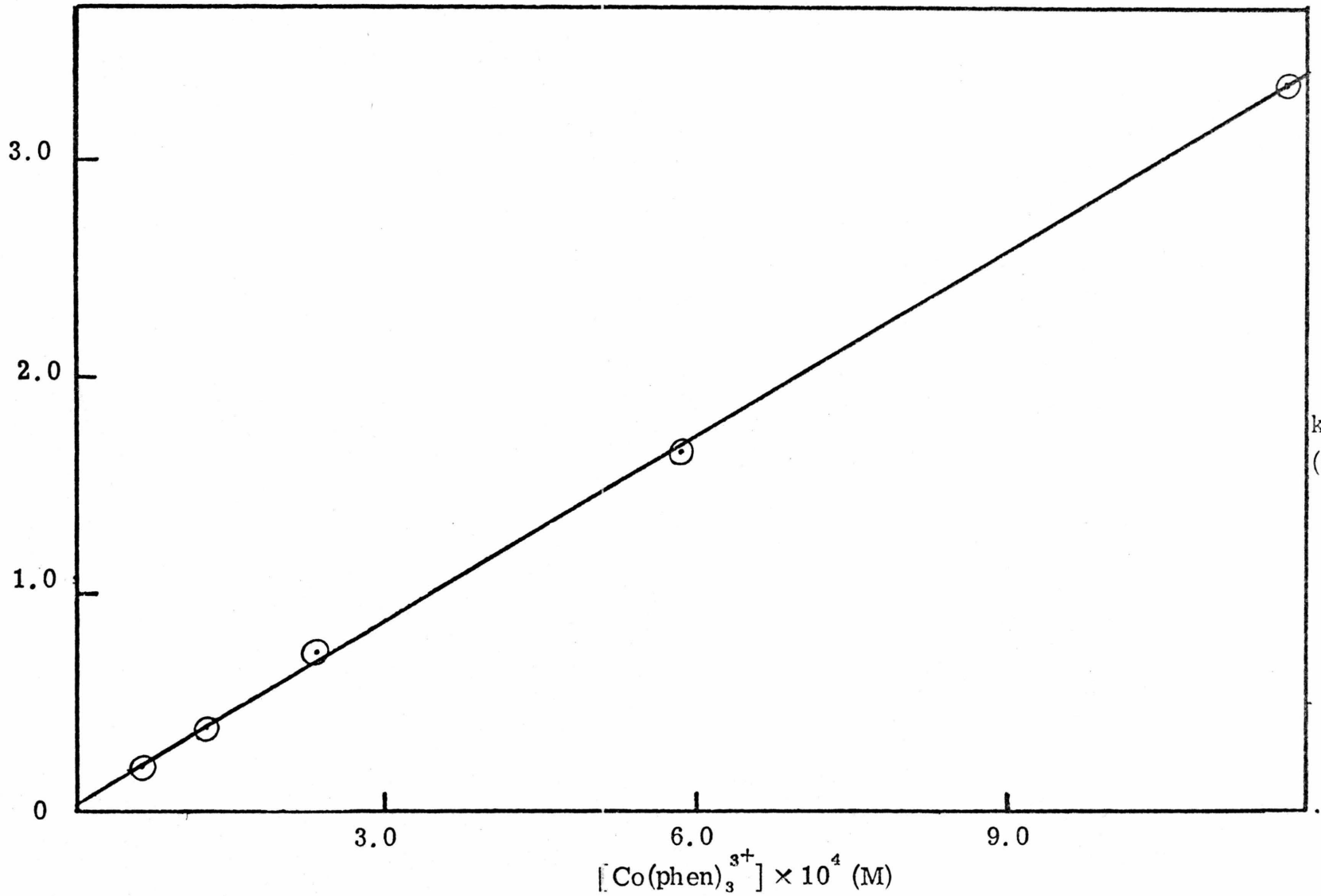
3.0
2.0
1.0
0
3.0
6.0
9.0
$[Co(phen)_3^{3+}] \times 10^4$ (M)
k_{obs} (sec^{-1})

Table 9

Temperature Dependence of the Observed Rate Constants for the Reaction of $Fe(CN)_6^{3-}$ with Reduced HiPIP; $\mu = 0.1$ phosphate, pH 7.0, $[Fe(CN)_6^{3-}] = 1.05 \times 10^{-4}$ M, [HiPIP] = 8.1×10^{-6} M, 480 nm

Temperature (°C)	k_{obs} (sec^{-1})
12.0	0.186
	0.185
17.5	0.187
	0.186
25.0	0.189
	0.185

Figure 7. Eyring plot for the reaction of HiPIP and $Fe(CN)_6^{3-}$ ($\mu = 0.1$ phosphate, pH 7.0, $[Fe(CN)_6^{3-}] = 1.05 \times 10^{-4}$ M, [HiPIP] $= 8.1 \times 10^{-6}$ M).

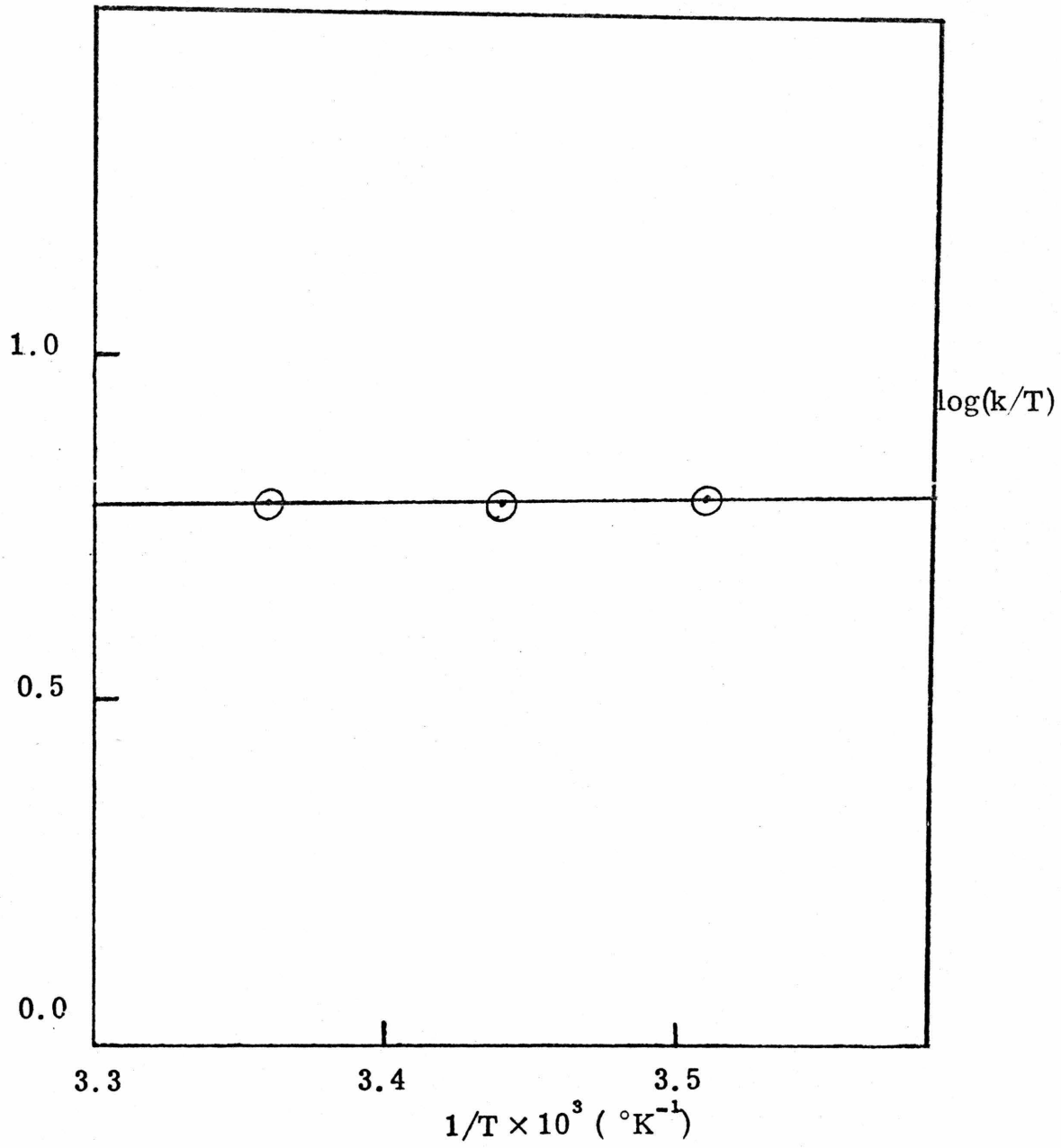

Table 10

Temperature Dependence of the Observed Rate Constants for the Reaction of $Co(phen)_3^{3+}$ with Reduced HiPIP; μ = 0.1 phosphate, pH 7.0, $[Co(phen)_3^{3+}]$ = 1.42×10^{-4} M, [HiPIP] = 6.5×10^{-6} M, 480 nm

Temperature (°C)	k_{obs} (sec^{-1})
12.0	0.13
	0.12
18.0	0.21
	0.21
26.0	0.42
	0.40
33.0	0.85
	0.81

Figure 8. Eyring Plot for the Reaction of HiPIP and $Co(phen)_3^{3+}$ ($\mu = 0.1$ phosphate, pH 7, $[Co(phen)_3^{3+}] = 1.42 \times 10^{-4}$ M, $[HiPIP] = 6 \times 10^{-6}$ M).

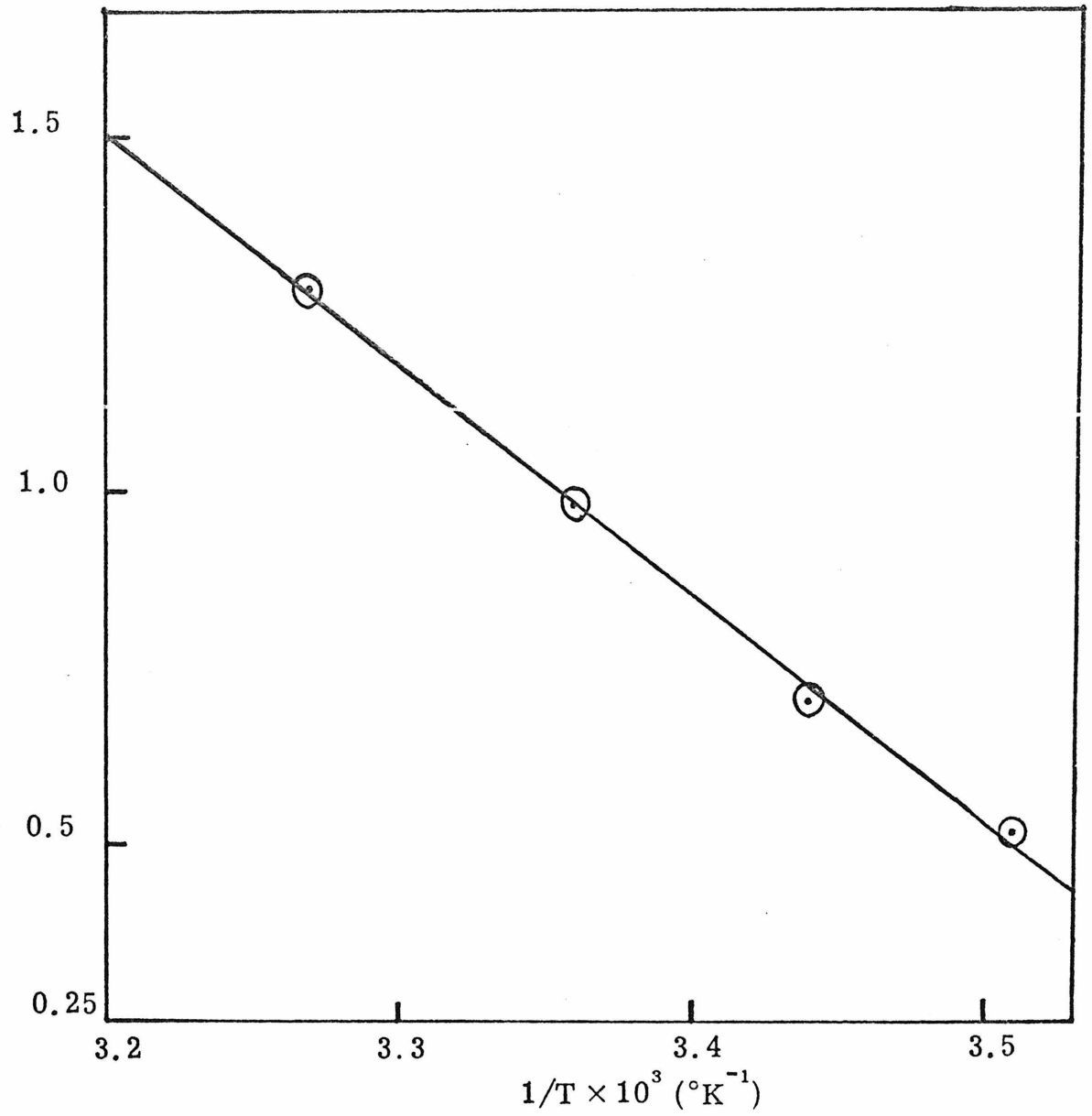

Table 11

pH Dependence of Observed Rate Constants for the Oxidation of HiPIP by $Co(phen)_3^{3+}$; 25.5°C, μ = 0.1 phosphate, $[Co(phen)_3^{3+}] = 1.27 \times 10^{-4}$ M, [HiPIP] = 6.5×10^{-6} M, 480 nm

pH	k_{obs} (sec^{-1})
5.2	0.28
	0.27
6.0	0.32
	0.32
7.0	0.38
	0.37
8.0	0.45
	0.46

Figure 9. pH Dependence of the Observed Rate Constants for the Oxidation of HiPIP by $Co(phen)_3^{3+}$ (25.5 °C, $\mu = 0.1$ phosphate, $[Co(phen)_3^{3+}] = 1.27 \times 10^{-4}$ M, [HiPIP] $= 6.5 \times 10^{-6}$ M).

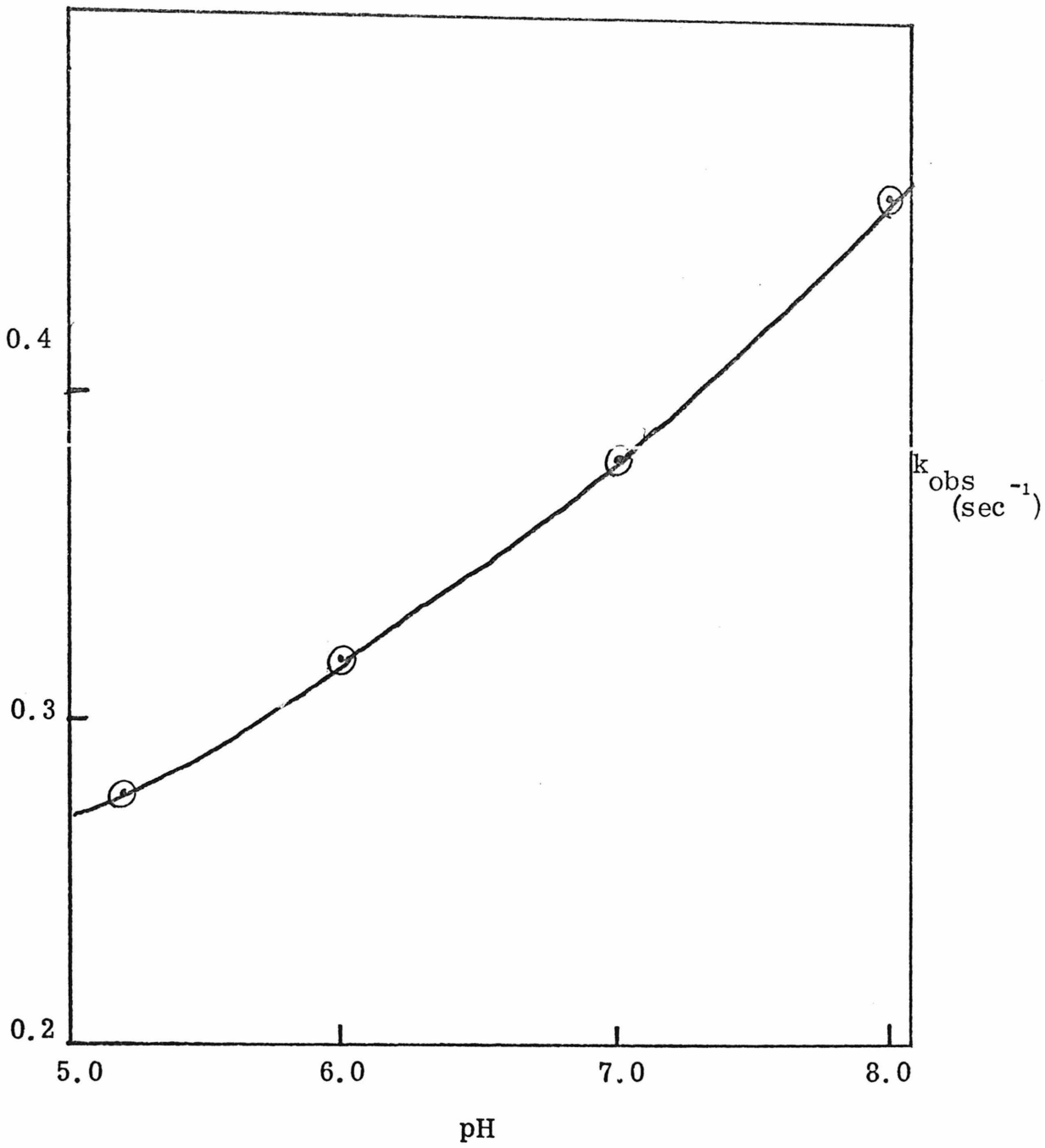

Table 12

Observed Rate Constants for the
Reactions of Flavins with Reduced Ferredoxin;
26°C, μ = 0.1 Tris-NaCl, pH 7.8, [Fd] = 1.5×10^{-5} M, 540 nm

FAD and Ferredoxin

$[FAD] \times 10^4$ (m)	k_{obs} (sec^{-1})
0.58	59
	57
2.35	304
	295
4.69	580
	550

FMN and Ferredoxin

$[FMN] \times 10^4$ (m)	k_{obs} (sec^{-1})
0.58	92
	88

Riboflavin and Ferredoxin

$[R] \times 10^4$ (m)	k_{obs} (sec^{-1})
0.58	560
	540

Table 13

$FADH_2$ Dependence of Observed Rate Constants for the Reaction of FAD with Reduced Ferredoxin;

26°C, μ = 0.1 Tris-NaCl, pH 7.8, [FAD] = 6.8×10^{-5} M, [Fd] = 1.5×10^{-5} M, 540 nm

$[FADH_2] \times 10^6$ (m)	k_{obs} (sec^{-1})
0	52.9
	55.0
0.28	63.5
	60.3
5.6	74.8
	72.6
33.2	116
	110
83	168
	160

Table 14

Temperature Dependence of the Observed Rate Constant for the Reaction of Reduced Ferredoxin with FAD;

μ = 0.1 Tris-NaCl, pH 7.8, [FAD] = 5.88×10^{-5} M, [Fd] = 1.5×10^{-5} M, 540 nm

Temperature (°C)	k_{obs} (sec^{-1})
14.0	43.2
	44.5
19.0	54.0
	52.1
26.0	60.0
	61.8

Figure 10. Eyring Plot for the Reaction of FAD and Ferredoxin ($\mu = 0.1$ Tris-NaCl, pH 7.8, $[FAD] = 5.85 \times 10^{-5}$ M, $[Fd] = 1.5 \times 10^{-5}$ M).

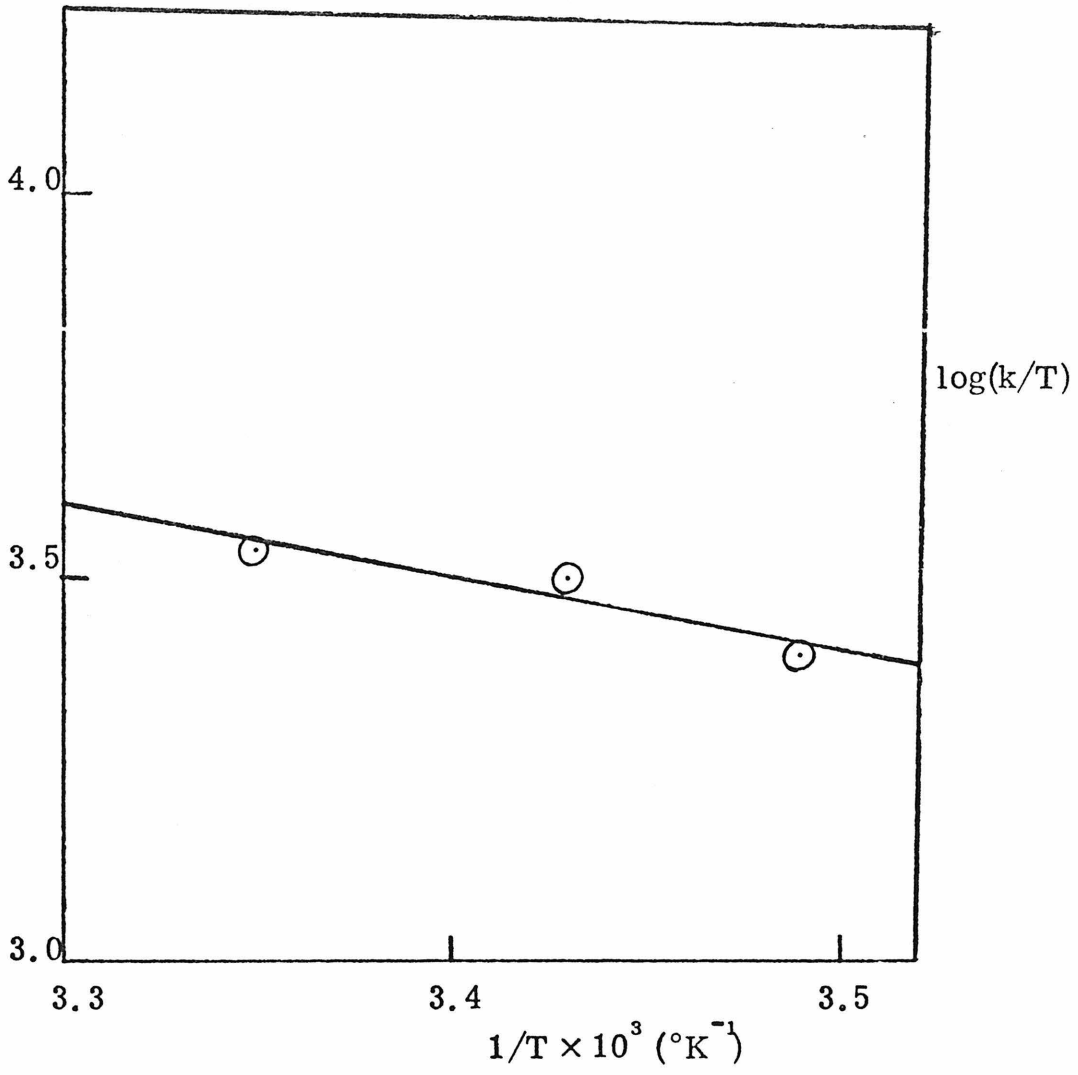

Table 15

Ionic Strength Dependence of the Observed Rate Constants for the Reaction of Reduced Ferredoxin with FAD;

26°C, Tris-NaCl buffer, pH 7.8, [FAD] = 3.59×10^{-5} M, [Fd] = 1.5×10^{-5} M, 540 nm

Ionic Strength	k_{obs} (sec^{-1})
0.01	29.1
	28.0
0.33	72.0
	71.6
0.50	94.5
	93.8
0.80	124
	120

Figure 11. Ionic Strength Dependence of Observed Rate Constants for the Oxidation of Ferredoxin by FAD (26 °C, Tris-NaCl buffer, pH 7.8, [FAD] = 3.59×10^{-5} M, [Fd] = 1.5×10^{-5} M).

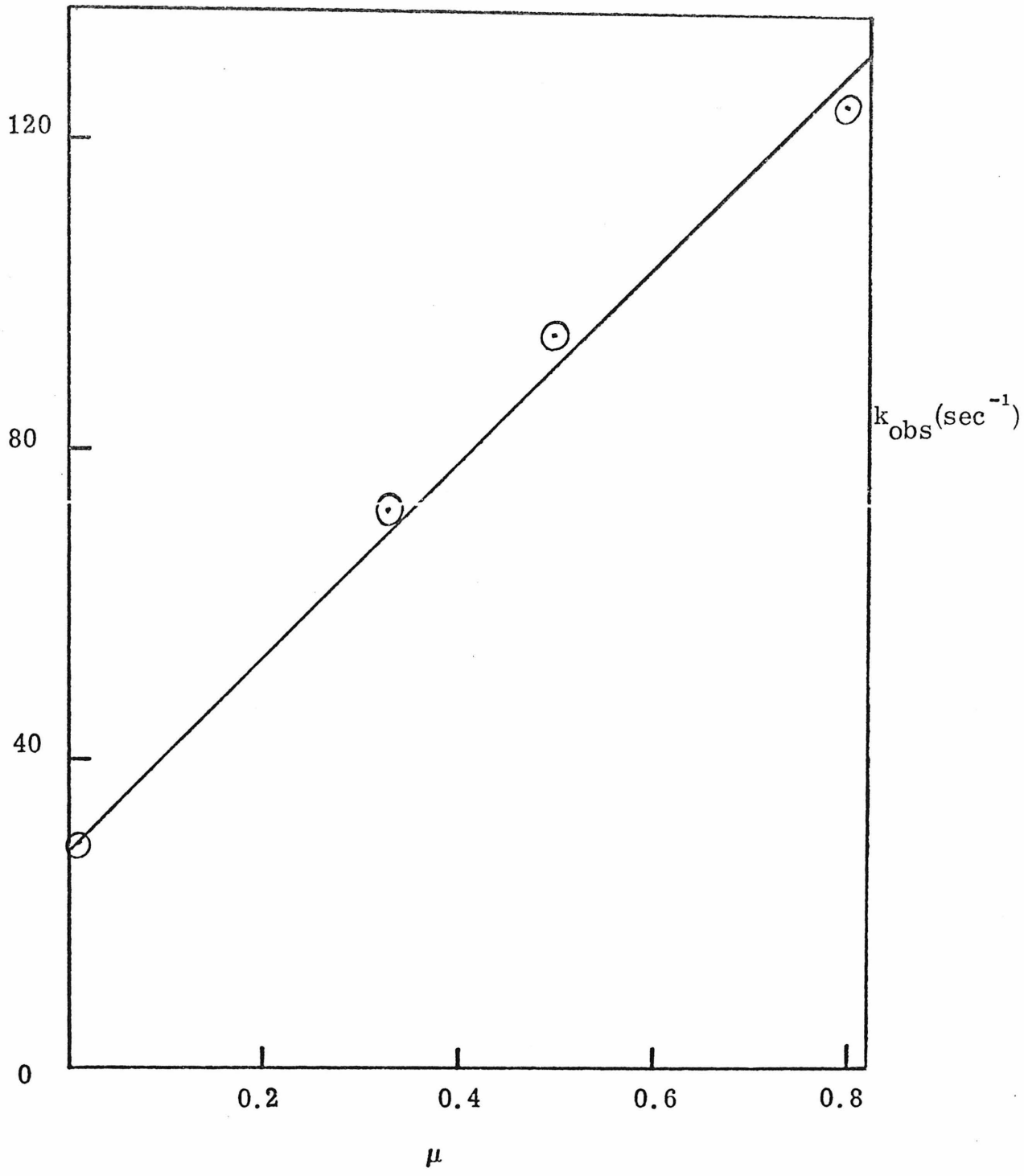

Table 16

Rate Data for the Reduction of FTR by Ferredoxin

Temperature Dependence of the Observed Rate Constants:
μ = 0.1 Tris-NaCl, pH 7.8, [FTR] = 6.3×10^{-6} M,
[Fd] = 5.4×10^{-5} M, 510 nm

Temperature (°C)	k_{obs} (sec^{-1})
12.0	0.50
	0.48
18.0	0.44
	0.46
25.0	0.50
	0.50

Ionic Strength Dependence of the Observed Rate Constants;
25°C, Tris-NaCl buffer, pH 7.8, [FTR] = 6.3×10^{-6} M;
[Fd] = 5.4×10^{-5} M, 510 nm

Ionic Strength	k_{obs} (sec^{-1})
0.10	0.50
	0.50
0.80	1.80
	1.74

Figure 12. Eyring Plot for the Reaction of Ferredoxin and FTR (μ = 0.1 Tris-NaCl, pH 7.8, [FTR] = 6.3×10^{-6} M, [Fd] = 5.4×10^{-5} M).

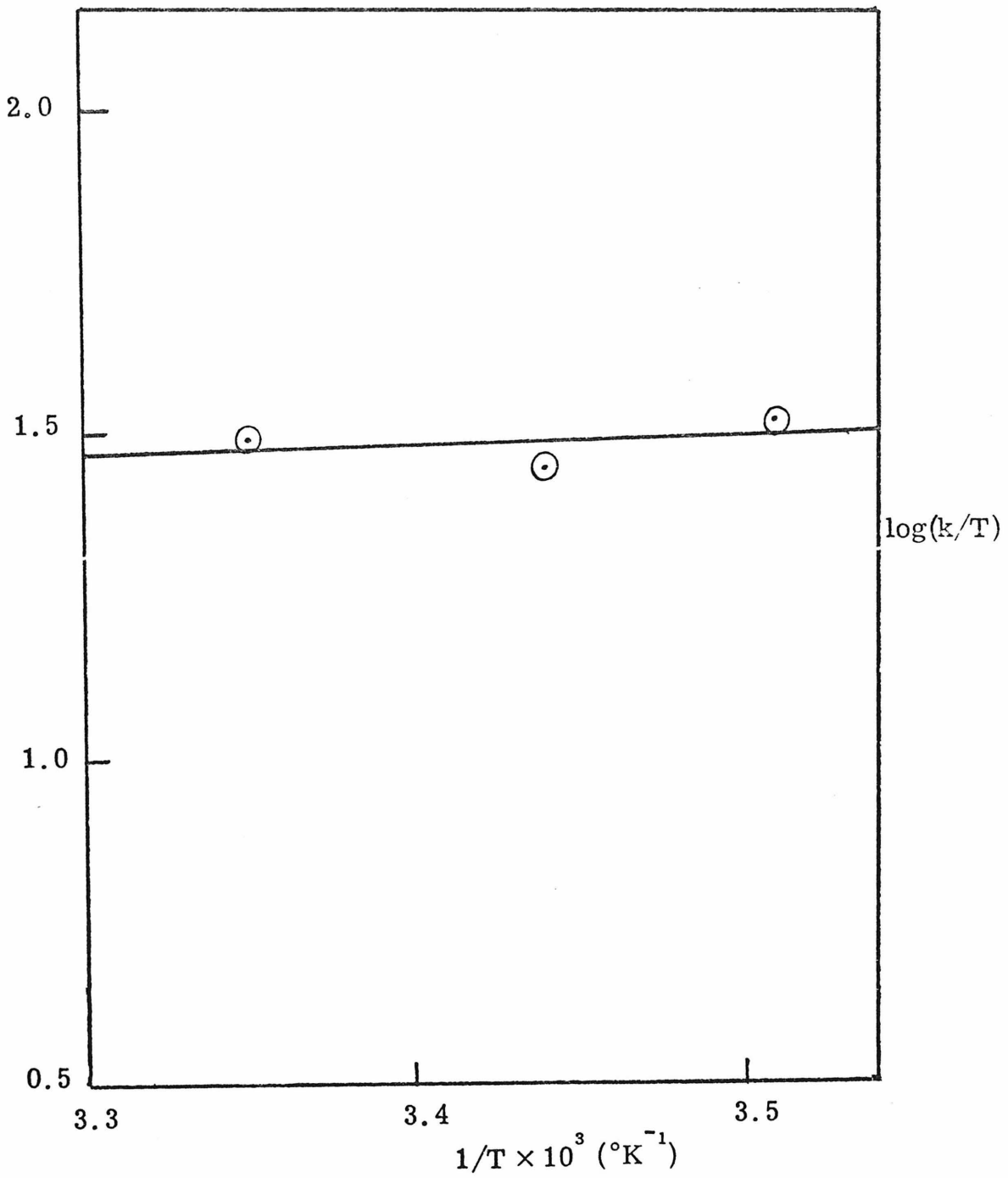

Table 17

Observed Rate Constants for the Oxidation of Ferredoxin by Heme Proteins

Metmyoglobin and Ferredoxin;

25°C, μ = 0.1 phosphate, pH 7.0, [Fd] = 5×10^{-6} M, 560 nm

[mMb] $\times 10^5$ (M)	k_{obs} (sec^{-1})
1.85	52
	49
2.84	80.3
	78.2
3.68	94.3
	92.8
3.97	96.5
	99.0
5.6	141
	140

Cytochrome c and Ferredoxin;

25°C, μ = 0.1 phosphate, pH 7.0, [Fd] = 2.5×10^{-6} M, 550 nm

[Cyt c] $\times 10^5$ (M)	k_{obs} (sec^{-1})
2.05	1.7
	1.8
2.7	2.1
	2.1
3.26	2.7
	2.5
3.67	3.2
	3.4
6.0	4.9
	4.8

Figure 13. Observed Rate Constants for the Reduction of MetMyoglobin by Ferredoxin (25 °C, $\mu = 0.1$ phosphate, pH 7.0, $[Fd] = 5 \times 10^{-6}$ M).

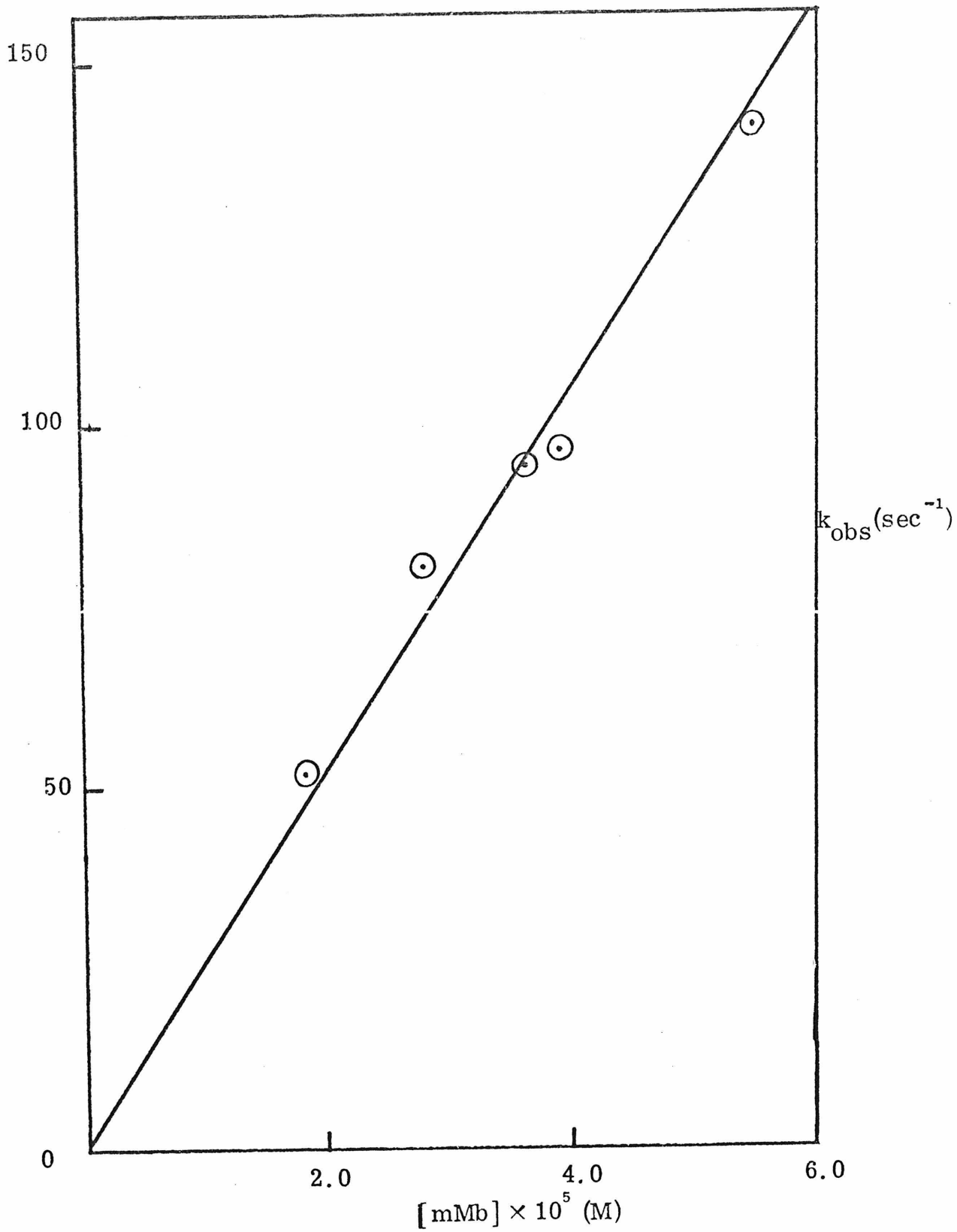
150
100
50
0
2.0
4.0
6.0
$k_{obs}(sec^{-1})$
$[mMb] \times 10^5$ (M)

Table 18

Temperature Dependence of the Observed Rate Constants for the Reactions of metMyoglobin and Cytochrome c with Reduced Ferredoxin

metMyoglobin and Ferredoxin;
μ = 0.1 phosphate, pH 7.0, [mMb] = 5.6×10^{-5} M,
[Fd] = 5×10^{-6} M, 560 nm

Temperature (°C)	k_{obs} (sec^{-1})
12.5	145
19.0	142
25.0	141

Cytochrome c and Ferredoxin;
μ = 0.1 phosphate, pH 7.0, [Cyt c] = 2.05×10^{-5} M,
[Fd] = 2.5×10^{-6} M, 550 nm

Temperature (°C)	k_{obs} (sec^{-1})
13.0	0.77
	0.72
18.0	1.06
	1.03
21.0	1.20
	1.24
25.0	1.66
	1.71

Figure 14. Eyring plot for the reaction of Ferredoxin and MetMyoglobin ($\mu = 0.1$ phosphate, pH 7.0, [mMb] $= 5.6 \times 10^{-5}$M, [Fd] $= 5 \times 10^{-6}$M).

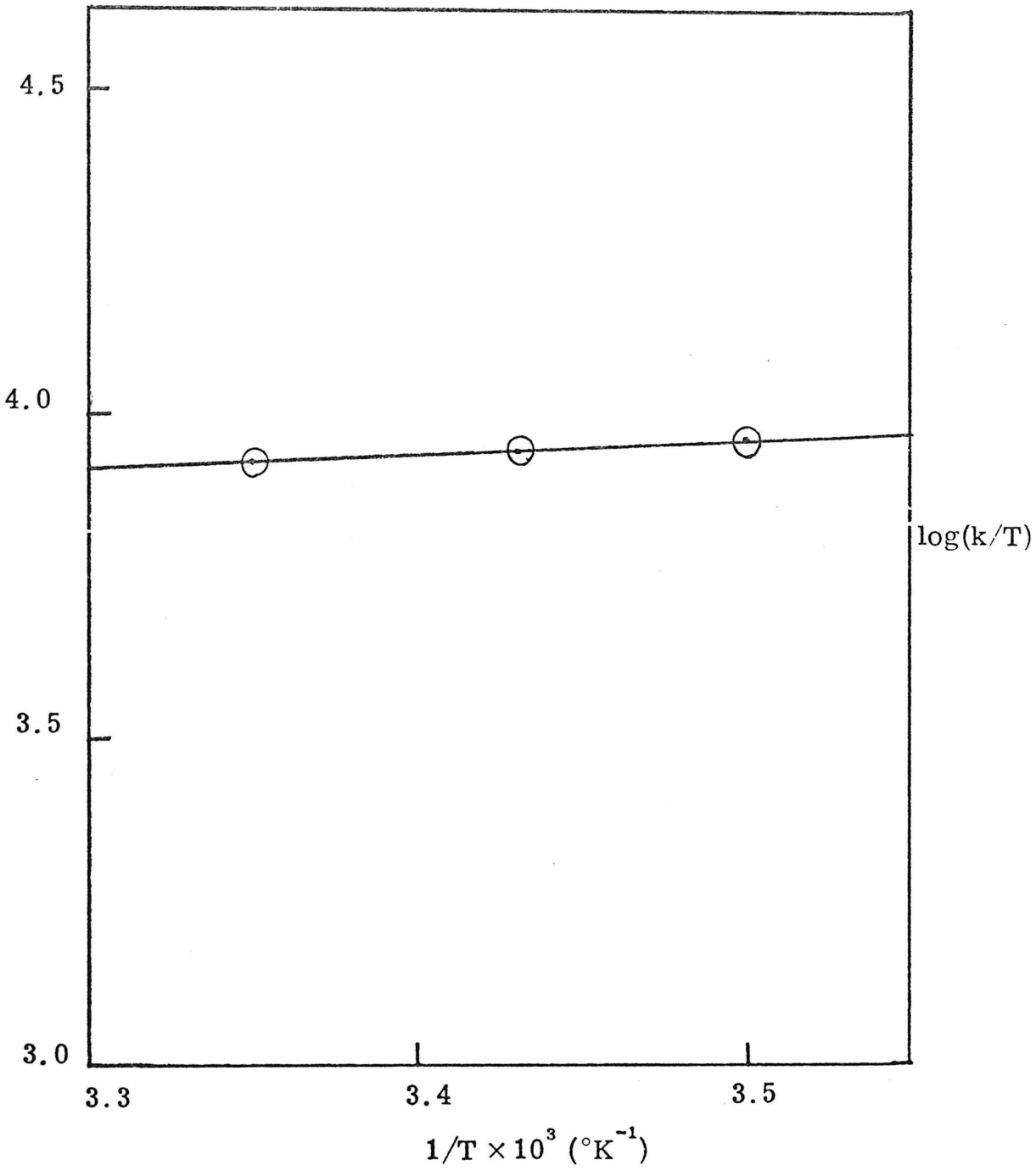

Table 19

pH Dependence of the Observed Rate Constants for the Reaction of metMyoglobin with Reduced Ferredoxin;

25°C, μ = 0.1 phosphate, [mMb] = 5.6×10^{-5} M, [Fd] = 5×10^{-6} M, 560 nm

pH	k_{obs} (sec^{-1})
6.0	408
	390
7.0	141
	138
8.0	80.5
	79.4

Figure 15. pH Dependence of the Observed Rate Constants for the Reaction of Ferredoxin and MetMyoglobin (25.5 °C, $\mu = 0.1$ phosphate, [mMb] $= 5.6 \times 10^{-5}$ M, [Fd] $= 5 \times 10^{-6}$ M).

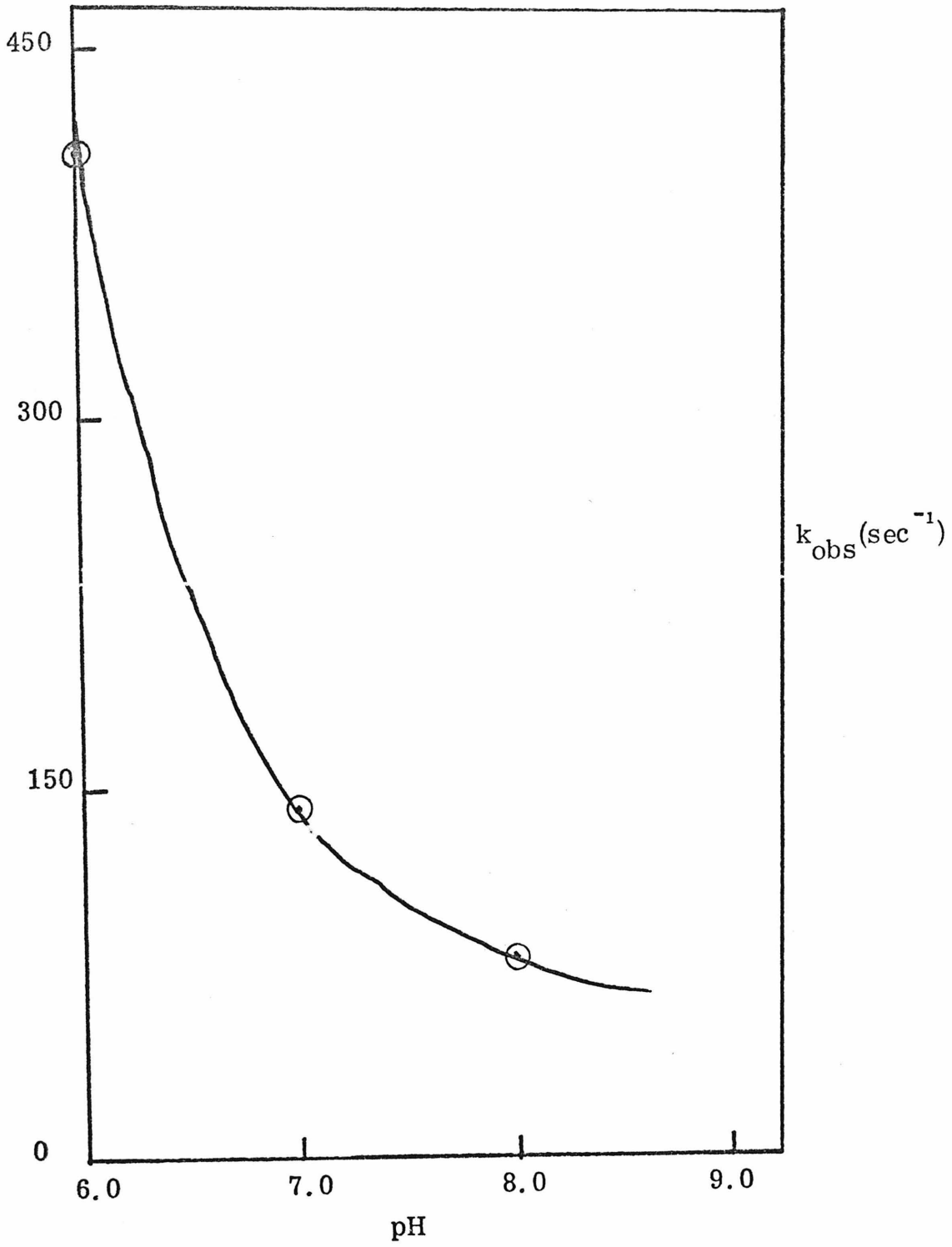

Table 20

Observed Rate Constants for the
Reaction of Ferredoxin with metMyoglobin-Fluoride;
25°C, μ = .8 Tris-Cl + NaF, pH 7.7, [Fd] = 5×10^{-6} M, 610 nm

$[mMb\text{-}F] \times 10^5$ (m)	k_{obs} (sec^{-1})
3.03	.38
	.39
5.28	.29
	.40
6.62	.43
	.44
7.12	.41
	.43
10.3	.46
	.44
15.4	.45
	.45

PROPOSITIONS

PROPOSITION I

Although the iron-sulfur proteins have been well characterized by many physical techniques,[1] there still remain a number of intriguing problems. One, for example, is concerned with the description of the electronic structure of the various cluster proteins. It seems clear that the model cluster, $(Et_4N)_2[Fe_4S_4(SCH_2Ph)_4]$, is a completely delocalized electronic system.[2] However, the spectral work on reduced HiPIP would seem to indicate that there may be some protein-induced inequivalence in the cluster.[3] The nature of the protein effect on the cluster is not well understood.

In addition to perturbing the electronic spectrum, the protein must also influence the oxidation levels that the cluster exhibits. Thus, the cluster proteins are isolated in an even electron state. However, the 8 iron protein can add an electron to this state, at a very low potential, while the 4 iron protein shows an oxidation from this even electron state. The factors that govern this redox behavior must reflect the influence of the protein, since the structural details of the clusters are so similar.[4]

Another type of protein has recently been described which has four iron but a low potential. Shethna reported a protein from Bacillus Polymyxa that contained four iron but had the low potential (E° = -.33v) characteristic of the 8 iron protein.[5] Similar proteins

were subsequently found in D. gigas[6] and D. desulfuricans.[7] It is not clear, however, what type of electronic structure these proteins have, or if they are functionally similar to the eight iron protein. By studying a variety of types of iron-sulfur proteins, it may be possible to understand the nature of the protein influence on the cluster, which must influence the redox behavior and the electronic structure. It is thus proposed that these four iron low potential proteins be studied by the full array of physical methods which have been used on HiPIP. By contrasting the various types of proteins, one might better understand the forces governing the structures, potentials, and reactivity of cluster proteins. A comprehensive view of the iron-sulfur proteins must include an understanding of the similarities and differences of HiPIP, bacterial ferredoxins, and four iron ferredoxins.

A comparison of the sequence data on these proteins should provide useful information. The sequences and structures of a number of HiPIPs and ferredoxins are known.[8,9] The amino acid composition of three four iron proteins have been reported,[7] and the sequence of the D. gigas protein has been reported.[10] The sequence of the D. gigas protein is fairly similar to the bacterial proteins for amino acid residues 1 to 29, with a phenylalanine present in the sequence instead of the tyrosine found in the eight iron proteins. However, the protein from D. desulfuricans apparently has no aromatic residues.[7] A study of the amino acids that would be near the cluster in this protein could indicate whether or not the cluster requires a hydrophobic environment.

It has been postulated that aromatic groups function in the protein's redox reaction and are perhaps necessary to stabilize the cluster.[11] Thus, a comparison of several of the eight and four iron protein sequences could indicate what parts of the sequence must be conserved to create an environment favoring a low potential.

The similarity of the electronic structures of these proteins could be studied by use of optical spectra. The visible spectra of these four iron low potential proteins have been reported and reveal the broad absorption band centered at 390 nm typical of the cluster proteins.[6] However, the near infrared spectra of these proteins have not been reported. The comparison between the spectra of these proteins and of reduced HiPIP, super-reduced HiPIP, Holm's model cluster, and the eight iron bacterial ferredoxins should be most informative. One would expect near infrared spectra of the low potential proteins to be similar. However, it is not known whether the low potential proteins show any evidence of localized electronic structure such as the 1040 nm band in HiPIP. Thus, a near IR study of the eight and four iron proteins is necessary for a complete description of the electronic structures. It is possible that these low potential iron proteins are the best analogues of the model compound $(Et_4N)_2[Fe_4S_4(SCH_2Ph)_4]$. It is a possibility that the protein induced electron delocalization and the redox behavior are related. Thus, HiPIP is characterized by an oxidation and a 1040 nm band; it may be that the low potential proteins, which show a reduction,

have no 1040 nm band, are completely delocalized, and are the best examples of the delocalized model.

The question of electronic structures of the four iron, low potential proteins can also be studied by use of Mossbauer spectroscopy and ESCA. Inequivalent iron could be revealed by broadening of the Mossbauer lines or a splitting in the ESCA spectra. One should also be able to compare the Mossbauer parameters and the binding energies of the two low potential proteins to determine how similar these iron clusters are.

There is some reason to expect that the four iron low potential protein might show some anomalies. This protein has unusual magnetic behavior, showing an esr spectrum in both reduced and oxidized states. The $g = 2.0$ signal found for the oxidized protein disappears on the one electron reduction with sodium dithionite to give the typical $g = 1.94$ type of signal found for the reduced eight iron ferredoxins.[5] The intensities of these signals are approximately equal, thus ruling out impurity as a cause of the $g = 2.0$ signal. The nature of this signal is thus in doubt. It may reflect the presence of an excited state very close to the ground state, or it could indicate an unpaired electron associated more with the protein. Magnetic susceptibility studies could help determine the ground states of these species. In particular, one would want to determine if the ground state of the reduced protein was an $S = 1/2$ state, of if there was any antiferromagnetic coupling present. NMR contact shifts could also indicate antiferromagnetic coupling.

Thus, a number of studies can be made on the four iron proteins having low potentials. These studies can reveal the similarities between the electronic structure of this protein and the other proteins and model compound that contain the four iron cluster. By making a complete study of the different examples, one can come to an understanding of the forces that govern the redox behavior and electronic structures of these cluster proteins.

References

1. W. R. Dunham, G. Palmer, R. H. Sands, and A. J. Bearden, Biochem. Biophys. Acta., 253, 373 (1971)

2. R. H. Holm, B. A. Averill, T. Herskovitz, R. B. Frankel, H. B. Gray, O. Siiman, and F. J. Grunthaner, J. Amer. Chem. Soc., 96, 2644 (1974).

3. J. Rawlings and H. B. Gray, J. Amer. Chem. Soc., in press.

4. C. W. Carter, Jr., J. Kraut, S. T. Freer, R. A. Alden, L. C. Sieker, E. Adman, and L. H. Jensen, Proc. Nat. Acad. Sci. U. S., 69, 3526 (1972).

5. Y. I. Shethna, N. A. Stombaugh, and R. H. Burris, Biochem. Biophys. Res. Comm., 42, 1108 (1971).

6. J. LeGall and N. Dragoni, Biochem. Biophys. Res. Comm., 23, 145 (1966).

7. J. A. Zubieta, R. Mason, and J. R. Postgate, Biochem. J., 133, 851 (1973).

8. M. Tanaka, J. Biol. Chem., 246, 3953 (1971).

9. K. Dus, S. M. Tedro, R. G. Bartsch, and M. D. Kamen, Biochem. Biophys. Res. Comm., 43, 1239 (1971).

10. J. Travis, D. J. Newman, J. LeGall, H. D. Peck, Jr., Biochem. Biophys. Res. Comm., 45, 452 (1971).

11. R. Mason and J. A. Zubieta, Angew. Chem., 85, 390 (1973).

PROPOSITION II

Magnetic circular dichroism has provided a new spectroscopic tool for the characterization of metal systems;[1,2] it can provide information on the ground and excited states of many complexes. This technique has recently been applied to several biological systems of the heme type. For example, studies of methemoglobin and its derivatives in the near infrared spectral region have shown a correlation between the band position and the spin state of the heme; the near IR bands of hemoproteins are a sensitive indicator of metal coordination, oxidation state, and spin state.[3] MCD has also been applied to several other problems of heme protein chemistry. For example, the technique has been used to study spin-state equilibrium in some hemoproteins[4] and to study the dissociation of hemoglobin into subunits at high pH.[5] Thus, the MCD spectrum of a heme compound can provide very sensitive information about the iron atom structure.

A number of heme proteins are involved in the hydroxylations of biological compounds; these proteins incorporate one or both atoms of molecular oxygen into the compound. L-tryptophan-2,3-dioxygenase, for example, catalyzes the conversion of tryptophan to formylkynurenine by incorporating both atoms of molecular oxygen into the substrate.[6] The enzyme occurs in a variety of sources; the protein isolated from Pseudomonas acidovorans has a molecular weight of 122,000 and consists of four subunits of identical molecular weight.[6] The dioxygenase

isolated from rat liver has a slightly higher molecular weight, but also consists of four subunits, tentatively identified as an $\alpha_2\beta_2$ arrangement.[7] Both proteins contain two heme and two copper.[8]

Another heme system which hydroxylates camphor has been isolated from Pseudomonas putida. This system consists of a flavoprotein, an iron-sulfur protein, and a heme protein known as P450.[9] This protein has a molecular weight of 45,000 and contains one molecule of ferriprotoporphyrin IX.[10] This cytochrome functions both by binding oxygen and by its ferric-ferrous redox capacity. It has been suggested that one of the ligands is a cysteine.[10]

Although much work has been done on this type of heme protein, a number of questions remain unanswered. In particular, what is the nature of the enzyme-substrate interaction and what is the reaction mechanism. Schemes have been proposed for the mechanism of these reactions, but have not been verified. It is thus proposed to use the MCD and absorption spectroscopy in the near IR spectral region to study these proteins and the intermediates of the reaction cycle to determine the nature of their spin state and oxidation state.

A mechanism for the reaction of tryptophan-2,3-dioxygenase has been proposed by Feigelson.[11] In this mechanism, the active enzyme is proposed to be in a ferriheme-cuprous state. Adding substrate causes changes in the visible spectrum, perhaps because of a transition of the heme components from a high spin to a low spin state.[12] However, it has been suggested by esr studies that only one of the hemes becomes

low spin; the other remains high spin.[12] The nature of the spin state change on adding substrate can easily be determined with MCD, since high and low spin ferrihemes have quite different spectra. If these heme are functionally distinct, the MCD spectra should be able to distinguish between them. The MCD spectra may also indicate whether binding substrate to one heme results in changes in the environment of the presumably unbound heme. Comparison with other heme proteins may indicate something about the mode of binding or possible changes in the heme ligands. MCD may also decide whether the enzyme-substrate complex should be formulated as $E\text{-}Fe^{3+}\text{-}Cu^{+}\text{-}Tryp$ or $E\text{-}Fe^{2+}\text{-}Cu^{2+}\text{-}Tryp$.

Tryptophan-2,3-dioxygenase has long been known to be controlled by a complex regulatory mechanism. The existence of an allosteric site on the protein has been postulated from studies with α-methyltryptophan; saturation of an allosteric site with α-methyltryptophan in the presence of low amounts of tryptophan alters the protein so that it has a much higher affinity for the second substrate, O_2.[13] Tryptophan can bind to the catalytic and control sites, but α-methyltryptophan can bind only to the control site.[12] Other tryptophan metabolites can inhibit the protein. However, little is known about the nature of the enzyme modification which occurs on binding effectors. Thus, spectroscopic methods could indicate the nature of the changes in the heme environment as α-methyltryptophan is bound.

Similar problems of the P450 system can be studied by MCD. The P450 as isolated is a low spin ferric protein. On adding substrate,

a partial change to high spin ferric protein is reported. [14] This change in spin state could have significant implications since the potential for the heme reduction changes on adding substrate. [15] Since the amount of high spin fraction increases with temperature, a spin state equilibrium has been postulated. MCD could be used to evaluate the parameters characterizing this equilibrium and could monitor how the equilibrium is affected by pH, buffer, or other influences.

Adding one reducing equivalent and oxygen to the P450-substrate complex forms a new stable species, with a distinctive visible spectrum. [9] This species has been suggested to be an oxygenated intermediate in the hydroxylation cycle. [9] The cycle then ends by adding one more reducing equivalent; the hydroxylated substrate splits off the enzyme with the production of water and restoring the ferric form of the hemoprotein. However, the nature of this intermediate is not well understood. It has variously been described as a ferric or ferrous enzyme in combination with oxygen or superoxide. A similar oxygenated species has been found with the tryptophan-2,3-dioxygenase system. [16] Thus, a spectroscopic comparison of these intermediates with various heme proteins and the new porphyrin-oxygen model compounds [17] may reveal some of the details of the oxygen binding.

References

1. P. N. Schatz and A. J. McCaffery, Quart. Rev., 23, 552 (1969).

2. A. D. Buckingham and P. J. Stephens, Ann. Rev. Phys. Chem., 17, 399 (1966).

3. J. C. Cheng, G. A. Osborne, P. J. Stephens, and W. A. Eaton, Nature, 241, 193 (1973).

4. J. C. Sullivan and P. J. Stephens, personal communication.

5. N. A. Sharonova, Y. A. Sharonova, and M. V. Volkenstein, Biochem. Biophys. Acta., 271, 65 (1972).

6. W. N. Poillon, H. Maenoa, K. Koike, and. P. Feigelson, J. Biol. Chem., 244, 3447 (1969).

7. G. Schutz and P. Feigelson, J. Biol. Chem., 247, 5327 (1972).

8. F. O. Brady, M. E. Monaco, H. J. Forman, G. Schutz, and P. Feigelson, J. Biol. Chem., 247 7915 (1972).

9. Y. Ishinura, V. Ulrich, and J. A. Peterson, Biochem. Biophys. Res. Comm., 42, 140 (1971).

10. I. C. Gunsalus, J. R. Meeks, J. D. Lipscomb, P. Debrunner, and E. Munck, in Molecular Mechanisms of Oxygen Activation , O. Hayaishi, ed., Academic Press, New York, 1974, p. 564.

11. H. Maeno and P. Feigelson, J. Biol. Chem., 242, 596 (1967).

12. F. O. Brady, P. Feigelson, K. V. Rajogopalan, Arch. Biochem. Biophys, 157, 63 (1973).

13. P. Feigelson and H. Maeno, Biochem. Biophys. Res. Comm., 28, 289 (1967).

14. J. A. Peterson, Arch. Biochem. Biophys., 144, 678 (1971).

15. R. Tsai, L. A. Yu, I. C. Gunsalus, J. Peisach, W. Blumberg, W. H. Orme-Johnson, and H. Beinert, Proc. Nat. Acad.Sci. U. S., 66, 1157 (1970).

16. Y. Ishimura, M. Nozaki. O. Hayaishi, T. Nakamura, M. Tamura, I. Yanazaki, J. Biol. Chem., 245, 3593 (1970).

17. J. P. Collman, R. R. Gagne, C. A. Reed, W. T. Robinson, G. A. Rodley, Proc. Nat. Acad. Sci. U. S., 71, 1326 (1974).

PROPOSITION III

The development of model systems by inorganic chemists has recently provided much information about a variety of biological systems. Model oxygen carriers[1] and model iron-sulfur compounds[2] have contributed greatly to the understanding of several proteins. It is to be expected that model building can contribute to the understanding of other types of protein. Thus, it is proposed to synthesize and characterize a series of iron compounds which may mimic the catalytic behavior of the enzyme pyrocatechase.

Pyrocatechase is an enzyme which oxidizes catechol to cis, cis-muconic acid by incorporating both atoms of molecular oxygen into the product.[3] It is a reddish enzyme with a broad absorption band between 390 and 650 nm (ϵ = 4670 at 440 nm) in addition to the protein peak at 280 nm.[4] Its molecular weight is 90,000, and it contains two iron atoms. ESR measurements show a g value of 4.28, indicating the presence of ferric ion.[4] There have been some suggestions that the iron is bound by sulfur in the active site, but Tsibris[5] concludes that there is no good information for this conclusion. The spectral properties are certainly more typical of the oxygen bound iron enzymes. None of these reported properties indicates an unusual coordination site.

It is also known that the enzyme forms a very stable complex with catechol in the absence of oxygen.[6] The optical spectrum shows

a poorly resolved band at about 600 nm and shows additional absorption at longer wavelengths; the enzyme-substrate complex is blue-grey. The esr signal is lost.

Thus, to build a model system for the enzyme, coordination of ferric iron is necessary, along with a site in which the aromatic compound can bind. The closest inorganic models relating to the enzyme would be a mixed ligand complex, comprised of Fe(III), catechol, and other ligands such as nitrilotriacetate (NTA) or HEDTA serving the role of protein. These models may answer questions about the mechanism of the pyrocatechase reaction. Specifically, does the enzyme form a ferric-catechol complex, or is there an electron transfer, with the enzyme forming a ferrous-semiquinone complex? Also, does the oxygen directly attack the catechol or must it coordinate to iron?

A number of related compounds and systems have been studied. Iron catechol complexes have been well characterized and are found to be very stable.[7] Interesting effects have been noted with copper mixed ligand systems containing catechol and other aromatic ligands.[8] A number of model hydroxylating systems are known, although the active species are somewhat in doubt. The Udenfriend system, consisting of Fe(II), ascorbic acid, and EDTA, will hydroxylate aromatic compounds in the presence of O_2.[9] Another system in which aromatic compounds are hydroxylated by H_2O_2 in the presence of catalytic amounts of catechol and Fe(III) has been described by Hamilton.[10] The oxidizing agent is suggested to be a complexed iron oxide formed by the elimination of

a molecule of water from an intermediate containing ferric ion, H_2O_2, and the catechol. However, none of these systems results in cleavage of the aromatic ring, as found in the enzyme reaction.

Several possible mechanisms have been suggested for the enzyme reaction. A reaction with a four-membered ring dioxetane as an intermediate has been suggested.[11] Another proposed sequence is outlined below.[12,13]

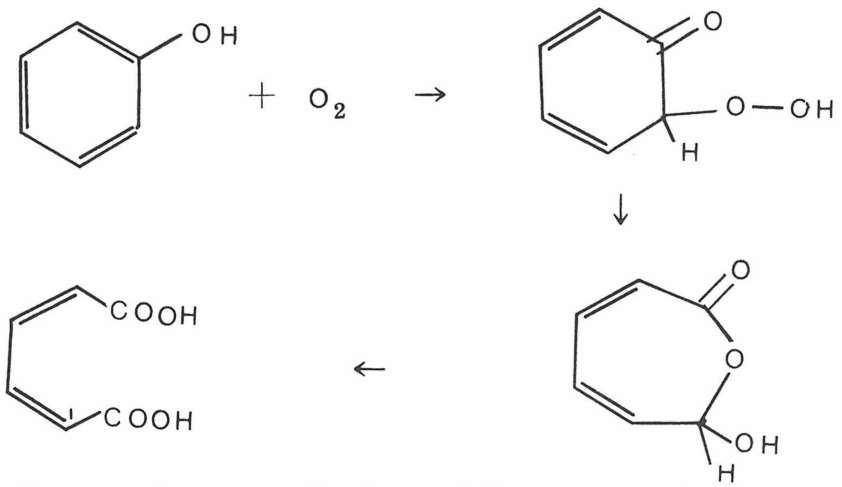

In this mechanism, the iron of the enzyme functions by coordinating oxygen in the first step. Although this mechanism is energetically feasible and consistent with oxygen-18 tracer results,[14] little other evidence is available about the enzymic mechanism. Thus, additional studies are needed.

Studies of an iron(III)-catechol-NTA complex could indicate something about the structure of the enzyme-substrate complex. This mixed ligand complex is readily formed and is relatively stable,[15] suggesting it can be isolated and characterized. Analysis can be

performed to determine the stoichiometry. The IR spectrum should distinguish between the diol form, the semiquinone, or possibly even the quinone form of catechol. The magnetic susceptibility could be measured, determing whether such mixed complexes form the ferric or ferrous complex. Photoelectron spectroscopy would also provide information about the charge distribution. Thus, one can readily determine whether mixed complexes are formed which have a partially oxidized catechol present.

The interaction of the iron-catechol complex with oxygen can be studied on the same inorganic system. Oxidizing agents which cannot coordinate to iron, such as $K_3Fe(CN)_6$, react with iron-catechol-NTA complexes, but the electronic spectrum of reactant and product are very similar.[15] This suggests that the oxidation involved only the catechol. This oxidized product is also relatively stable, suggesting that the state of the iron and catechol can be determined as described previously.

However, agents which can coordinate to iron, such as H_2O_2, show a very different reaction, suggesting that the catechol has extensively rearranged. The products of this reaction should be studied. The reaction pattern in the inorganic system would indicate that the enzyme can function only by first coordinating oxygen to the iron, instead of direct attack of oxygen on the catechol.

Thus, although the coordination sphere of this enzyme is imperfectly understood, it is possible to obtain some information about the interaction of iron, catechol, and oxygen in pyrocatechase.

References

1. J. P. Collman, R. R. Gagne, C. A. Reed, W. T. Robinson, G. A. Rodley, Proc. Nat. Acad. Sci., 71, 1326 (1974).

2. T. Herskovitz, B. A. Averill, R. H. Holm, J. A. Ibers, W. D. Phillips, and J. F. Weiher, Proc. Nat. Acad. Sci. U.S., 69, 2437 (1972).

3. O. Hayaishi, M. Katagiri, S. Rothberg, J. Biol. Chem., 229, 905 (1957).

4. T. Nakazawa, N. Mishiro, O. Hayaishi, T. Yamano, J. Biol. Chem., 244, 119 (1969).

5. J. C. M. Tsibris and R. W. Woody, Coord. Chem. Rev., 5, 417, (1970).

6. Y. Kojima, H. Fujisawa, A. Nakazawa, T. Nakazawa, F. Kanetsuna, H. Tanuchi, M. Nozaki, O. Hayaishi, J. Biol. Chem., 242, 3270 (1967).

7. J.B. Neilands, in Inorganic Biochemistry, G. L. Eichhorn, ed., Elsevier, Amsterdam, 1973, p. 167.

8. F. A. Walker, H. Sigel and D. B. McCormick, Inorg. Chem., 11, 2756 (1972).

9. G. A. Hamilton, R. J. Workman, and L. Woo, J. Amer. Chem. Soc., 86, 3390 (1964).

10. G. A. Hamilton, J. W. Hanifin, Jr., and J. P. Friedman, J. Amer. Chem. Soc., 88 5269 (1966).

11. O. Hayaishi, M. Katagir, and S. Rothberg, J. Amer. Chem. Soc., 77, 5450 (1955).

12. R.O. C. Norman and J. R. Smith, in Oxidases and Related Redox Systems, T. E. King, H. S. Mason, and M. Morrison, eds., Wiley New York, 1965, p. 150.

13. G. A. Hamilton, in Molecular Mechanisms of Oxygen Activation, O. Hayaishi, ed., Academic Press, New York, 1974, p. 444.

14. O. Hayaishi, in The Enzymes, P. D. Boyer, H. Lardy, and K. Myrback, eds., Vol. 8, Academic Press, New York, 1963, p. 353.

15. J. Rawlings, unpublished observations.

PROPOSITION IV

Cytochromes are ubiquitous in nature and serve many varied functions. In unusual circumstances, unusual cytochromes have evolved to perform the functions required for life. Thus, purple sulfur bacteria, which are obligate anaerobes using sulfur compounds as electron donors, have developed many types of cytochromes to perform the functions needed for photosynthesis and electron transfer.[1] One cytochrome, which is present in large amounts in Chromatium, is a diheme protein, molecular weight 70,000 which also contains a flavin.[2]

The function of the protein has been tentatively identified as serving as a shuttle between reduced sulfur compounds such as S^{2-} and $S_2O_3^{2-}$ and other cytochromes.[3,4,5] Thus, this protein functions as an electron transfer protein. Although much work has been done on the kinetics of the simple cytochromes,[6] the functioning of complex cytochromes has not been much investigated. This flavoprotein offers an opportunity to study the interactions between components in a complex cytochrome. Its ready availability, functional groups, spectral properties, water solubility, and stability make the protein an excellent candidate for kinetic studies using a rapid scan spectrophotometer.

The nature of multi-electron transfer has attracted increasing attention. Many important enzymes, such as cytochrome oxidase and nitrogenase, have the capacity to transfer several electrons to a substrate.[6] However, the interactions between the redox sites and

substrates are not well understood. For example, does electron transfer to substrate occur in steps or simultaneously, and is there any "communication" between the redox sites?

Cytochrome C552 offers an opportunity to study such a multi-electron system. The oxidation or reduction of the flavin can be followed at 455 nm; in addition, the appearance of the semiquinone form of the flavin can be followed at longer wavelengths. The heme can be followed at the Soret band. Thus, the kinetics of the components can be followed in reactions with one electron donors or multi-electron donors. The behavior of the system with a multi-electron donor such as its substrate sulfur compounds could indicate whether the protein accepts electrons in a concerted fashion or whether each chromophore acts independently.

One might expect some unusual behavior with this protein, since there is evidence that the heme in the molecule are close enough to interact. The CD spectrum of this protein is quite unusual.[1] There has also been a suggestion that only one of the heme in the protein can combine with CO.[1] It might then be possible to study the reaction of the CO-blocked protein. In this case, only one heme would be capable of reacting, and thus, kinetic parameters relating to this heme alone could be determined. A large difference in the heme reactivity on adding CO could indicate the protein acts by a cooperative mechanism.

It is also possible to study this protein in the absence of flavin. Several treatments have been described which remove the flavin but

leave the heme intact.[7] Thus, one could look for any differences in the kinetics of the heme redox reactions with the deflavo protein.

A very similar protein from Chlorobium has been described.[4] This protein, however, has only one heme and one flavin. Thus, rapid scan kinetics could reveal the interaction between the two components in this simpler system.

Thus, studies of the kinetics of a variety of cytochromes with the same redox reactants can give new insights into the relation of structure to function. Also, by studying complex cytochromes that may function as multi-electron donors or acceptors, one can gain some understanding of the multi-electron redox process.

References

1. R. G. Bartsch, Ann. Rev. Microbiol., 22, 181 (1968).

2. R. G. Bartsch, and M. D. Kamen, J. Biol. Chem., 235, 825 (1960).

3. M. A. Cusanovich, R. G. Bartsch, and M. D. Kamen, Biochem. Biophys. Acta., 153, 397 (1968).

4. T. E. Meyer, R. G. Bartsch, M. A. Cusanovich, and J. H. Mathewson, Biochem. Biophys. Acta., 153, 854 (1968).

5. G. D. Glace and W. W. Parson, Biochem. Biophys. Acta., 253, 187 (1971).

6. L. E. Bennett, in Current Research Topics in Bioinorganic Chemistry, S. J. Lippard, ed., Wiley, New York, 1973, p. 1.

7. R. Hendricks and J. R. Cronin, Biochem. Biophys. Res. Comm., 44, 313 (1971).

PROPOSITION V

Platinum compounds have been used in recent years in the treatment of cancer.[1, 2] Compounds like cis-$[Pt(NH_3)_2Cl_2]$ have proved quite effective. However, the design of such drugs has often been approached nonsystematically; a wide range of compounds may be clinically tested and the ones which work are used. Thus, there is no clear understanding of the structural requirements for a good anti-cancer drug.

One hypothesis about drug action is that the effective platinum compound has two cis ligands approximately 3 Å apart which are relatively labile.[1] Thus, the compounds bind to the DNA of the cancer cell, inhibiting replication. Some compounds, however, would seem not to fit these requirements.[3] Thus, there is no clear picture of the nature of the good cancer drug. Thus, it would prove valuable to study the existing cancer drugs to determine the structure and properties of these compounds.

Some platinum complexes containing uracil or thymine have been reported which show a good anti-cancer effect.[4] However, not much is known about the structure of these compounds. It is thus proposed that these compounds be characterized. By doing so, one may hope to gain further information about the design of a good drug.

While most platinum complexes are yellow or palely colored, these complexes are blue. This might be indicative of a polymeric

nature.[5] Thus, the compound should be analyzed and a molecular weight determination made. However, other blue or green platinum-amide complexes have been reported which are monomeric and square planar.[6,7] One of these complexes, $Pt[(CH_3)_3(CCONH]_2Cl_2$, has been formulated as a Pt(IV) complex, with two amide anions complexed to the platinum.[6] This assignment has been questioned,[1] but the similarity between these amides and the platinum-uracil complex is obvious.

Thus, these platinum complexes could be studied by IR and nmr to determine which tautomeric form of the ligand is involved in the binding. Information on the metal oxidation state can be obtained by ESCA studies.[8] Ideally, it would be useful to do an X-ray crystal structure.

Since the stoichiometry of this compound is not yet known, it is not clear whether these platinum-uracil complexes contain labile ligands. Determining the formula of the compound may indicate whether labile ligands are an absolute requirements for an effective drug. It may be that this type of compound is exhibiting a significantly different binding mechanism. It is well known that nucleotide-like substances "stack",[9] with their aromatic rings parallel. Thus, it may be possible for the platinum-uracil compound to insert the uracil in the DNA sequence; the resulting complex may be bulky enough to seriously interfere with the DNA structure and replication. The base

stacking of nucleotides has been well characterized by nmr.[9] Therefore, an nmr study of the Pt-uracil complex with various polynucleotides could indicate if serious disruption of the structure has taken place.

Thus, characterizing what may be a substantially different type of platinum complex which is an effective cancer drug may indicate more about the structural requirements for drug design.

References

1. M. J. Cleare, Coord. Chem. Rev., 12, 349 (1974).

2. D. R. Williams, Chem. Rev., 72, 203 (1972).

3. M. J. Cleare and J. D. Hoeschele, Bioinorg. Chem., 2, 187 (1973).

4. S. Mansy and B. Rosenberg, in Ref. 1, p. 399.

5. K. Krogman and H. D. Hausen, Z. Anorg. Allgem. Chem., 358, 67 (1968).

6. D. B. Brown, R. D. Burbank, and M. B. Robin, J. Amer. Chem. Soc., 91, 2895 (1969).

7. K. A. Hoffman and G. Bugge, Chem. Ber., 41, 312 (1908).

8. W. M. Riggs, Proc. Symp. on Electron Spectroscopy, Asilomar California, 1971, Abstract V. 2.

9. M. P. Schweizer, S. I. Chan, P. O. P. Ts'o, J. Amer. Chem. Soc., 87, 5241 (1965).